

# A HEALING SYSTEM FOR FAILED ANTENNA ARRAY USING EVOLUTIONARY COMPUTATIONAL TECHNIQUES

Ph.D. THESIS

*by*

OM PRAKASH ACHARYA



DEPARTMENT OF ELECTRONICS AND COMMUNICATION ENGINEERING  
INDIAN INSTITUTE OF TECHNOLOGY ROORKEE  
ROORKEE-247667 (INDIA)  
JANUARY, 2016



**A HEALING SYSTEM FOR FAILED ANTENNA ARRAY USING  
EVOLUTIONARY COMPUTATIONAL TECHNIQUES**

**A THESIS**

*Submitted in partial fulfilment of the  
requirements for the award of the degree*

*of*

**DOCTOR OF PHILOSOPHY**

*in*

**ELECTRONICS AND COMMUNICATION ENGINEERING**

*by*

**OM PRAKASH ACHARYA**



**DEPARTMENT OF ELECTRONICS AND COMMUNICATION ENGINEERING  
INDIAN INSTITUTE OF TECHNOLOGY ROORKEE  
ROORKEE-247667 (INDIA)  
JANUARY, 2016**





**©INDIAN INSTITUTE OF TECHNOLOGY ROORKEE, ROORKEE- 2016  
ALL RIGHTS RESERVED**



# INDIAN INSTITUTE OF TECHNOLOGY ROORKEE ROORKEE

## CANDIDATE'S DECLARATION

I hereby certify that the work which is being presented in the thesis entitled "**A HEALING SYSTEM FOR FAILED ANTENNA ARRAY USING EVOLUTIONARY COMPUTATIONAL TECHNIQUES**" in partial fulfilment of the requirements for the award of the Degree of Doctor of Philosophy and submitted in the Department of Electronics and Communication Engineering of the Indian Institute of Technology Roorkee, Roorkee is an authentic record of my own work carried out during a period from July, 2010 to January, 2016 under the supervision of Dr. A. Patnaik, Associate Professor and Prof. S. N. Sinha, Emeritus Professor, Department of Electronics and Communication Engineering, Indian Institute of Technology Roorkee, Roorkee, India.

The matter presented in this thesis has not been submitted by me for the award of any other degree of this or any other Institute.

**(OM PRAKASH ACHARYA)**

This is to certify that the above statement made by the candidate is correct to the best of our knowledge.

**Dr. A. Patnaik**  
**Supervisor**  
**Date: 18<sup>th</sup> January 2016.**

**Prof. S. N. Sinha**  
**Supervisor**

The Ph.D Viva-Voce Examination of **Mr. OM PRAKASH ACHARYA**, Research Scholar, has been held on **09<sup>th</sup> May 2016.**

**Chairman, SRC**

**Signature of External Examiner**

This is to certify that the student has made all the corrections in the thesis.

**Signature of Supervisor**  
**Date: 09<sup>th</sup> May 2016.**

**Signature of Supervisor**

**Head of the Department**





# Acknowledgements

*“The will of God will never take you where Grace of God will not protect you”*

First of all, I am extremely grateful to The Almighty God who has always taught me to follow the right path of the life. Without his grace this work could never have come true.

I would like to express my sincere gratitude to my supervisors, Dr. Amalendu Patnaik, Associate Professor and Prof. S.N. Sinha, Emeritus Professor, Department of Electronics and Communication Engineering, IIT Roorkee for their continuous support and valuable guidance in carrying out this research work. Their commendable patience, motivation, enthusiasm, and immense knowledge have been a source of inspiration in my research and writing of this thesis. This work would not have been possible without them. I have been fortunate enough to get the excellent environment for work with ample facilities and academic freedom from them. I will remain ever indebted to them. I could not have expected having better advisors and mentors for me.

Besides my supervisors, I am very grateful to the other members of my research committee, Dr. M. V. Kartikeyan, Dr. N. P. Padhy and Dr. D. Singh for their suggestions and contribution during my Ph.D. I also offer my sincere thanks to all the faculty and staff members of Electronics and Communication Engineering Department for their needful support. I also pay my thanks to the laboratory technicians, Mr. Rajaram and Mr. L. Giri for their assistantship in the advanced microwave lab.

The years spent at IIT Roorkee would not have been as wonderful without my friends, including Aswini, Debasis, Anuradha, Jagannath, Arjun, Prateek, Ajith Ku M. M, who contributed through their support, knowledge and friendship in this work.

Special thank to my friend Dr. Trilochan Panigrahi.

I take this opportunity to express my regards and obligation to my father whose support and encouragement I can never forget in my life. My sincere thanks to my wife Ipsa, for her patience, support, encouragement and understanding, without which, I could hardly be able to complete my work. I

wish to appreciate and thank my daughter Juju for her love which inspired me.

Finally, this thesis is dedicated to my mother. Her blessings have been a constant support to me throughout my life.

For anyone I forgot to thank, I am sorry, I just wish them to know that I could not have done this without them.

**OM PRAKASH ACHARYA**

# Abstract

Antenna arrays are an integral part of many signal acquisition systems such as sonar, radar, and satellite communication, since they provide additional dimensions of flexibility and control to system designer. The arrays used for these applications utilize the spatial diversity effectively, known as beam-forming in array terminology, for improving the quality of signal and reducing interference. Because of the presence of the large number of radiating elements in an antenna array, there is always a possibility that some of the elements may malfunction. One of the reasons for this is that the active components like transistor and switches, T/R modules, power supplies used in phased array antennas have a finite lifetime. Alternatively, the degradation in array performance may occur due to some unforeseen reasons like vagaries of weather or natural calamities. Thus, over a period of time, as the components of the antenna fail, the antenna performance will degrade which is a matter of concern to the system designer.

Faults in an array degrade the far field radiation pattern of the antenna. This degradation may be in the form of increased side lobe levels (SLL), decreased gain and directivity, and the removal of nulls. Thus, entire system performance is affected due to element failure. One possible solution to this problem could be the replacement of the defective element(s). However, this increases the overall cost of the antenna and system downtime. Furthermore, replacement of the faulty elements is not always possible, particularly when the array is on a space platform or placed in a difficult geographical location. Thus, it is a tremendous challenge for the engineers to establish an uninterrupted and reliable communication by maintaining the radiation properties of the array. Therefore, methods need to be developed to tackle this problem of element failure by means of remote handling in an antenna array, so that the antenna system can heal itself as much and as fast as possible, till more elaborate repairs can be undertaken. The possibility of failure correction for digital beam-forming arrays by remotely changing the excitation of the functioning elements without removing the faulty elements provides a cost-

effective alternative to hardware replacements. This extends the effective usefulness of the phased array and its dependent systems.

The malfunctioning of one or more radiating elements makes the array asymmetric and hence, it becomes difficult to handle the problem of compensation analytically. It was, therefore, proposed to use computational techniques after converting the compensation problem to an optimization problem. However, classical optimization techniques, like conjugate-gradient method increase in complexity for multi-variable systems. A good alternative is the use of evolutionary computing techniques which have gained currency in recent years. These tools fall under the broad category of soft-computing methods. Over the years, biologically inspired evolutionary computational techniques have been used in all engineering branches for design and optimization. The methods can tolerate imprecision, uncertainty and approximation to achieve robust and low cost solution in a small time frame. Researchers have successfully used techniques like Neural Networks (NN), Genetic Algorithm (GA), Particle Swarm Optimization (PSO), Ant Colony Optimization (ACO), Bacteria Foraging Optimization (BFO) and many more for finding an easy solution for their problems. The robustness of these techniques has been tested for the problems encompassing every engineering field. For the last decade or so, antenna engineers have also frequently used these techniques.

The aim of the present research work is to develop methods of compensation for SLL suppression, null steering, DoA estimation and beam-forming for a failed phased antenna array with the help of evolutionary computational techniques, viz. particle swarm optimization and bacteria foraging optimization techniques. Although the results of compensation are presented for a typical array structure, through extensive simulation it has been found that it is equally applicable for other arrays also. The overall aim is to make the faulty array to work as a normal one.

# Table of Contents

<b>Acknowledgements</b>	<b>i</b>
<b>Abstract</b>	<b>iii</b>
<b>Table of Contents</b>	<b>v</b>
<b>List of Figures</b>	<b>vii</b>
<b>List of Tables</b>	<b>xi</b>
<b>List of Abbreviations</b>	<b>xiii</b>
<b>Chapter 1: Introduction</b>	<b>1</b>
1.1 Motivation	1
1.2 Research Objectives	3
1.3 Organization of the Thesis	4
<b>Chapter 2: Revisiting Array Synthesis and Evolutionary Computational Techniques</b>	<b>7</b>
2.1 Antenna Array Synthesis	8
2.1.1 Synthesis in a Failed Array	9
2.2 DOA Estimation and Beamforming	11
2.3 Evolutionary Computational Techniques	13
2.3.1 Particle Swarm Optimization	14
2.3.2 Bacteria Foraging Optimization	20
<b>Chapter 3: Recovery of Sidelobe Level (SLL) in Failed Antenna Array</b>	<b>27</b>
3.1 Introduction	27
3.2 Problem Formulation	29
3.3 Test Antenna Array	30
3.4 SLL Recovery Using PSO	33
3.4.1 Analysis for Amplitude-only Control	34
3.4.2 Analysis for Amplitude-phase Control	46
3.5 SLL Recovery Using BFO	49
3.6 Performance Comparison of PSO with BFO for SLL Recovery	53
3.7 Summary	56
<b>Chapter 4: Null Steering in Failed Antenna Array</b>	<b>57</b>
4.1 Introduction	57
4.2 Problem Formulation	58
4.3 Null Recovery Using PSO	59
4.3.1 Analysis for Amplitude-Only Control	60
4.3.2 Analysis for Amplitude-Phase Control	74

4.4	Null Recovery Using BFO	80
4.5	Performance Comparison of PSO with BFO for Null Recovery	83
4.6	Summary	85
<b>Chapter 5: Limits in Compensation in a Failed Antenna Array</b>		<b>87</b>
5.1	Introduction	87
5.2	Investigation on Minimum Number of Element Excitations Required for Pattern Restoration	88
5.2.1	Observations	96
5.3	Investigation on Maximum Numbers of Element Failure That Can Be Compensated	96
5.4	Summary	100
<b>Chapter 6: Effect on Direction of Arrival Estimation (DoA) in a Failed Antenna Array and Beamforming</b>		<b>103</b>
6.1	Introduction	103
6.2	Problem Formulation	104
6.3	PSO for DoA Estimation	107
6.3.1	DoA Estimation in a Failed Antenna Array for Single Source	108
6.3.2	DoA Estimation in a Failed Antenna Array for Two Sources	109
6.3.3	Observations	111
6.4	Beamforming in Failed Array	112
6.5	Beamforming Implementation	114
6.6	Summary	115
<b>Chapter 7: Conclusion and Future Scope of work</b>		<b>117</b>
7.1	Future Scope	119
<b>References</b>		<b>121</b>
<b>Author's Publications</b>		<b>131</b>

# List of Figures

Figure No.	Title of Figure	Page No.
Figure 2.1	Flow chart for PSO	19
Figure 2.2	Flow chart for BFO	25
Figure 3.1	A linear antenna array	29
Figure 3.2	Desired SLL considered for Chebyshev and Taylor pattern	30
Figure 3.3	Array factor of 32 element linear Chebyshev and Taylor array	31
Figure 3.4	Recovered power pattern by PSO in a two element failed Chebyshev antenna array	35
Figure 3.5	Amplitude distribution of recovered pattern by PSO versus original Chebyshev array (Two element failure)	35
Figure 3.6	Recovered power pattern by PSO in a two element failed Taylor antenna array	36
Figure 3.7	Amplitude distribution of recovered pattern by PSO versus original Taylor array (Two element failure)	36
Figure 3.8	Recovered power pattern by PSO in a two element failed Chebyshev antenna array with inter element spacing of $0.75 \lambda$ .	37
Figure 3.9	Recovered power pattern by PSO in a three element failed Chebyshev antenna	37
Figure 3.10	Amplitude distribution of recovered pattern by PSO versus original Chebyshev array (Three element failure)	38
Figure 3.11	Plot of corrected pattern by PSO in a four element failed (at 3 <sup>rd</sup> , 4 <sup>th</sup> , 5 <sup>th</sup> and 6 <sup>th</sup> positions) Chebyshev array	39
Figure 3.12	Plot of corrected pattern by PSO in a four element failed (at 5 <sup>th</sup> , 6 <sup>th</sup> , 29 <sup>th</sup> and 30 <sup>th</sup> positions) Chebyshev array	39
Figure 3.13	Amplitude distribution of recovered pattern by PSO versus original Chebyshev array (Four elements failure located at 3 <sup>rd</sup> , 4 <sup>th</sup> , 5 <sup>th</sup> and 6 <sup>th</sup> positions)	40
Figure 3.14	Amplitude distribution of recovered pattern by PSO versus original Chebyshev array (Four elements failure located at 5 <sup>th</sup> , 6 <sup>th</sup> , 29 <sup>th</sup> and 30 <sup>th</sup> positions)	40
Figure 3.15	Error performance of PSO for different types of element failure in the Chebyshev array	44
Figure 3.16	Plot of corrected pattern obtained by amplitude-phase compensation in a two element failed Chebyshev antenna	47
Figure 3.17	Plot of corrected pattern obtained by amplitude-phase compensation in a three element failed Chebyshev antenna	47
Figure 3.18	Recovered power pattern by PSO and BFO in a two element failed Chebyshev antenna array	50

Figure 3.19	Amplitude Distribution of recovered pattern versus Original Chebyshev array (Two element failure case)	51
Figure 3.20	Convergence of fitness function for PSO and BFO	51
Figure 3.21	Recovered power pattern by PSO and BFO in a two element failed Taylor antenna array	52
Figure 3.22	Amplitude distribution of recovered pattern versus Original	52
Figure 4.1	A 32-element Chebyshev array pattern with SLL of -35dB.	60
Figure 4.2	Radiation pattern of 32 element linear broadside array with null at $20^{\circ}$	61
Figure 4.3	Radiation pattern with element failure at 2 <sup>nd</sup> and 5 <sup>th</sup> positions and null at $20^{\circ}$	62
Figure 4.4	Radiation pattern with element failure at 2 <sup>nd</sup> , 5 <sup>th</sup> and 6 <sup>th</sup> positions and null at $20^{\circ}$	63
Figure 4.5	Radiation pattern with element failure at 2 <sup>nd</sup> , 3 <sup>rd</sup> , 5 <sup>th</sup> and 6 <sup>th</sup> positions and null at $20^{\circ}$	64
Figure 4.6	Convergence curve for recovery of pattern nulling in the presence of faulty elements in the antenna array.	64
Figure 4.7	Radiation pattern of 32 element linear broadside array with null at $20^{\circ}$ and $40^{\circ}$	66
Figure 4.8	Performances of PSO for placing nulls at $20^{\circ}$ and $40^{\circ}$ with element failure.	67
Figure 4.9	Radiation pattern of the linear array with imposed nulls at $20^{\circ}$ , $33^{\circ}$ and $50^{\circ}$	68
Figure 4.10	Performances of PSO for placing nulls at $20^{\circ}$ , $33^{\circ}$ and $50^{\circ}$ with element failure	69
Figure 4.11	Radiation pattern of a linear broadside array with a broad null at $30^{\circ}$	71
Figure 4.12	Performances of PSO for placing broad null with element failure	72
Figure 4.13	Radiation pattern obtained by controlling both the amplitude and the phase with one null at $20^{\circ}$	75
Figure 4.14	Recovered radiation pattern of a failed antenna array obtained by controlling both the amplitude and the phase with one null at $20^{\circ}$	76
Figure 4.15	Radiation pattern obtained by controlling both the amplitude and the phase excitations to impose null at $20^{\circ}$ and $40^{\circ}$ (Test array pattern)	77
Figure 4.16	Recovery of pattern with failed elements and have nulls at $20^{\circ}$ and $40^{\circ}$ directions	77
Figure 4.17	Three nulls in the pattern, obtained by re-optimizing complex weights (Test array pattern)	78
Figure 4.18	Recovery of three nulls in element failure	78
Figure 4.19	Performances of PSO and BFO for placing a null at $20^{\circ}$ with element failure	81
Figure 4.20	Performances of PSO and BFO for placing two nulls at $20^{\circ}$ and $40^{\circ}$ with element failure	82
Figure 4.21	Performances of PSO and BFO for placing three nulls at $20^{\circ}$ ,	83



	33° and 50° with element failure	
Figure 5.1	Compensation for element failure at 5 <sup>th</sup> position by adjusting 6 of the remaining elements	89
Figure 5.2	Compensation for element failure at 6 <sup>th</sup> position by adjusting 8 of the remaining elements	90
Figure 5.3	Compensation for element failure at 7 <sup>th</sup> position by adjusting 12 of the remaining elements	91
Figure 5.4	Compensation for element failure at 8 <sup>th</sup> position by adjusting 14 of the remaining elements	91
Figure 5.5	Compensation for element failure at 9 <sup>th</sup> position by adjusting 16 of the remaining elements	92
Figure 6.1	Linear uniform array for DoA estimation	105
Figure 6.2	RMS error of the estimated DoA vs SNR (Single source incident on the antenna array having different number of faulty elements)	108
Figure 6.3	RMS Error of the estimated DoA vs SNR (Two sources incident on the antenna array having different number of faulty elements)	110
Figure 6.4	Probability of resolution (PR) vs SNR for DOA estimation by PSO in a failed antenna array (Two sources separated by 10°)	110
Figure 6.5	RMS Error of the estimated DoA vs SNR (Two sources separated by 5° incident on the antenna array having different number of faulty elements)	111
Figure 6.6	Probability of resolution (PR) vs SNR for DOA estimation by PSO in a failed antenna array (Two sources separated by 5°)	111
Figure 6.7	Beamformer	114
Figure 6.8	Beamforming in a 32- element linear array having two failed elements	115



# List of Tables

Table No.	Title of Table	PageNo.
Table 3.1	Parameters of the test array	31
Table 3.2	Normalized amplitude excitations for two test arrays	32
Table 3.3	PSO Parameters	33
Table 3.4	Parameters obtained in amplitude-only compensation in a 32-element linear Chebyshev array	42
Table 3.5	Computation time for PSO in dealing with element failure in Chebyshev antenna array	42
Table 3.6	Optimized amplitude excitations obtained by PSO for different number of element failure in the Chebyshev array	43
Table 3.7	Normalized amplitude excitations obtained from PSO optimizer to correct the radiation pattern of 32- element Taylor pattern array having two element failures	45
Table 3.8	Parameters obtained by PSO in amplitude-phase compensation for Chebyshev array	48
Table 3.9	BFO parameters	50
Table 3.10	Optimized amplitude-excitation obtained for two element failure at 2nd and 5th position in a 32-element linear Chebyshev and Taylor array	55
Table 3.11	Parameters obtained in compensation of two element failure in Chebyshev Array	56
Table 3.12	Parameters obtained in compensation of two element failure in Taylor Array	56
Table 4.1	Comparison of recovered patterns for the different configurations discussed in Case I	64
Table 4.2	Element excitations corresponding to recovery of single null	65
Table 4.3	Pattern characteristics obtained in recovery of two nulls with two element failure in a Chebyshev array	66
Table 4.4	Element excitations corresponding to Case II	67
Table 4.5	Pattern characteristics obtained in recovery of three null with two element failure in a Chebyshev array	69
Table 4.6	Element excitations corresponding to Case III	70
Table 4.7	Pattern characteristics obtained for the configurations discussed in Case IV	72
Table 4.8	Element excitations corresponding to Case IV	73
Table 4.9	Pattern characteristics of the array with single null	75
Table 4.10	Pattern characteristics obtained in recovery of two nulls in a failed antenna array	79
Table 4.11	Pattern characteristics obtained in recovery of three nulls in a failed antenna array	79
Table 4.12	BFO parameters	80
Table 4.13	Comparison of pattern properties obtained in recovery of single null with two element failure	81

Table 4.14	Comparison of pattern properties obtained in recovery of two nulls with two element failure	82
Table 4.15	Comparison of pattern properties obtained in recovery of three nulls with two element failure	82
Table 4.16	Element excitations obtained using BFO	84
Table 5.1	Compensation for single element failure at different positions in the array carried out by optimizing minimum number of working elements	90
Table 5.2	Compensation for multiple element failure in the array carried out by optimizing minimum number of working elements	93
Table 5.3	Amplitude weights computed for single element failure at different positions (as given in Table 5.1) in a 32- element array	94
Table 5.4	Optimized amplitude weights computed for multiple element failure at different positions (as given in Table 5.2) in a 32- element array	95
Table 5.5	Pattern Recovery for maximum number of element failure in a 32-element linear array	98
Table 5.6	Pattern recovery for maximum number of element failure in a 20-element linear array	98
Table 5.7	Optimized amplitude weights computed for multiple element failure at different positions (as given in Table 5.5) in a 32- element array	99
Table 5.8	Optimized amplitude weights computed for multiple element failure at different positions (as given in Table-5.6) in a 20- element array	100

# List of Abbreviations

ACO	Ant Colony Optimization
BFO	Bacteria Foraging Optimization
BWFN	Beamwidth between First Null
CDMA	Code Division Multiple Access
dB	Decibel
DE	Differential Evolution
DoA	Direction of Arrival
ESPRIT	Estimation of Signal Parameters via Rotational Invariance Technique
FDMA	Frequency Division Multiple Access
GA	Genetic Algorithm
GBEST	Global Best
HPBW	Half-Power Beamwidth
ML	Maximum Likelihood
MUSIC	Multiple Signal Classification
NDL	Null Depth Level
NN	Neural Network
PBEST	Personal Best
PR	Probability of Resolution
PSO	Particle Swarm Optimization
RMSE	Root Mean Square Error
SA	Simulated Annealing
SLL	Side Lobe Level
SNR	Signal to Noise Ratio
TDMA	Time Division Multiple Access
Wi-Fi	Wireless Fidelity
WiMAX	Worldwide Interoperability of Microwave Access



## Chapter 1

# Introduction

---

Boeing in August 2001, said in a statement that five of the 18 communication services provided by the NASA operated TDRS-8 (TDRS-H) satellite that was launched in June 2000, are performing at less than specified capability because of the performance shortfall on the multiple access phased array antenna [1]. The cause of the problem was rooted in one specific material used in the assembly of antenna, because of which the array was malfunctioning. Few similar instances forced antenna engineers to think of ways and means of remotely handling arrays, particularly for the arrays placed in space platforms. The main focus was how to restore the antenna pattern when few of the radiating elements of the phased array start malfunctioning. It is indeed a matter of concern, because the active components like transistor and switches, T/R modules, power supplies used in phased array antennas have limited lifetime [2]. So over a period of time, as the components of the antenna fail, the antenna performance degrades. The work done in this thesis is an attempt to restore the performances of a failed phased array antenna.

## 1.1 Motivation

Antenna arrays are an integral part of many signal acquisition applications such as sonar, radar, satellite communications and cellular phones etc. The array used for these applications utilize the spatial diversity effectively, which in array terminology is known as beam-forming, for improving the quality of signal and reducing the interference. Because of the presence of the large number of radiating elements, possibility of having a fault in individual antenna element(s) during the array operation cannot be ruled out at all times [3]. The failure may occur due to the degradation in the

performance of the associated circuitries such as transmitter/receiver modules and power supplies as they have finite life time. This may also be due to some unforeseen reasons like vagaries of weather or natural calamities. The effect of such fault in an array, i.e. presence of elements that are not contributing to the radiation, distort the antenna radiation pattern, mostly in the form of increased sidelobe levels (SLL), decreased gain and directivity and the removal of nulls. Thus, the entire system performance is affected due to element failure [4, 5]. One possible solution to this element failure problem could be replacement of the defective element(s). But this increases the overall antenna cost. Furthermore, replacement of the fault elements is not always possible, particularly when the array is in space platform or placed in a difficult geographical location. Therefore, this is a challenge for the engineers to establish an uninterrupted communication by maintaining the radiation properties of the array. This prompted us to take, development of healing system for failed antenna array as the topic of research for the present thesis. Restoration of radiation pattern of a phased array antenna with failed elements provides a cost effective alternative to hardware replacement, thereby increasing the array availability [6, 7]. Presence of one or more non-radiating elements makes the array asymmetric and thereby making it difficult to find an analytical solution for this problem. Therefore, we have approached the problem as an optimization problem and solved using evolutionary computational techniques.

Evolutionary computational techniques are a set of tools whose working principle originates from replicating different biological phenomenon. These tools fall under the broad category of soft-computing methods. Over the years, biologically inspired evolutionary computational techniques have gained popularity among the researchers in every branch of engineering [8, 9]. Researchers are using techniques like Neural Networks (NN), Genetic Algorithm (GA), Particle Swarm Optimization (PSO), Ant Colony Optimization (ACO), Bacteria Foraging Optimization (BFO) and many more for finding an easy solution for their problems. The robustness of these techniques has been tested in problems encompassing every field of



engineering. These techniques have been used in antenna engineering since 1990s. A number of applications of these evolutionary computational methods have been reported for the design of antennas [10-20].

Evolutionary optimization techniques [21, 22] offer some unique advantages, over their classical counterparts making these suitable to use for the present research problem. These are summarized below:

- The use of evolutionary computational techniques does not require extensive mathematical formulation of the problem. Thus, the requirement on the necessity of exclusive domain specific knowledge can be reduced.
- These tools can handle many variables simultaneously.
- Use of global optimization methods can avoid the chances of being trapped in local minima, if the problem in hand can be formulated as an optimization problem.
- They provide low cost solutions to the user, thereby reducing the dependency on costly electromagnetic simulations up to some extent.
- These methods are adaptive and scalable.

## **1.2 Research Objective**

The objectives of our research work are as stated below:

- To analyze the effects of element failure on the radiation properties of antenna array.
- To develop compensation techniques based on evolutionary computational methods, which can optimize the array performance in the presence of one or more failed elements.
- To test the performance of evolutionary computational techniques for speedy implementation in view of their use in real-time operation.

In order to meet the above mentioned research objectives the following tasks were considered and solved successfully.

- The task of sidelobe level suppression in a failed antenna array using PSO.
- In the next phase of work, the task of null steering in failed antenna array for interference suppression was carried out using PSO.
- BFO being relatively new to microwave community, its capability was investigated for failed antenna array, for the same two tasks handled by PSO.
- Investigation was made to find the limits of the compensation for a failed antenna array.
- In the last part of the research work, attempt was made to find the effect on direction of arrival (DoA) estimation in a failed antenna array.

## **1.3 Organization of the Thesis**

The thesis consists of seven chapters. Chapter-1 gives an introduction of the entire work. It also includes the motivation and objectives of the research. The organization of the later chapters is as follows: Chapter-2 presents a comprehensive review on the synthesis of antenna array with and without element failure. Various analytical methods for antenna array pattern synthesis have been reviewed. The different optimization techniques (both classical and evolutionary computational techniques) used for compensation of failed array is discussed. The capabilities of the two evolutionary optimization techniques, PSO and BFO that are actually being used in our work are also discussed in this chapter.

Chapter-3 of the thesis deals with the use of PSO for sidelobe level suppression in the antenna array with element failure. In order to solve the problem, at the outset the task was converted to an optimization problem. Then a suitable cost function was framed to solve it using PSO. A similar approach was adopted to solve the same problem using BFO. A detailed analysis of time of computation has also been done for both PSO and BFO implementation.

Another aspect of radiation pattern is the placement of nulls. The problem of null steering in failed antenna array is the content of chapter-4. Both PSO

and BFO were used to solve the null steering problem in failed antenna arrays.

Chapter-5 describes the limits of compensation in failed antenna arrays. In one approach, the minimum number of operational elements was found out, which can restore the radiation pattern. The second approach is to determine the maximum number of element failure, for which the compensation technique is able to recover the pattern with acceptable performance.

The effect on the direction of arrival (DoA) estimation and the corresponding beamforming in a failed array is discussed in chapter-6.

Finally chapter-7 summarizes the contributions made in the thesis and the scope for the future work is outlined.



# Revisiting Array Synthesis and Evolutionary Computational Techniques

---

Recent advances in wireless communications and electronics have made the antenna as an integral part of human life and are widely used in their day to day activity. The use of antenna in different applications has been reported in literature [23-28]. The research on antenna was started from its date of inception, to improve the performances in terms of gain, efficiency, control of directivity, polarization and reconfigurability by introducing different techniques [29-36]. But in many long distance wireless applications, there was always a demand for very high directive antennas. This high gain characteristic was achieved by arranging several antennas in space, which was referred to as an array antenna. The concept of array was developed in 1940.

The antenna array is a geometrical configuration of multiple antenna elements whose far-field radiation patterned can be tailored by adjusting the different design parameters. Thus, an antenna array can enhance the spatial diversity of transmitted/received signals [37, 38]. There are several array design variables that can be controlled to achieve the desired radiation pattern. These are:

- general array shape (linear, planar, circular, etc.)
- element spacing
- element excitation amplitude
- element excitation phase
- patterns of the individual element in array

Synthesis of antenna array is a systematic procedure to produce desired radiation characteristics by finding the antenna configuration, its

geometrical dimensions and excitation distribution. This chapter presents a brief review of the techniques for the optimization of the radiation pattern of an antenna array with element failures. In the beginning a comprehensive overview of the antenna array synthesis techniques reported so far are introduced. In this chapter the available techniques for the direction of arrival (DoA) estimation and beamforming are also briefly discussed. A review on evolutionary computational techniques has also been presented with special emphasis on particle swarm optimization (PSO) and bacteria foraging optimization (BFO) that are actually used to solve the problem in this thesis.

## **2.1 Antenna Array Synthesis**

The most widely used analytical techniques, such as ‘Taylor’ [39] and ‘Dolph-Chebyshev’ [40, 41] are the two classical amplitude distributions available to achieve radiation patterns with a narrow beamwidth for a given sidelobe level. Other classical means of pattern synthesis procedures are the Schelkunov form [42] and Woodward synthesis [43]. These analytical techniques were developed during the initial phases of antenna arrays and gained popularity till the introduction of the computer processing in array synthesis. These methods are not found suitable for more sophisticated antenna patterns, which require new methods of finding optimal values of the different parameters of the antenna array. With the introduction of computer processing for antenna analysis, optimization based array synthesis techniques were developed. Most of the earlier array synthesis methods in this category are based on the conventional optimization techniques, which are deterministic in nature. In this process, the objective function based on antenna array parameters is minimized or maximized iteratively as per the requirement. Typical deterministic optimization techniques which are applied successfully to problem of array synthesis are Conjugate Gradient [44], Newton’s Method, Simplex Method, Least Squares [45], Projection methods [46-47] etc. A unified formulation for super directive end-fire array design by using Chebyshev and Legendre polynomials is discussed in [48].

In addition to these classical optimization techniques, recently the antenna array synthesis has been under investigation using optimization techniques governed by stochastic principles such as GA, PSO, simulated annealing (SA), BFO etc. [49-54]. Each one of these techniques has its own capabilities, advantages and drawbacks. GA has been applied for the pattern synthesis with arbitrary geometrical configurations in an antenna array [49-50]. In [51] the desired radiation pattern is obtained by simultaneously optimizing the values of the weight coefficients and inter-element spacing of a linear aperiodic array, with the help of GA. The design of reconfigurable antenna array based on GA was discussed in [52]. Khodier and Christodoulou [53] used the PSO to determine the physical layout of the array that produces a radiation pattern that is closest to the desired pattern. In [54], the parameters of array, such as, the amplitude, phase and locations are optimized by PSO for linear and circular arrays. Application of PSO for array analysis and design is discussed in [55-59]. Recently BFO has been applied for pattern synthesis for minimizing sidelobes, along with null-placement of antenna arrays [60-62]. Other optimization techniques which have been successfully implemented for the antenna array synthesis are Simulated Annealing (SA) [63-64] and differential evolution (DE) [65].

### **2.1.1 Synthesis in a Failed Array**

In a large antenna array, there is always a possibility that some of the elements may develop a fault. The fault may occur either due to manufacturing defects during its fabrication or due to adverse weather conditions or aging during its operation. A number of optimization techniques based on either numerical algorithms or stochastic principles have been reported for array failure correction [66-77].

Peters [66] proposed a method to reconfigure the amplitude and phase distribution of the remaining elements for minimizing the average sidelobe level via a Conjugate Gradient Method. Bu et. al. [67] used the biquadratic programming method in reconfiguring the array by changing the phase of each of the remaining active elements. Mailloux [68] used the method of replacing the signals from failed elements in a digital beamforming receiving

array. A practical failure compensation technique for active phased arrays was introduced by Levitas et al. [69]. The orthogonal method has also been used to improve the radiation patterns of an array in the presence of failed elements [70].

In addition to the above classical optimization methods, several heuristic search based evolutionary techniques have also been successfully applied to handle the problem of failed antenna array [71-77]. An approach based on GA is applied for array failure correction in digital beamforming of a linear antenna array in [71]. A cost function was proposed for a given configuration of failed elements in a 32-element linear array and was minimized iteratively to obtain amplitude and phase for all working elements in order to correct the damaged pattern. Another GA based method was proposed in [72] for transmitter/receiver failure compensation in an antenna array by resynthesizing the optimal beam pattern from the damaged pattern using an adaptively weighted beam pattern mask. This approach allows improved resynthesis flexibility and computation speed. The same GA technique is also applied by S. A. Mitilneos *et. al* to deal with dual band operation for the application in WiFi/WiMAX and element failure in a dipole antenna array [73].

Simulated annealing (SA) technique has also been applied for optimizing the performance of the antenna array with the failed elements. In [74] problem of array failure correction in a planar array has been considered. The developed method was applied to a 10×10 rectangular grid planar array with three element failures for recovery of the sum pattern. Another 16×16 element planar array with rectangular grid and a  $\lambda/2$  inter element spacing with two element failure was considered for a shaped beam pattern. SA has also been used in [75] for recalculating linear antennas to compensate for the failed elements.

Hybrid optimization approach based on the combination of GA and fast fourier transform (FFT) was applied to improve the array pattern in the presence of failed elements [76]. This method can obtain all the sampling



points of the pattern by using FFT, hence, providing the possibility of speeding up of the operation of GA. Thus, the process of array failure correction is faster in this case. In another approach, an efficient method based on the artificial neural network (ANN) was introduced for array failure correction in a planar antenna array [77].

## **2.2 DoA Estimation and Beamforming**

The spatial diversity achieved by an antenna array is called array beamforming. Beamforming techniques are used to design a radiation pattern in a manner that the main beam is placed in the direction of the desired target and nulls in the direction of the interfering sources. This maximizes the system performance. Thus, the knowledge of the direction from which the signal is arriving is necessary to place the main beam of the antenna in the direction of the source. The direction of arrival (DoA) estimation involves a correlation analysis of the array signals. DoA estimation has applications in many communication systems, such as, SONAR, track-and-scan RADAR, radio astronomy and in cellular systems [78-80].

In practice, number of signals from unknown directions with unknown amplitude and phase impinge simultaneously on the array. Noise also overlaps with the received signal. Therefore, accurate DoA estimation is always a challenging problem in the area of array signal processing. Nevertheless, there are methods available to estimate the number of signals and their directions. The most widely used techniques are super resolution algorithm, Multiple Signal Classification (MUSIC), Estimation of Signal Parameters via Rotational Invariance Techniques (ESPRIT) and their variants (e.g. Root-MUSIC) [81-83]. MUSIC was developed by Schmidt [81] and it is one of the most popular techniques for estimating DoAs of multiple signal sources and also multiple parameters per source. In the MUSIC algorithm, the desired signal response is orthogonal to the noise subspace. The noise and signal subspaces are identified using eigen value decomposition of the received signal covariance matrix. Then the DoAs are

estimated from the computed values of MUSIC spatial spectrum. A special case of MUSIC is Root-MUSIC algorithm which is described in [82]. Roy and Kailath proposed another efficient and robust DoA estimation method is ESPRIT in 1989 [83]. This method exploits the rotational invariance in the signal subspace which is created by two arrays with translational invariance structure.

Recently, meta-heuristic techniques are gaining popularity in every field of engineering. They also find the application in the field of array signal processing to estimate the DoA. In the recent years, the DoA estimation problem has been solved by using different meta-heuristic optimization techniques like Genetic algorithms (GAs), Particle Swarm optimization (PSO), Ant Colony Optimization (ACO), and Simulated Annealing (SA) etc [84-91]. It is well acknowledged that these techniques are quite successful, reliable and efficient. In [84] Minghui Li and Yilong Lu have described DoA estimation based on maximum likelihood (ML) principle and implemented using GA. The proper selection of all the GA parameters made the estimator to achieve fast global convergence. Authors in [85] introduced ACO to work with MUSIC to overcome the problem of high computational cost in spectrum search in multidimensional case. A new kind of ACO for continuous domain featured by Gauss kernel function is used to sample the MUSIC spectrum, which is regarded as the fitness function in the process.

PSO has also been applied in many cases for DoA estimation [86-91]. In [86] PSO is proposed for single snapshot direction of arrival (DoA) estimation of a set of signals impinging on a uniform linear array. The validity of this approach was verified by doing a performance analysis for infinite signal-to-noise ratio (SNR). A modified PSO was considered to deal with the problem of DoA estimation for code-division multiple access (CDMA) signals in [87].

PSO technique was also applied by B. Errasti et. al. in [88-90] and they tried to find the DoA of the signal as well as other parameters of the signal such as amplitude, phase and frequency. The performance of PSO was analyzed under single snapshot scenarios. In [91] the performance of most

popular metaheuristic optimization methods towards the single-snapshot DoA estimation was addressed.

Once the DoA is obtained, the next task is to form a highly directional beam to track the target i.e. beamforming. So placing the beam in the desired direction is the key issue in the phased arrays used in military and commercial applications. Several studies on beamforming are available in literature [78, 79, 80, 92, 93, 94].

## **2.3 Evolutionary Computational Techniques**

Optimization is the process of obtaining the best solution to meet the design objective of a problem under a given set of circumstances. In the design of engineering systems, the objective is to minimize the effort and cost required or maximization of the efficiency or both by optimally using the valuable resources under various constraints. The systematic and efficient way to reach an optimal design is by the use of optimization algorithms. As optimization algorithm deals with the problem in hand in a particular format, it has to address the issues of mathematical modeling of the process by identifying the design variables which affect the objective function, constraints and variable bounds.

The optimization techniques can be classified as *classical* and *evolutionary optimization* techniques. Most of the classical optimizers are deterministic in nature. Some deterministic optimizers are gradient based, that is, they use the function values and their derivatives [22, 95]. These optimizers do not work well when the complexity of objective function increases.

Classical optimization techniques have the following demerits:

- (1) they are mostly time consuming
- (2) these techniques fail to deal with complex problems involving several parameters

(3) these are local search methods and involve the derivative of functions and

(4) these techniques are computationally unstable or less efficient.

The advent of computers and powerful computational techniques has led the researchers to focus on the evolutionary computation based optimizers. The metaheuristic approach to solve these complex optimization problems is based on the stochastic algorithms. The major components of these algorithms are intensification and the diversification. Diversification is to generate diverse solutions, so that the search space can be explored on a global scale. Intensification is to intensify the focus on the search in a local region by exploiting the current information, so that a recent good solution can be obtained for that region. This selection of the best solution helps in reaching at the optimal solution. At the same time, the diversification via randomization avoids the solution being trapped in the local optima. So the combination of both intensification and the diversification is helpful in reaching a global optimal solution [96]. Simple and powerful nature-based optimization techniques that are available in the form of Genetic Algorithm (GA), Particle Swarm Optimization (PSO), Ant Colony Optimization (ACO), Bacteria foraging optimization (BFO) are stochastic in nature and are global optimizers. Each one of these techniques has its own capabilities, advantages and drawbacks. They are less prone to converge to a weak local optimum than the classical methods and are most suitable for highly non-linear problems.

For the sake of completeness, a brief discussion of PSO and BFO algorithms is presented here while more elaborate descriptions can be found elsewhere [97, 98]. In this dissertation, we have used PSO which is simple to use and BFO which is relatively new to microwave community.

### **2.3.1 Particle Swarm Optimization**

PSO was introduced by Kenedy and Eberhart in 1995, while investigating the idea of collective intelligence in biological populations. The concept of PSO was developed from the simulation of the simplified social systems such

as the ability of flocks of birds, schools of fish to adapt to their environment, find rich sources of food and avoid predators by implementing an information sharing approach [99, 100]. The PSO has been effectively applied in optimizing a wide range of multidimensional problems in different fields of science and engineering [101-103]. Antenna engineering is no exception and PSO has found useful applications in antenna engineering [16-18, 104-106].

According to PSO terminology, every individual swarm is called a *particle* and the position of the particle in the space represents a solution to the problem. The initial choice of a bunch of random solutions is called a *population*. The parameters of each solution are to be optimized within the permissible range. Depending on the number of such parameters, (say  $N$ ), the PSO searches for the optimal solution in the  $N$ -dimensional solution space. The effectiveness of the solution is evaluated by the fitness function of the optimization process. The fitness function, which depends on the user's requirements, takes the value of all  $N$  parameters that represent a possible solution in the solution space and return a single number representing the goodness of that particular solution. The particles remember the position where it encountered best fitness values and share the information with the other particles so that the entire swarm is able to know about the global best solution. Each particle in the solution space is associated with a *velocity*, which is controlled by the best personal solution encountered by the individual particle and the global best solution obtained by the entire swarm. The locations and velocities of particles are initialized randomly within the search space but are updated according to the best position already found by themselves i.e. *personal best* and according to the experience of their companions i.e. *global best*. The particles fly through the multidimensional search space in order to reach the best solution [16].

### **2.3.1.1 PSO Algorithm**

Formally the algorithm can be described as below [16]:

- Define the solution space

In this step the parameters to be optimized by PSO are defined. Each parameter is provided with a range for searching the optimal solution. So the minimum and maximum value for each dimension is specified to define the solution space of the problem.

- Define a fitness function

Fitness function relates the physical problem to the optimization algorithm. It takes the value of all  $N$  parameters that represents a possible solution of the problem and measures the goodness of that particular solution. It should be carefully selected to return a single number. The fitness function should exhibit a functional dependence with each parameters being optimized.

- Random initialization of swarm positions and velocities

Let the initial position and velocity of each particle in the swarm (a population of particles) are  $X_i = (x_{i1}, x_{i2}, \dots, x_{iN})$ , and  $V_i = (v_{i1}, v_{i2}, \dots, v_{iN})$  (where  $N$  is the number of design parameters of the optimization problem), respectively. In the first run, the initial positions of the each particle is designated as the best position encountered by the each individual and is represented as  $P_i = (p_{i1}, p_{i2}, \dots, p_{iN})$ . The global best position of all particles is selected from these initial positions by evaluating the fitness function at each solution space and is represented by  $P_g = (p_{g1}, p_{g2}, \dots, p_{gN})$ .

- Update the particle velocity

The velocity of each particle is updated according to the individual best position and the global best position of the swarm.

The velocity is updated in each time step using the relation:

$$v_{id}(t+1) = wv_{id}(t) + c_1r_1(p_{id} - x_{id}) + c_2r_2(p_{gd} - x_{id}) \quad (2.1)$$

Where  $c_1$ (cognitive constant) and  $c_2$ (social constant) are two positive constants,  $r_1$  and  $r_2$  are two random numbers with uniform distribution in the interval  $[0, 1]$ . The parameter  $w$  is the inertial

weight that correlates the particle's current velocity to its previous velocity. The convergence of PSO depends on the values of  $w$  in each iteration. The values of  $c_1$  and  $c_2$  are considered to be equal in most PSO literature to balance movement of particles in both cognitive and social components. Equation (2.1) describes the flying trajectory of a population of particle. This equation consists of three parts. The first part is the momentum part implying that the velocity can't be changed abruptly. The second part is the "cognitive" part which represents the learning from its own flying experience. The third part is the "social" part i.e. learning from flying experiences of the group. The velocity of each particle is restricted by the maximum velocity vector  $V_{\max}$  on each dimension.

- Update the position

In this step, the position of the each particle is updated and the particle moves to a new location. The velocity determined from eqn. (2.1) is applied for a given time step and the new position is obtained by:

$$x_{id} = x_{id} + \Delta t \times v_{id} \quad (2.2)$$

- Fitness function evaluation:

The updated positions of the particles are used to evaluate the fitness function  $f(X_i)$ .

This fitness value of each particle is compared with the previously obtained best fitness value of the corresponding particle.

If  $f(X_i) < f(P_i)$  then  $P_i = X_i$

Similarly the global best position ( $P_g$ ) is updated, if the best particle in the current swarm has lower  $f(X)$  than  $f(P_g)$ .

- Termination Criteria:

The velocities of the particles are updated in each time step and the particles change their locations towards its personal best and

global best positions. The process is continued till a specified number of iterations or a minimum error criterion is attained.

**Parameter Selection:**

In the above described algorithm, the selection of parameters is an important part for the iterative process to reach the optimal solution. Population size is a parameter which requires a careful selection. A larger population means a more thorough exploration of the solution space but require more computation time. It has been found that, in case of PSO, a relatively small population size can satisfactorily explore a solution space while avoiding excess fitness evaluations. Parametric studies show that a population size of about 30 is optimal for many engineering problems. Other parameter values such as  $w$ ,  $c_1$  and  $c_2$  are problem dependent. These parameters are selected by a trial and error approach [107]. The block diagram of the PSO algorithm is shown in Fig.2.1.



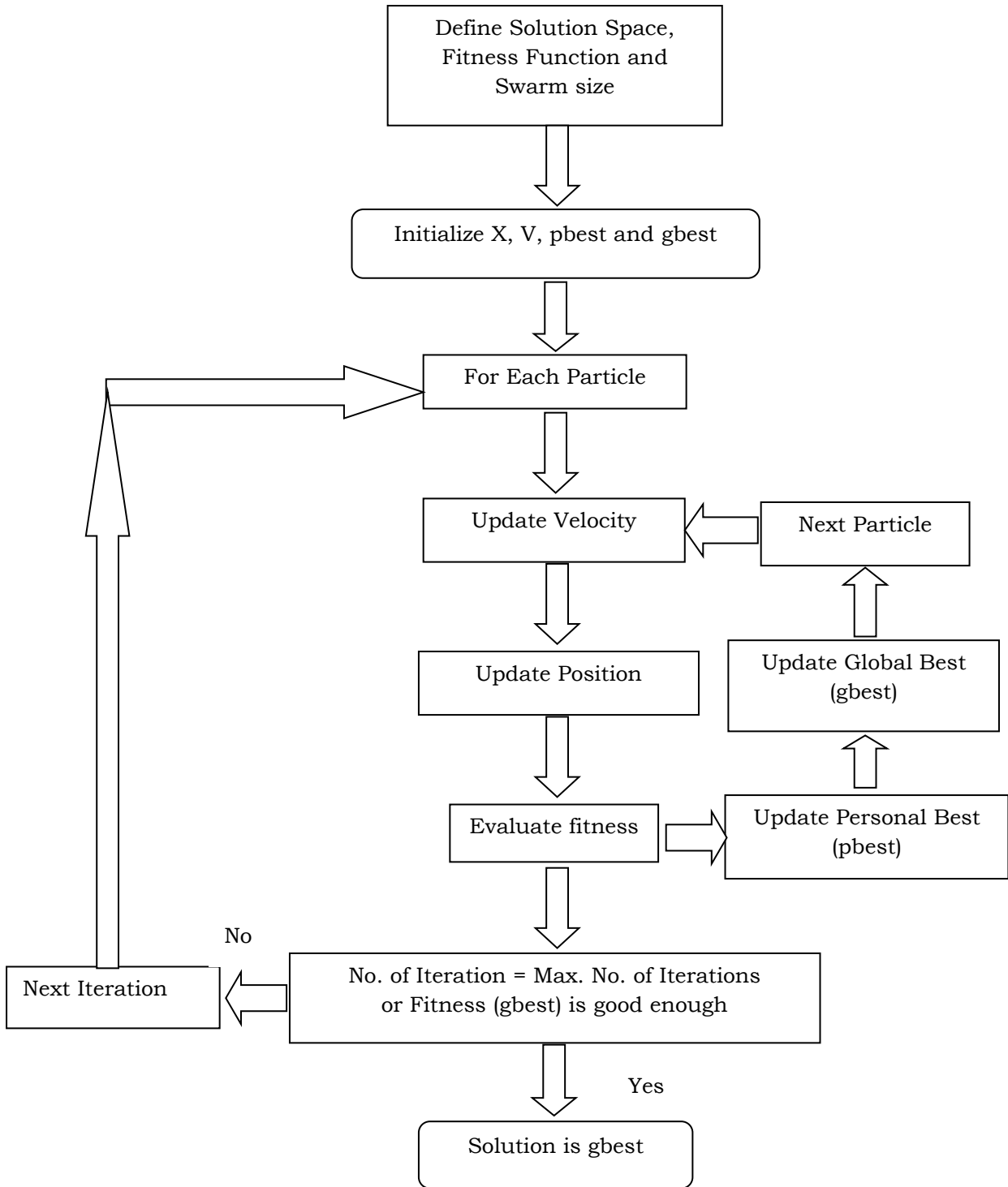


Figure 2.1: Flow chart for PSO

### 2.3.2 Bacteria Foraging Optimization

Foraging is the search for food resources by the animals to survive in the nature. At the same time the searching and capturing the food require both energy and time. So the *optimal foraging theory* is the strategy by which an animal can gain most benefits (net energy intake) for lowest cost (least possible time) during the process of foraging. The optimal foraging provides maximum fitness to the animals. The foraging theory is based on the assumption that, the animals search for and obtain food resources in such a manner, that maximizes the net energy intake (E) per unit time (T) spent for foraging [108]. The natural foraging strategy can be modeled as an optimization process where an animal aims to maximize its fitness by obtaining maximum food per unit time.

In 2002 Passino introduced an optimization technique which is inspired from the food-ingesting (foraging) behavior of *E-Coli* bacteria which are present in our intestines [98]. In this method, a group of bacteria move in search of rich nutrient concentration and away from noxious elements. The BFO proceeds by selecting or eliminating bacteria based on their foraging strategies. The natural selection tends to eliminate animals with poor foraging strategies and favor those having successful foraging strategies. After many generations, the poor foraging strategies are refined into the good ones. The foraging strategy is consists of four different steps [109]:

#### *Chemotaxis:*

The movement of *E-Coli* bacteria towards the nutrient-rich area is simulated by an activity called chemotaxis. This process is achieved by swimming and tumbling. In *swimming*, bacteria move in a predefined direction with fixed swim length. In *tumbling* the bacteria position themselves in some random direction in which swimming is performed. Hence the modes of operation that a bacterium performs in its entire lifetime are that of running (swimming for a period of time), tumbling or switching between running and tumbling. This behavior results in a random search for nutrients. However,

when the bacterium encounters an increasing nutrient gradient, it runs for longer duration till the gradient continues to increase.

Suppose  $\theta^i(j,k,l)$  represents the position of  $i^{\text{th}}$  bacterium at  $j^{\text{th}}$  chemotactic,  $k^{\text{th}}$  reproductive,  $l^{\text{th}}$  elimination-dispersal step. The process of chemotaxis can be represented as

$$\theta^i(j+1,k,l) = \theta^i(j,k,l) + C(i)\Phi(j) \quad (2.3)$$

where  $\Phi(j)$  is a random unit vector which is used to define the direction of movement after a tumble.  $C$  is termed as “run length unit”.  $C(i)$  is the size of the step in the direction specified by  $\Phi(j)$ . When the activity is run,  $\Phi(j)$  is same as  $\Phi(j-1)$ , otherwise  $\Phi$  is a random angle within a range  $[0, 2\pi]$ . If at  $\theta^i(j+1,k,l)$ , the cost function is lower than that at  $\theta^i(j,k,l)$ , another step size  $C(i)$  is taken in the same direction, otherwise it is allowed to tumble.

#### *Swarming:*

It is group behavior or cell-to-cell signaling exhibited by bacteria while moving towards rich nutrient area. It is always desired that the bacterium that has searched the optimum path of food should try to attract other bacteria. This helps them propagate collectively as concentric patterns of swarms with high bacterial density while moving up in the nutrient gradient. Mathematically swarming is modeled as

$$\begin{aligned} J_{cc}(\theta, P(j,k,l)) &= \sum_{i=1}^S J_{cc}^i(\theta, \theta^i(j,k,l)) \\ &= \sum_{i=1}^S \left[ -d_{attract} \exp\left(-w_{attract} \sum_{m=1}^p (\theta_m - \theta_m^i)^2\right) \right] \\ &+ \sum_{i=1}^S \left[ h_{repellant} \exp\left(-w_{repellant} \sum_{m=1}^p (\theta_m - \theta_m^i)^2\right) \right] \end{aligned} \quad (2.4)$$

$J_{cc}(\theta, P(j,k,l))$  is the objective function value to be added to the actual cost function to make a time varying objective function.  $\theta = [\theta_1, \theta_2, \dots, \theta_p]^T$  is point in a  $p$ -dimensional search space.  $S$  and  $p$  indicate the total number of bacteria and total number of design parameters to be optimized respectively.  $d_{attract}$ ,  $w_{attract}$ ,  $h_{repellant}$  and  $w_{repellant}$  are different coefficients and should be chosen carefully.

### *Reproduction:*

After the completion of all chemotaxis steps, a reproduction step takes place. The fitness values of the bacteria are sorted in ascending order. The least healthy bacteria constituting half of the bacterial population are eliminated. Each of the remaining healthy bacteria split into two identical ones, with the result that the population size remains unchanged.

### *Elimination and Dispersal:*

In this event, bacteria in a region are eliminated or a group is dispersed into a random location due to the local environmental effect. This event changes the life of the bacteria either gradually by consumption of nutrients or suddenly due to some other effect. This event possibly destroys chemotactic progress but also assists it, since dispersal may place bacteria near good food source. Elimination and dispersal helps in reducing stagnation, i.e., being trapped in a premature solution point or local optima.

## **2.3.2.1 BFO Algorithm**

The classical BFO algorithm is as described below:

### *Initialization:*

1. Initialize parameters  $D_{im}$ ,  $S$ ,  $N_c$ ,  $N_s$ ,  $N_{re}$ ,  $P_{ed}$ ,  $N_{ed}$ ,  $C(i)$  with  $(i = 1, 2, \dots, S)$ ,  $\theta_i$  where,

$D_{im}$ : Dimension of the search space

$S$ : Number of bacteria in the population

$N_c$ : Number of chemotactic steps

$N_{re}$ : Number of reproduction steps

$N_s$ : Length of swimming

$N_{ed}$ : Number of elimination-dispersal events

$P_{ed}$ : Probability of elimination-dispersal events

$C(i)$ : Size of the step taken in the random direction specified by the tumble

$\theta^i(j,k,l)$ : Position vector of the  $i^{\text{th}}$  bacterium, in  $j^{\text{th}}$  chemotactic step,  $k^{\text{th}}$  reproduction step and  $l^{\text{th}}$  elimination-dispersal event.

*Iterative process:*

2. Elimination-dispersal loop:  $l=l+1$

3. Reproduction loop:  $k=k+1$

4. Chemotaxis loop:  $j=j+1$

(a) For  $i = 1, 2, \dots, S$ , take a chemotactic step for bacterium  $i$  as follows:

(b) Compute fitness function  $J(i, j, k, l)$ , and then let,

$$J(i, j, k, l) = J(i, j, k, l) + J_{cc}(\theta^i(j, k, l), P(j, k, l))$$

$P(j, k, l)$  (i.e. add on the cell to cell attractant effect to the nutrient concentration) is the location of the bacterium corresponding to the global minimum cost function out of all the generations and chemotactic loops until that point.

(c) Let  $J_{last} = J(i, j, k, l)$  to save this value since we may find a better cost via run.

(d) Tumble: Generate a random unit vector  $\Phi(i)$  with each element  $m(i)$ ,  $m = 1, 2, \dots, D_{im}$ , a random number on  $[-1, 1]$ .

(e) Move: Following the eqn.  $\theta^i(j+1, k, l) = \theta^i(j, k, l) + C(i)\Phi(i)$

(f) Compute  $J(i, j+1, k, l)$  as

$$J(i, j+1, k, l) = J(i, j+1, k, l) + J_{cc}(\theta^i(j, k, l), P(j+1, k, l))$$

(g) Swim: Consider only the  $i^{\text{th}}$  bacterium is swimming while the others are not moving, then,

i. Let  $m = 0$  (counter for swim length)

ii. While  $m < N_s$

- Let  $m = m + 1$
  - If  $J(i, j + 1, k, l) < J_{last}$  (if doing better) then,
  - $J_{last} = J(i, j + 1, k, l)$   
and  $\theta^{i(j+1,k,l)} = \theta^{i(j+1,k,l)} + C(i)\Phi(i)$   
and use this  $\theta^{i(j+1,k,l)}$  to compute new  $J(i, j + 1, k, l)$
  - Else, if  $m = N_s$ , then end while loop.
- (h) If  $i \neq S$ , then  $i = i + 1$  and go to (b) to process  $(i + 1)$  bacterium.
5. If  $j < N_c$  go to step 4 (i.e., continue chemotaxis as the life of the bacteria is not over)
  6. Reproduction: Sort bacteria in ascending order of their fitness values ( $J$ ). Now, let  $S_r = S/2$ . The  $S_r$  bacteria with highest cost function (or fitness) values ( $J$ ) die and the other half of bacteria population with the best values split and the copies that are made are placed at the same location as their parent.
  7. If  $k < N_{re}$ , go to step 3. This implies that we have not reached the specified number of reproduction steps. So we start the next generation of the chemotaxis loop.
  8. Elimination-dispersal: For  $i = 1, 2, \dots, S$ , eliminate and disperse each bacterium with probability  $P_{ed}$ . (If any bacterium is eliminated, then disperse other bacterium to random location in optimization domain in order to keep the number of bacteria in population constant.) If  $k < N_{ed}$  then, go to step 2; otherwise end.

The detailed flow of the BFO algorithm is shown in Fig. 2.2.

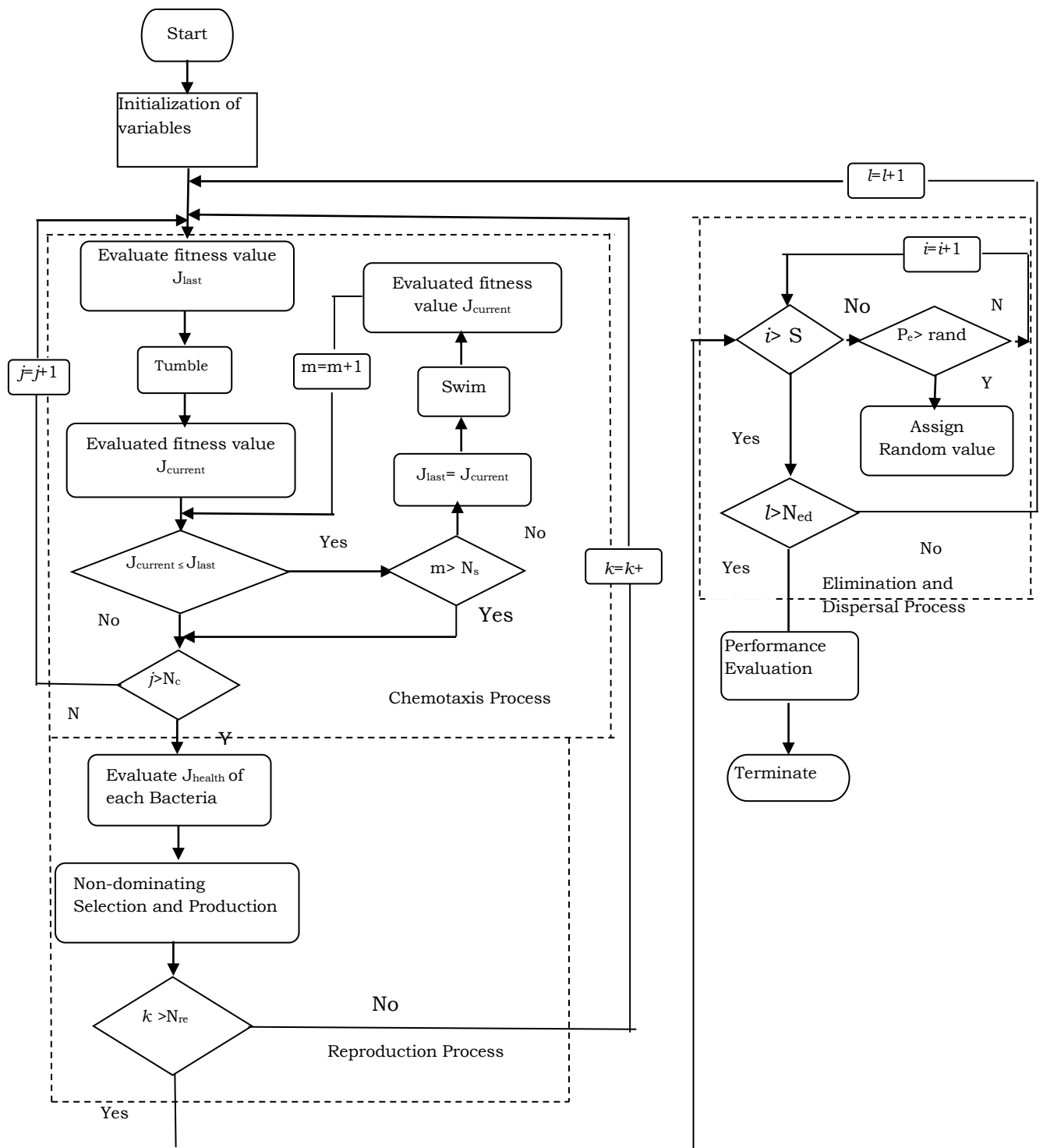


Figure 2.2: Flow chart BFO





# **Recovery of Sidelobe Level (SLL) in Failed Antenna Array**

---

## **3.1 Introduction**

The demand for large aperture antennas exhibiting increased capabilities and reduced cost and complexity is growing day by day. Because of large size of these arrays, possibility of failure of one or more elements is always there due to the degradation of performance of the associated circuitries, such as, transmit/receive modules and power supplies as they have finite life time. The failure in array elements may also be due to some unforeseen reasons like vagaries of weather or natural calamities. The effect of such failures usually manifests itself in terms of a degradation in the antenna pattern resulting in sharp variations in the field intensity, increased sidelobe levels (SLL), and decrease in the gain and directivity of the antenna. Thus, the entire system performance gets affected due to element failure. The replacement of the defective element is not possible on every occasion and it is a tremendous challenge for the engineers to establish an uninterrupted communication by restoring the main beam in the direction of interest and also reducing the sidelobe level to maximize the signal to noise ratio. Since in an active antenna array it is possible to control the excitations of the array elements remotely [6], the restoration of the beam pattern, close to the original pattern, can be achieved by reconfiguring the excitations of the remaining functional elements. This provides a cost effective alternative to hardware replacement, thereby increasing the array life.

In view of increased demand of antenna arrays in radar and communication systems, the development of healing systems for failed arrays has received considerable attention in recent years. A number of methods have been investigated to improve the radiation pattern of the array in the presence of

the failed elements by re-optimizing the excitations applied to the remaining elements. The synthesis of failed antenna array can employ amplitude-only, phase-only, or amplitude-phase approach to improve the damaged radiation pattern. Out of the three methods, phase-only approach has a very less effect on the SLL of the pattern. So the problem of SLL suppression due to element failure can be efficiently handled by the amplitude-only or amplitude-phase approach. The amplitude-phase approach provides a greater degree of freedom for the solution space in the process of optimization, but the computational complexity is more in that case.

However, presence of faulty elements makes the array unsymmetrical, thereby making it difficult to handle the problem analytically. Considerable research efforts have been directed worldwide on investigating methods to improve the patterns of the array in the presence of the failed elements and several research papers have been reported [66-77]. Some of these approaches are based on classical optimization techniques [66-70]. In addition to that, various bio-inspired optimization techniques have also been used for this purpose, because of the inherent advantages offered by these methods [71-77].

In this chapter, the issue of array failure compensation is treated as an optimization problem and solved by using PSO [97] and BFO [98] based on amplitude-only and amplitude-phase approach. The result obtained by PSO is validated by implementing the same formulation with the new evolutionary technique i.e. BFO [98]. The purpose is to study the performances of both the optimization methods in terms of recovered sidelobe level, directivity and computation time. BFO is relatively new to microwave community and its performance in dealing with faulty antennas has to be verified in order to choose a fast and efficient method for developing possible array compensation techniques.

### 3.2 Problem Formulation

The array factor of a linear array comprising  $N$  equally spaced elements, as shown in Figure 3.1, having non-uniform amplitude and progressive phase excitation is given by [37]

$$AF(\theta) = \sum_{n=1}^N w_n e^{j(n-1)(kd \cos \theta + \beta)} \quad (3.1)$$

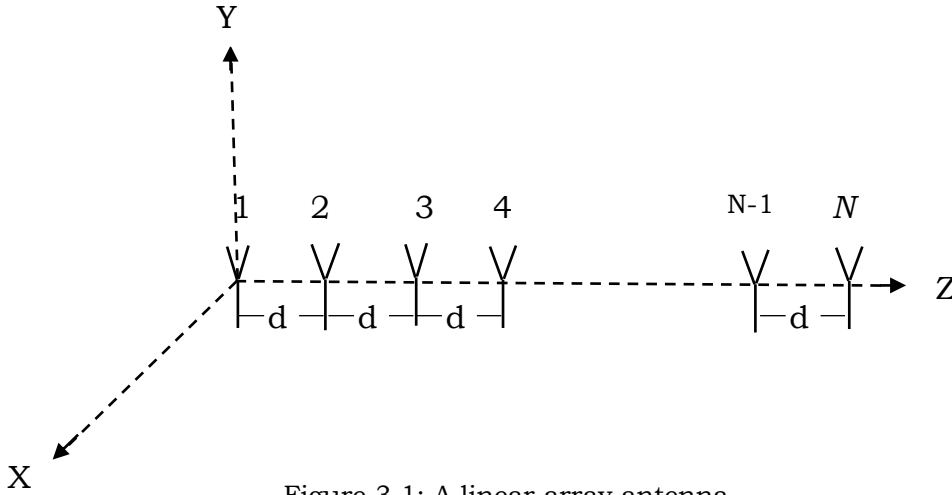


Figure 3.1: A linear array antenna

where  $w_n$  denotes the complex weight of each element,  $d$  is the spacing between the elements,  $\beta$  is the progressive phase shift and  $\theta$  is the angle measured from broadside.

Element failure in an antenna array causes sharp variations in the field intensity, increasing both sidelobe and ripple levels of power pattern. Assuming no radiation from the failed elements, the optimization techniques are applied to recover the SLL close to the desired level, by reconfiguring the amplitude and phase of the current, exciting each of the working elements. It minimizes a cost function, and returns the optimum current excitations for working elements that will lead to the desired radiation pattern with suppressed SLL. The following cost function was used for the optimization process:

$$C = \sum_{i=1}^{N_f} \left[ |AF(\theta_i)| - \text{DesiredSLL}(\theta_i) \right]^2 \quad (3.2)$$

where  $DesiredSLL$  is an upper limit on the array factor in the region  $|\theta| > BWFN$  (beamwidth between first nulls). The main lobe region is defined as the region  $|\theta| \leq BWFN$ . In this region the pattern is valued as 0 dB. The  $AF(\theta)$  is computed using the optimizer at the samples of  $\theta_i$  of size  $N_I$  that exceed the  $DesiredSLL$ . This compensation method is tested for Chebyshev and the Taylor arrays. The aim is to transform the excitations of the all the working elements to new values in a failed array, so that the sidelobe level remains within an acceptable limit. The upper limit of the sidelobe level of the both Chebyshev and Taylor pattern is depicted in Figure 3.2.

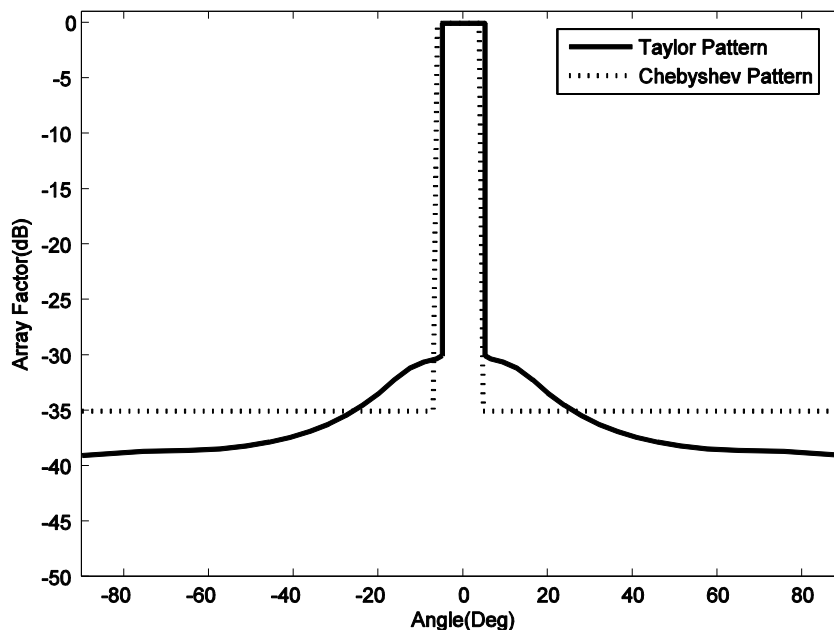


Figure 3.2: Desired SLL considered for Chebyshev and Taylor Pattern

### 3.3 Test Antenna Array

In this thesis, a 32 isotropic element linear broadside array with  $\lambda/2$  inter-element spacing was taken as the test antenna. In this work the mutual coupling between the elements was not taken into consideration. Two typical arrays, i.e., Chebyshev and Taylor array was considered to implement the developed procedure of array failure compensation. Although results for these two arrays are presented throughout the thesis, through extensive simulations for other array types it has been found that the results obtained are quite general in nature. Standard analytical method was applied to

obtain the amplitude excitations for the Chebyshev array having SLL of -35 dB [39]. Similarly the Taylor distribution was applied for determining the amplitude excitations of the elements to have a pattern with peak sidelobe power of -30dB near the main lobe and four numbers of constant sidelobes [40]. Figure 3.3 shows the radiation patterns of both Chebyshev and Taylor array. Table 3.1 shows the pattern parameters such as SLL, HPBW and BWFN of the test antenna array. The normalized amplitude excitations of the test array under consideration are given in Table 3.2.

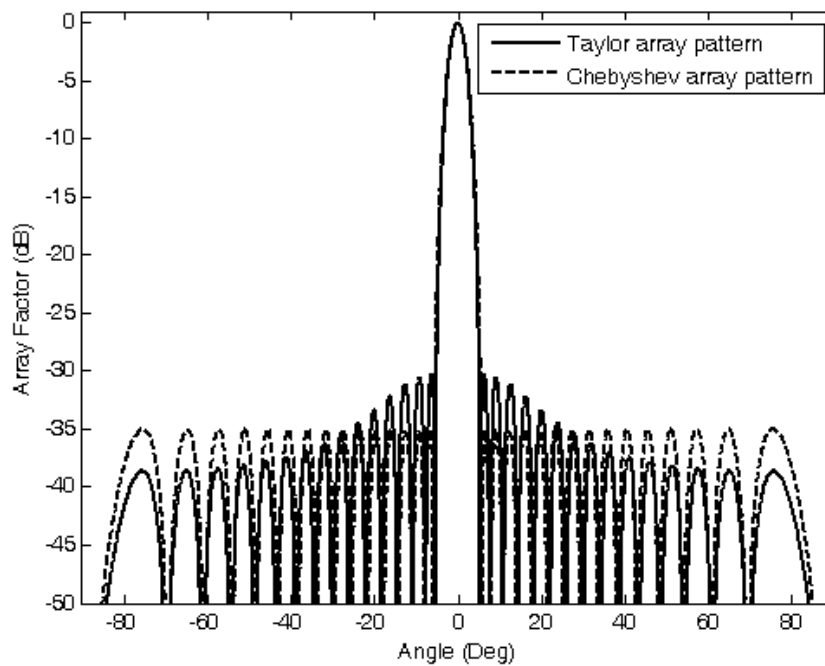


Figure 3.3: Array factor of 32-element linear Chebyshev and Taylor array

Table 3.1 Parameters of the test array

Test Array	Max <sup>m</sup> Sidelobe Level(SLL)	HPBW	BWFN
Chebyshev array	-35.0 dB	4.16°	11.6°
Taylor array	-30.0 dB	4.02°	10.8°

Table 3.2: Normalized amplitude excitations for two test arrays

Element Position	Chebyshev array	Taylor array
1	0.2503	0.2458
2	0.1774	0.2641
3	0.2341	0.2994
4	0.2976	0.3493
5	0.3669	0.4105
6	0.4406	0.4795
7	0.5170	0.5526
8	0.5943	0.6266
9	0.6703	0.6988
10	0.7431	0.7667
11	0.8103	0.8286
12	0.8700	0.8830
13	0.9202	0.9283
14	0.9594	0.9636
15	0.9863	0.9877
16	1.0000	1.0000
17	1.0000	1.0000
18	0.9863	0.9877
19	0.9594	0.9636
20	0.9202	0.9283
21	0.8700	0.8830
22	0.8103	0.8286
23	0.7431	0.7667
24	0.6703	0.6988
25	0.5943	0.6266
26	0.5170	0.5526
27	0.4406	0.4795
28	0.3669	0.4105
29	0.2976	0.3493
30	0.2341	0.2994
31	0.1774	0.2641
32	0.2503	0.2458

### 3.4 SLL Recovery Using PSO

The element failure in the array cause the unacceptable pattern distortion and mostly in the form of increased SLL. In this section the pattern recovery method was applied on the test array. So the faults in test antenna array was considered as complete (fully non-functional) and implemented by making the current excitation to the element as zero. PSO was applied to reconfigure only the amplitude excitations or both amplitude and phase excitations of the remaining functional elements in the failed array. Initially the performance of PSO was tested on both Chebyshev and Taylor arrays with failed elements at different positions.

PSO was applied with 30 initial particles and each particle performed the search in different dimensions, equal to the number of current excitations to be optimized. In order to obtain the optimum excitation values of each functional element, PSO minimizes the objective function defined in equation (3.2). The value of the objective/cost function was observed in each iteration and with increase in the number of iterations, this value decreases. The values of different parameters of PSO discussed in chapter 2, are mostly chosen based on trial and error approach and the best choics for the present problem are given in Table 3.3. PSO iteratively evaluates the excitations of all the working elements in the array. The completion of PSO iterations is based on the chosen error tolerance criteria. In order to get a better accuracy, the simulation was run for 30 times and the mean values of the element excitations were obtained.

Table 3.3: PSO Parameters

<b>Parameters</b>	<b>Value</b>
Number of Particles	30
Inertial weight ( $w$ )	linearly damped with iterations from 0.9 to 0.4
Cognitive parameter ( $c_1$ )	2
Social parameter ( $c_2$ )	2
Random function ( $rand()$ )	Range [0,1]

### 3.4.1 Analysis for Amplitude-only Control

In the amplitude-only approach, the amplitudes of currents exciting the working elements are calculated to restore the radiation performance of the failed array whereas the phase of excitation remains unchanged. As the probability of failure of large number of elements in an array is very less, simulations were carried out for failure of 2 to 4 elements.

#### ***Case-I: Two element failure compensation***

When the array suffered a failure in 2<sup>nd</sup> and 5<sup>th</sup> elements of the test array, the SLL power of distorted the Chebyshev pattern increased from -35dB to -27.15dB and the half-power beamwidth (HPBW) of the main lobe increased from 4.16° to 4.3°. The beamwidth between first nulls (BWFN) also increased from 11.6° to 12.2°. Here the goal was to restore the peak sidelobe level of the failed array near to its original value by re-optimizing the amplitude-only excitations of the remaining working elements. The optimizer was applied to evaluate the optimized amplitude weights  $\mathbf{a}_o = [a_{o1} \ a_f \ a_{o3} \ a_{o4} \ a_f \ a_{o6} \dots \ a_{o32}]$  for compensating the failed element weights ( $a_f$ ) by minimizing the cost function and the recovered patterns in this case exhibit a SLL of -35.26dB, HPBW of 4.68° and BWFN of 13.2°. The results for the correction of two element failure in the 32 element linear array are shown in Figure 3.4 which reveal that the recovered pattern is similar to the original Chebyshev pattern. Figure 3.5 shows the variation in the amplitude excitations to produce the corrected pattern.

This correction procedure was also applied to another test array (32-element linear Taylor array) to cross validate the methodology. Again, the element failure at position 2 and 5 was considered for this simulation. When the elements failed in the array, the peak SLL power of distorted pattern increased to -27.75dB and the HPBW of the pattern increased from 4.02° to 4.18°. The BWFN of the pattern became wider from 10.8° to 11.4°. The procedure of applying PSO was the same as was done for Chebyshev array. The optimizer recovered the pattern close to the original, having maximum SLL of -30.12 dB and HPBW 4.7°. The pattern obtained by the PSO



optimizer is shown in Figure 3.6 and it is similar to the reference Taylor pattern. The optimized amplitude distributions of non-defective elements are shown in Figure 3.7.

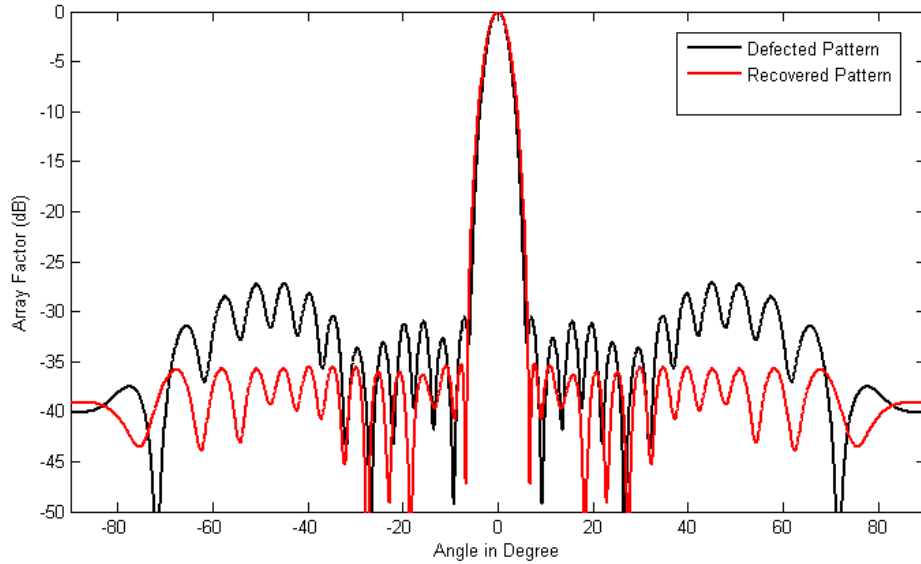


Figure 3.4: Recovered power pattern by PSO in a two element failed Chebyshev antenna array

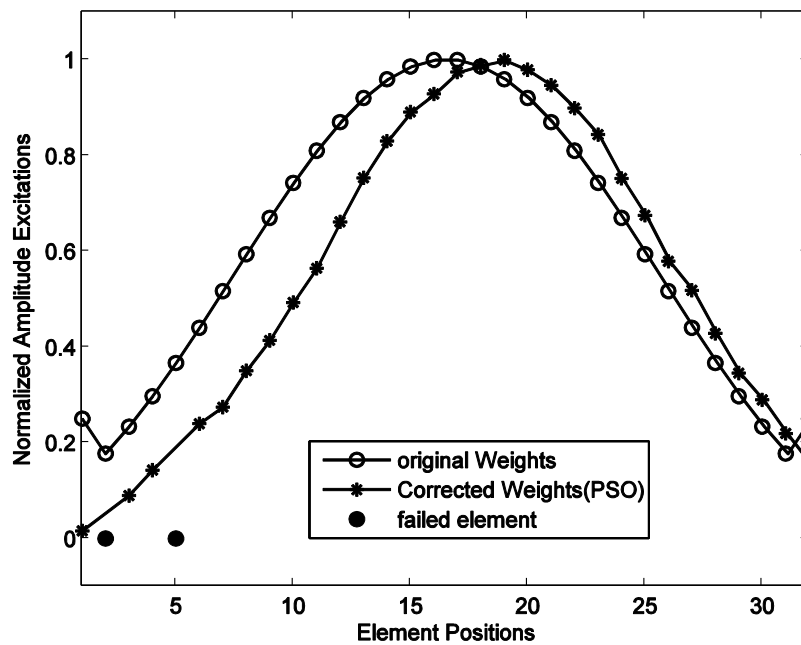


Figure 3.5: Amplitude distribution of recovered pattern by PSO versus original Chebyshev array (Two element failure)

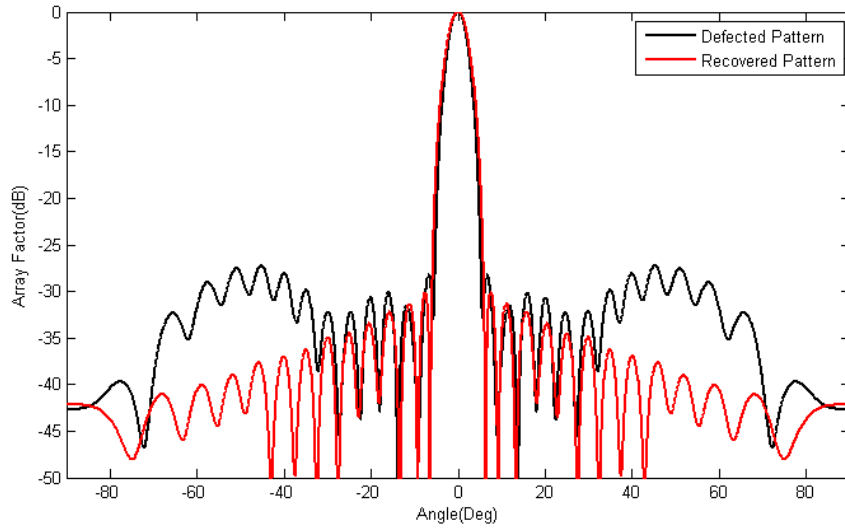


Figure 3.6 Recovered power pattern by PSO in a two element failed Taylor antenna array

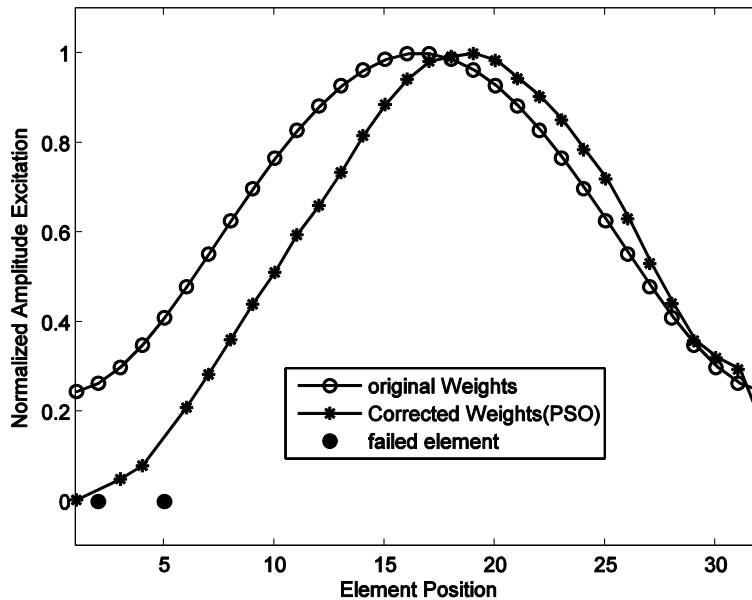


Figure 3.7 Amplitude distribution of recovered pattern by PSO versus original Taylor array (Two element failure)

After successfully recovering the radiation pattern for two element failure in the above mentioned test antenna array, PSO was further implemented on another uniformly spaced array having inter element spacing of  $0.75 \lambda$ . It was found that for the same two element failure PSO was also able to recover the damaged pattern successfully. The performance of PSO in handling this case is shown in Figure 3.8.

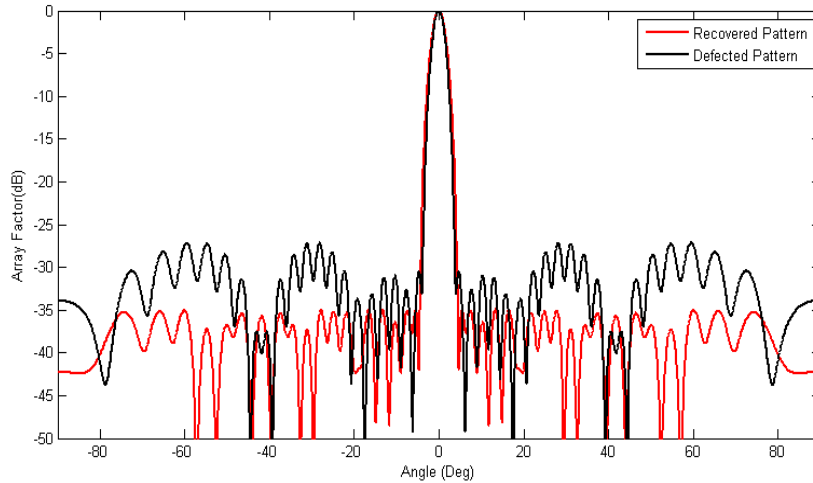


Figure 3.8: Recovered power pattern by PSO in a two element failed Chebyshev antenna array with inter element spacing of  $0.75 \lambda$ .

### ***Case-II: Three element failure compensation***

The same 32-element linear Chebyshev array was considered to study the performance of the compensation process in case of three element failure located at 2<sup>nd</sup>, 5<sup>th</sup> and 6<sup>th</sup> positions. The damaged array pattern due to the element failure has the SLL of -26.27dB. The HPBW and BWFN of the pattern became  $4.39^\circ$  and  $12.6^\circ$  respectively. The PSO applied for the pattern recovery produced a radiation pattern having SLL of -35.2dB, HPBW of  $5.1^\circ$  and BWFN of  $14.4^\circ$ . The performance of PSO in dealing with this problem is shown in Figure 3.9. The variations in the amplitude excitations of the functional elements are shown in Figure 3.10.

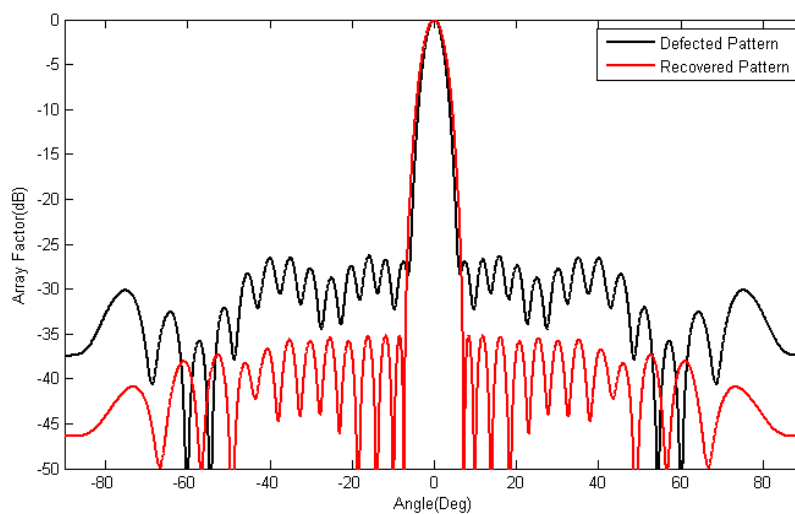


Figure 3.9: Recovered power pattern by PSO in a three element failed Chebyshev antenna

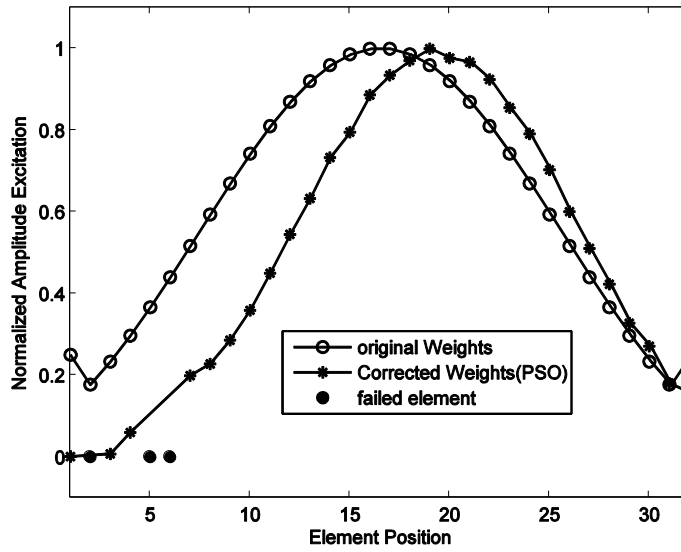


Figure 3.10: Amplitude distribution of recovered pattern by PSO versus original Chebyshev array (Three element failure)

### ***Case-III: Four element failure compensation***

Two different cases of four element failure were studied for the same Chebyshev array. In one case the faulty elements were located at 3<sup>rd</sup>, 4<sup>th</sup>, 5<sup>th</sup> and 6<sup>th</sup> positions, i.e. on one side of the centre of the array and in another case, the faulty elements were located on both sides of the centre of the array i.e. at 5<sup>th</sup>, 6<sup>th</sup>, 29<sup>th</sup> and 30<sup>th</sup> positions. The failure of elements on one side of the array made the radiation pattern with SLL, HPBW and BWFN of -23.45dB, 4.5° and 12.6°, respectively. Similarly the damaged patterns due to the element failure on both side of the centre of the array have the SLL of -22.53dB, the HPBW and BWFN of 4.47° and 13.6°, respectively. The new set of amplitude excitations obtained by the optimizer, produce a recovered radiation pattern having the SLL of -35.02 dB, HPBW of 5.23° and BWFN of 14.8° in case of the element failure in one side of the array centre. In the second case, the corrected radiation pattern has the SLL, HPBW and the BWFN of value -35.02 dB, 6.14° and 17.2°, respectively. The recovered patterns by the optimizer in both cases of four element failure are shown in the Figure 3.11 and Figure 3.12, respectively. The distribution of amplitude excitations in case of four element failure are shown in Figure 3.13 and Figure 3.14, respectively.

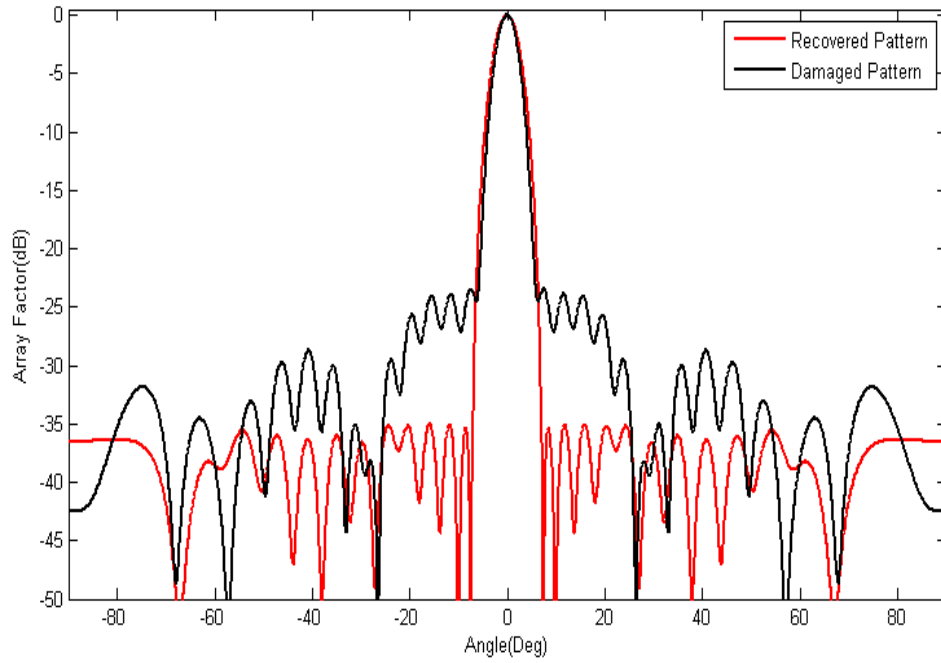


Figure 3.11: Plot of corrected pattern by PSO in a four element failed (at 3<sup>rd</sup>, 4<sup>th</sup>, 5<sup>th</sup> and 6<sup>th</sup> positions) Chebyshev array

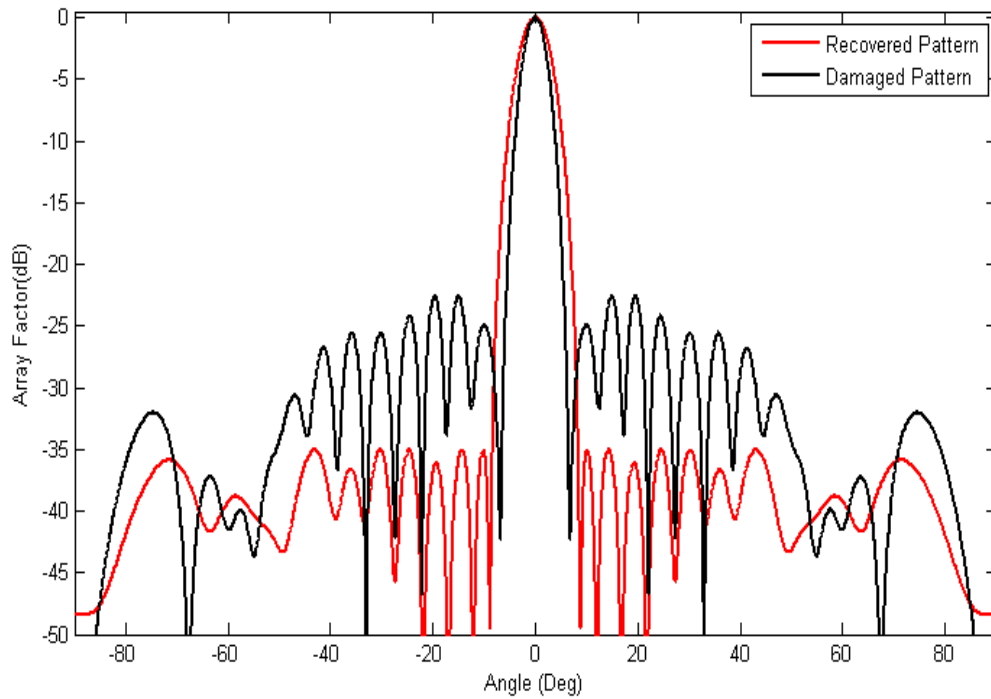


Figure 3.12: Plot of corrected pattern by PSO in a four element failed (at 5<sup>th</sup>, 6<sup>th</sup>, 29<sup>th</sup> and 30<sup>th</sup> positions) Chebyshev array

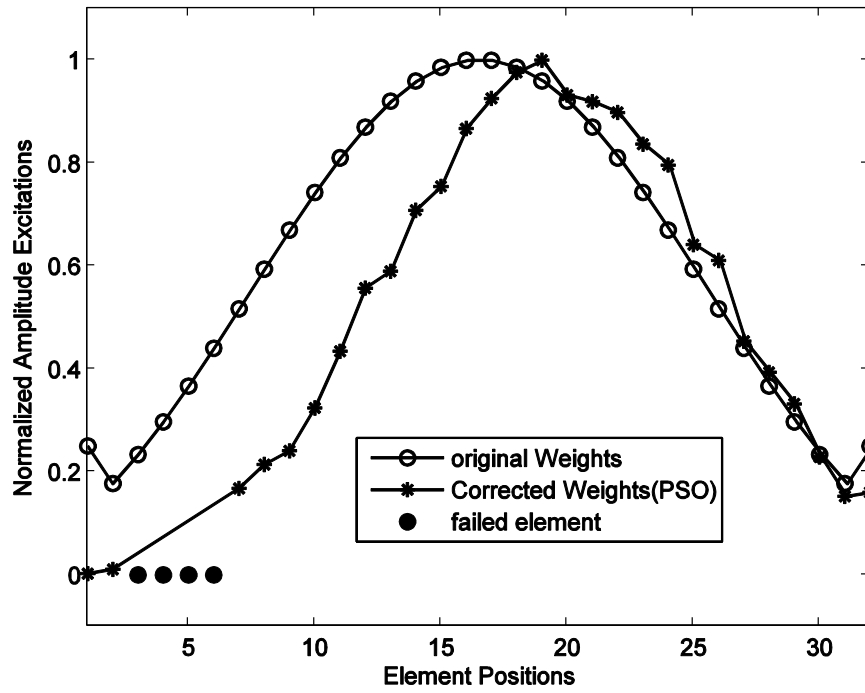


Figure 3.13: Amplitude distribution of recovered pattern by PSO versus original Chebyshev array (Four elements failure located at 3<sup>rd</sup>, 4<sup>th</sup>, 5<sup>th</sup> and 6<sup>th</sup> positions)

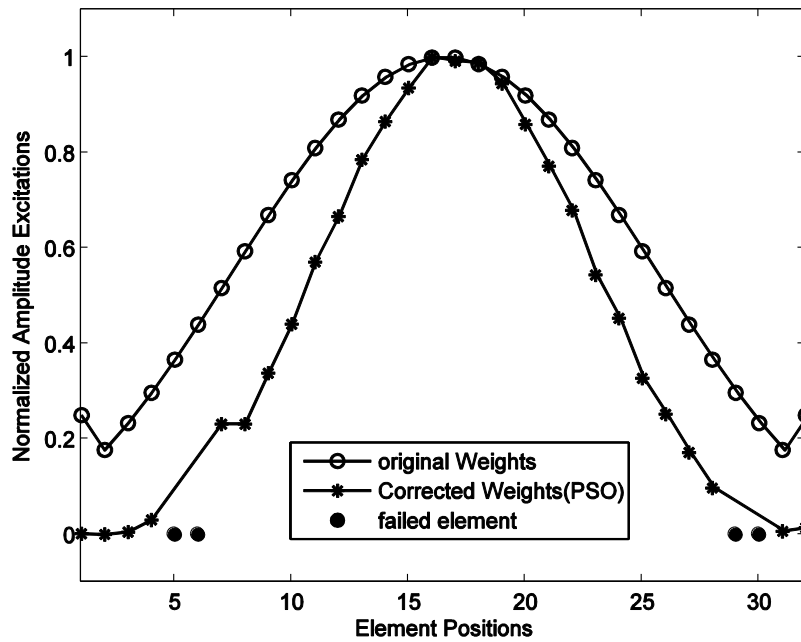


Figure 3.14: Amplitude distribution of recovered pattern by PSO versus original Chebyshev array (Four elements failure located at 5<sup>th</sup>, 6<sup>th</sup>, 29<sup>th</sup> and 30<sup>th</sup> positions)

### 3.4.1.1 Observations

In the course of optimization using PSO to improve the radiation performance in a failed array, the excitation amplitude of the elements was considered as the optimizing variables. The optimized amplitude values obtained from PSO give the corrected array pattern. This method of compensation was tested on arrays having different radiation pattern and faulty elements at different locations. All the simulations were performed on a 2.33 GHz workstation platform with 4GB RAM.

Table 3.4 shows the parameters of the recovered radiation pattern in amplitude-only compensation for all the different cases of element failure considered in section 3.4. It is observed from the results that the recovered Chebyshev array pattern have maximum SLL close to the original one and also maintains a good parity with the original pattern. However, recovery of SLL affects the directivity of the array. The value of HPBW and BWFN of the recovered pattern is increased by 12.5% and 13.8%, respectively compared to the original array value in case of two element failure. When the number of faulty element increases to three, the SLL of the damaged pattern increased to a higher level, compared to the case of two element failure. The improvement in the SLL is achieved at the cost of an increased beamwidth. In this case, the HPBW of recovered pattern increases by 22.5% compared to the original array and increase in the BWFN is of the order of 24%.

Next, we tried to compensate for the four element failure in the array by considering two different cases of fault locations. It was observed that, when the failed elements were located on both sides of the array centre, recovery of pattern is slightly difficult compared to the case when faulty elements are located on one side the centre. In both the cases of four element failure, the recovered patterns have SLL of -35.02dB. To achieve this value of SLL we have to pay the price in terms of the beamwidth and this trade-off between beamwidth and peak sidelobe power not only depends on the number of failed elements but also on the positions of the failure. The BWFN and HPBW of the recovered pattern increased by 27% and 25% of the original value when all the four failed elements were located on one side (3<sup>rd</sup>, 4<sup>th</sup>, 5<sup>th</sup>

and 6<sup>th</sup>) of the array center, whereas this increase was 46% and 45% for BWFN and HPBW respectively, when the failed elements were located at 5<sup>th</sup>, 6<sup>th</sup>, 29<sup>th</sup> and 30<sup>th</sup> position, i.e. when the failure of elements occurred on both sides of the array centre.

In order to have an idea about the average computation time, a stopping criteria was set for the optimizer. The optimization process was stopped when the cost function attained a zero value. The error plot of the cost function for different cases of element failure scenario is shown in Figure 3.15. It illustrates that the PSO converges faster when the number of faulty elements are less, and the convergence speed reduces as the number of faulty elements increases. The number of iterations required by PSO to reach at the desired cost function value is different for different numbers of element failure. Table 3.5 shows the time of computation in each case of the amplitude-only compensation described above. The numerical value of excitations for all the three cases of amplitude-only compensation described above is given in Table 3.6 for a Chebyshev array.

Table 3.4 Parameters obtained in amplitude-only compensation in a 32 element linear Chebyshev array

Fault Position	Number of Faults	Damaged Pattern			Recovered Pattern		
		SLL(dB)	HPBW	BWFN	SLL(dB)	HPBW	BWFN
2 <sup>nd</sup> ,5 <sup>th</sup>	2	-27.15	4.3°	12.2°	-35.26	4.68°	13.2°
2 <sup>nd</sup> ,5 <sup>th</sup> ,6 <sup>th</sup>	3	-26.27	4.39°	12.6°	-35.2	5.1°	14.4°
3 <sup>rd</sup> ,4 <sup>th</sup> ,5 <sup>th</sup> ,6 <sup>th</sup>	4	-23.45	4.5°	12.6°	-35.02	5.23°	14.8°
5 <sup>th</sup> ,6 <sup>th</sup> ,29 <sup>th</sup> ,30 <sup>th</sup>	4	-22.53	4.47°	13.6°	-35.02	6.14°	17.2°

Table-3.5: Computation time for PSO in dealing with element failure in Chebyshev antenna array

No of Failed elements	No. of Iteration for Convergence	Computation Time (Sec)
Two element failure (2,5)	826	81 Sec
Three element failure (2,5,6)	854	95 Sec
Four element failure(3,4,5,6)	890	101 Sec
Four element failure (5,6,29,30)	910	105 Sec



Table-3.6 Optimized amplitude excitations obtained by PSO for different number of element failure in the Chebyshev array

Element Position	Original Chebyshev Pattern	Two element failure (2,5)	Three element failure (2,5,6)	Four element failure	
				3,4,5,6,	5,6,29,30
1	0.2503	0.0160	0.0015	0.0025	0.0020
2	0.1774	0	<b>0</b>	0.0109	0.0001
3	0.2341	0.0899	0.0077	<b>0</b>	0.0052
4	0.2976	0.1429	0.0604	<b>0</b>	0.0308
5	0.3669	<b>0</b>	<b>0</b>	<b>0</b>	<b>0</b>
6	0.4406	0.2397	<b>0</b>	<b>0</b>	<b>0</b>
7	0.5170	0.2745	0.1993	0.1680	0.2318
8	0.5943	0.3503	0.2281	0.2145	0.2316
9	0.6703	0.4138	0.2862	0.2410	0.3385
10	0.7431	0.4928	0.3593	0.3243	0.4413
11	0.8103	0.5645	0.4501	0.4345	0.5714
12	0.8700	0.6616	0.5452	0.5573	0.6668
13	0.9202	0.7534	0.6331	0.5901	0.7860
14	0.9594	0.8301	0.7332	0.7083	0.8658
15	0.9863	0.8912	0.7956	0.7549	0.9363
16	1.0000	0.9289	0.8867	0.8671	1.0000
17	1.0000	0.9749	0.9350	0.9256	0.9922
18	0.9863	0.9892	0.9710	0.9764	0.9885
19	0.9594	1.0000	1.0000	1.0000	0.9451
20	0.9202	0.9794	0.9767	0.9324	0.8597
21	0.8700	0.9473	0.9668	0.9195	0.7722
22	0.8103	0.8994	0.9246	0.8986	0.6794
23	0.7431	0.8440	0.8554	0.8370	0.5444
24	0.6703	0.7523	0.7914	0.7965	0.4536
25	0.5943	0.6754	0.7033	0.6416	0.3277
26	0.5170	0.5793	0.6007	0.6111	0.2524
27	0.4406	0.5187	0.5111	0.4540	0.1721
28	0.3669	0.4289	0.4231	0.3935	0.0975
29	0.2976	0.3458	0.3279	0.3321	0
30	0.2341	0.2895	0.2714	0.2294	0
31	0.1774	0.2197	0.1804	0.1527	0.0069
32	0.2503	0.1566	0.1567	0.1602	0.0144

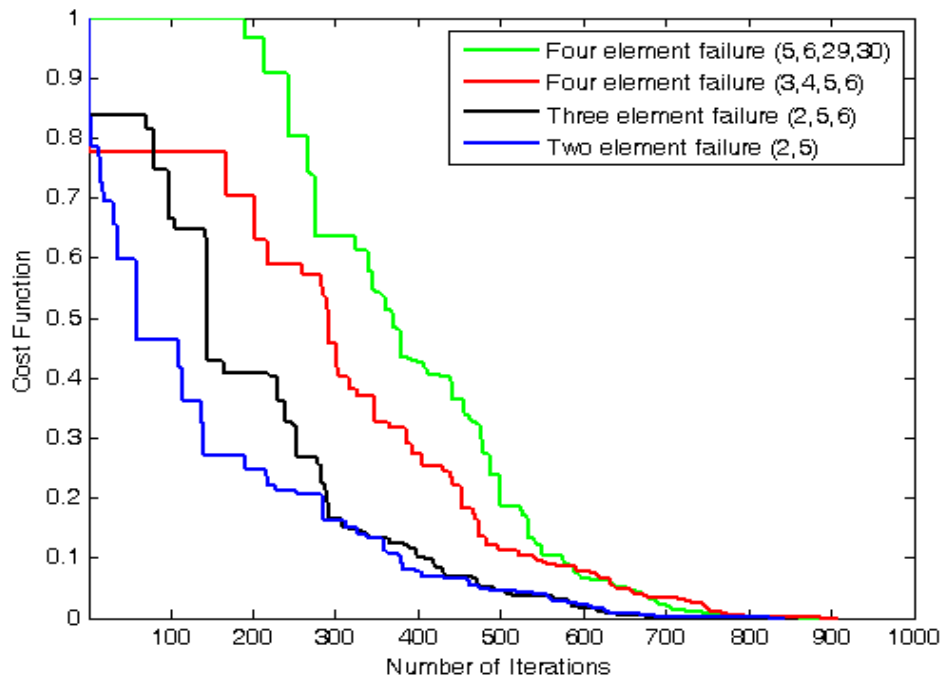


Figure 3.15: Error performance of PSO for different types of element failure in the Chebyshev array.

From Table 3.6, it can be observed that the number of iterations and computation time increases with the number of failed elements present in the array. With the increase in number of faulty elements, the complexity of the problem increases. In such case the time required will be more and also a price has to be paid in terms of reduced directivity while recovering the SLL.

While dealing with the case of Taylor array, PSO required more number of iterations for convergence compared to the iterations required for the Chebyshev array. It took an average of 1065 iterations to produce the corrected Taylor pattern when the failed elements were located at 2<sup>nd</sup> and 5<sup>th</sup> positions. The computation time required by PSO was 430 seconds. The recovered pattern has maximum sidelobe level close to the original one, whereas the BWFN and HPBW value obtained after correction are, respectively, 18% and 16.9% more than the original pattern. Table 3.7 shows the re-optimized amplitude excitations obtained for all the working elements for two element failure in Taylor array.

Table 3.7: Normalized amplitude excitations obtained from PSO optimizer to correct the radiation pattern of 32- element Taylor pattern array having two failed element

Element	Initial Taylor Excitations	Re-optimized excitations
1	0.2458	0.0039
2	0.2641	0
3	0.2994	0.0502
4	0.3493	0.0803
5	0.4105	0
6	0.4795	0.2099
7	0.5526	0.2840
8	0.6266	0.3615
9	0.6988	0.4404
10	0.7667	0.5116
11	0.8286	0.5956
12	0.8830	0.6609
13	0.9283	0.7348
14	0.9636	0.8168
15	0.9877	0.8862
16	1.0000	0.9429
17	1.0000	0.9825
18	0.9877	0.9930
19	0.9636	1.0000
20	0.9283	0.9847
21	0.8830	0.9443
22	0.8286	0.9038
23	0.7667	0.8518
24	0.6988	0.7854
25	0.6266	0.7203
26	0.5526	0.6314
27	0.4795	0.5317
28	0.4105	0.4420
29	0.3493	0.3590
30	0.2994	0.3207
31	0.2641	0.2953
32	0.2458	0.1712

### **3.4.2. Analysis for Amplitude-Phase Control**

The amplitude-phase approach for array failure correction employs complex weight synthesis to restore the damaged array pattern, i.e., both amplitude and phase of current exciting the functional elements were simultaneously optimized. As both the real and complex weights of the antenna elements take part in this method of compensation, it provides a greater degree of flexibility in correcting the damaged pattern. On the other hand, it increases the computational complexity. In order to present a comparative study of both amplitude-only and amplitude-phase approach for array failure compensation, we considered the same 32-element linear broadside Chebyshev array with faults located at same positions, that were taken in case of amplitude-only approach.

#### ***Case-I: Two element failure***

In this approach of array failure compensation, we have taken the same 32-element linear Chebyshev array having a constant SLL of -35 dB and faults at 2<sup>nd</sup> and 5<sup>th</sup> positions. The optimizer was applied to this problem to optimize the complex current excitations of the functional elements to restore the damaged radiation pattern. In this optimization process the particles search in 60 dimensions to obtain the optimum excitation values. The cost function for this optimization is also same as defined in equation (3.2). At the end of the iterative process a new set of optimized current excitations of the functional elements were obtained that are used to obtain recovered patterns. In this case the recovered pattern has a SLL of -35.16 dB, HPBW of 4.65° and BWFN of 13.5° and is shown in Figure 3.16.

#### ***Case-II: Three element failure:***

The procedure was extended to three element failure and the performance of PSO was investigated. The array elements at 2<sup>nd</sup>, 5<sup>th</sup> and 6<sup>th</sup> positions were considered to be faulty. The PSO optimizer was used to find the amplitude and phase of the functional elements. These re-optimized complex weights produce a pattern which has the value of SLL, HPBW and BWFN as -35.0 dB, 5.09° and 14.5°, respectively. The recovered radiation pattern which is

shown in Figure 3.17 has a close resemblance with the original Chebyshev pattern.

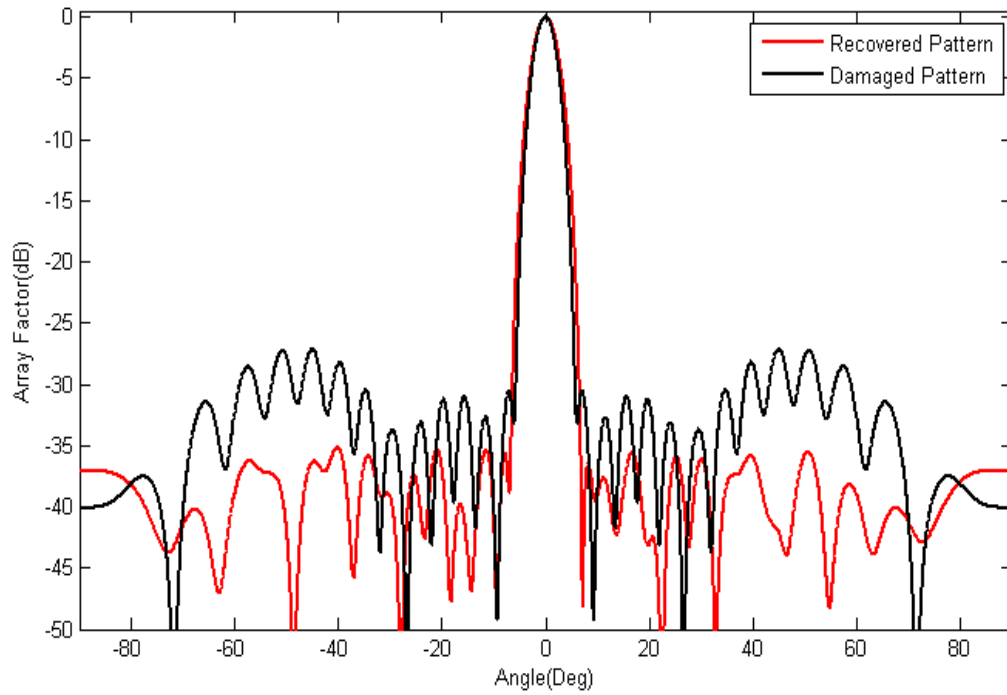


Figure 3.16: Plot of corrected pattern obtained by amplitude-phase compensation in a two element failed Chebyshev antenna array

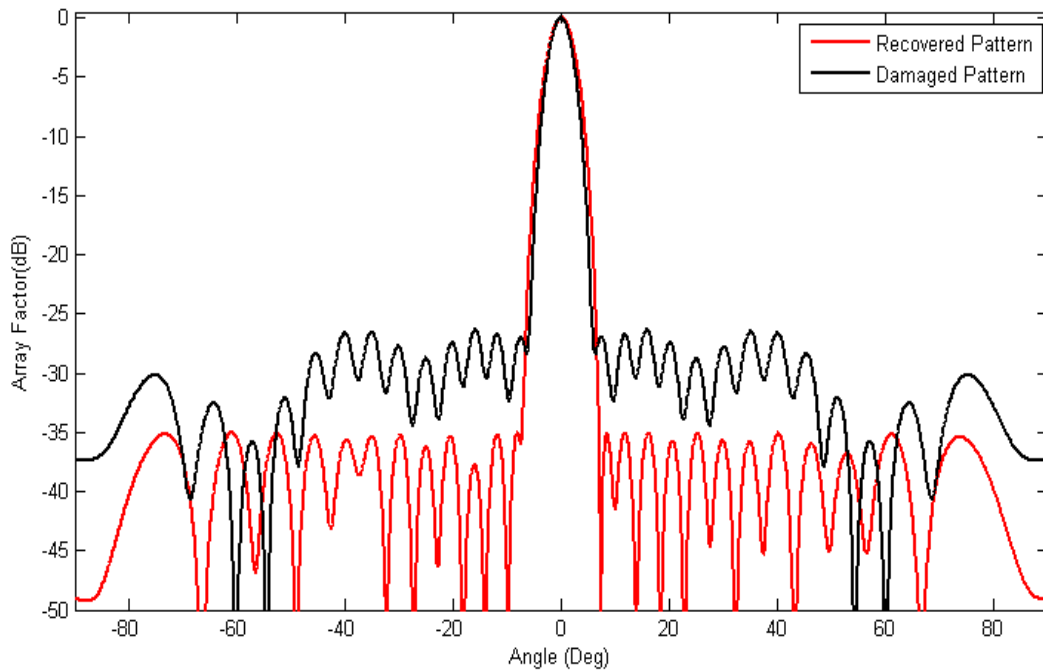


Figure: 3.17 Plot of corrected pattern obtained by amplitude-phase compensation in a three element failed Chebyshev antenna array

### 3.4.2.1 Observations

In this case, PSO improves the radiation performance in a failed array, by changing the excitation amplitude and phase of the working elements. The optimized amplitude-phase values obtained from the process of optimization give the corrected array pattern. This method of compensation was tested on arrays having faulty elements at different locations in the Chebyshev array. Table 3.8 shows the parameters of the compensated array, obtained from the amplitude-phase compensation method, when applied to the two and three element failures in the array. The results reveal that the recovered SLL, HPBW and BWFN of the pattern in both two element (2<sup>nd</sup>, 5<sup>th</sup>) and three element (2<sup>nd</sup>, 5<sup>th</sup> and 6<sup>th</sup>) failure cases are very much similar to the results obtained in the amplitude-only compensation approach. In amplitude-phase approach, both the amplitude and phase excitations were treated as the design variables for the optimizer. So the computational complexity and computation time for the optimizer was increased. Thus it can be concluded that since the amplitude-phase correction does not offer any advantage over the amplitude-only correction, the latter approach should be preferred owing to its simplicity and lower computational cost.

Table: 3.8: Parameters obtained by PSO in amplitude-phase compensation for Chebyshev array

No of Failed elements	Recovered Array Pattern Characteristics			No. of Iteration for Convergence	Computation Time (Sec)
	MAX <sup>m</sup> SLL (DB)	HPBW (DEG.)	BWFN (DEG.)		
Two element failure (2,5)	-35.16	4.65°	13.5°	860	485 Sec
Three element failure (2,5,6)	-35.0	5.09°	14.5°	873	540 Sec

### 3.5 SLL Recovery Using BFO

In order to have a comparative study of performance of evolutionary computational methods in dealing with failed array correction, BFO was also applied to the same test arrays and the results are presented in this section. The problem formulation was also kept same as used in case of PSO. As compared to PSO, the number of tuning parameters in BFO is more. The value of different parameters taken in this optimization process is shown in Table 3.9. BFO was tested on the test antenna array as described in section 3.3 with failure of elements at 2<sup>nd</sup> and 5<sup>th</sup> position. Since amplitude-phase compensation does not offer any significant advantage, the BFO implementation was implemented for amplitude-only compensation.

The compensated pattern for two element failure (2<sup>nd</sup> and 5<sup>th</sup>) in a Chebyshev array has a SLL of -35.12 dB, BWFN of 14° and HPBW of 4.88°. The parameters obtained for the recovered pattern has a SLL very close to the original one, but the beamwidth is increased. This increase is 17% in HPBW and 20% in BWFN of the pattern with respect to the original array. The corrected array pattern for two element failure is shown in Figure 3.18 and the figure reveals that the recovered pattern is similar to the original Chebyshev pattern. Figure 3.19 shows the variation in the amplitude excitations to produce the corrected pattern. For the sake of comparison, the result from PSO compensation is overlapped in the same figure. Since both PSO and BFO optimize the same cost function, their corresponding error performance plot in dealing with the element failure is shown in Figure 3.20.

In the next phase we applied BFO optimizer on the 32-element linear Taylor array with same fault locations as considered in case of PSO. BFO optimizer produced a corrected pattern having maximum SLL -30.01dB, BWFN 13° and HPBW 4.82°. The value of BWFN and HPBW increases by 20.3% and 19.9%, respectively compared to their original value. The pattern obtained by both the optimizers is shown in Figure 3.21 and the recovered patterns are similar to the reference Taylor pattern. The optimized amplitude distributions of working elements are shown in Figure 3.22. The normalized

amplitude weights of the working elements obtained by both the optimizers have similar distributions. The numerical results of Figure 3.19 and 3.22 are presented in Table 3.10. Although there is slight difference in the excitation values obtained by both the optimizers, but that doesn't affect the final results.

Table 3.9: BFO parameters

<b>Parameters</b>	<b>Value</b>
Number of Bacteria(S)	30
Swimming lenth( $N_s$ )	50
Number of Chemotactic steps $N_c(N_c > N_s)$	50
Number of reproduction ( $N_{re}$ )	10
Number of elimination dispersal events ( $N_{ed}$ )	2
Probability of elimination dispersal ( $P_{ed}$ )	0.25

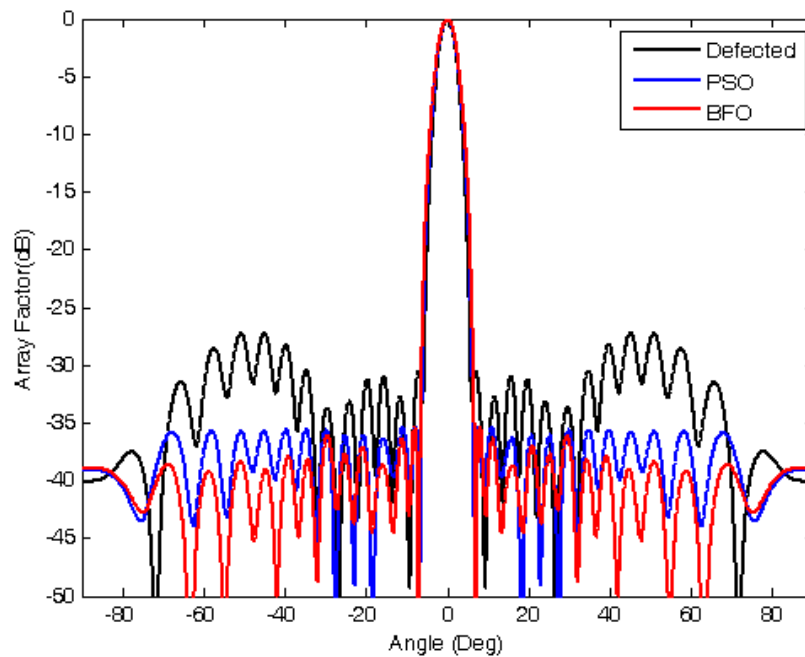


Figure 3.18 Recovered power pattern by PSO and BFO in a two element failed Chebyshev antenna array.



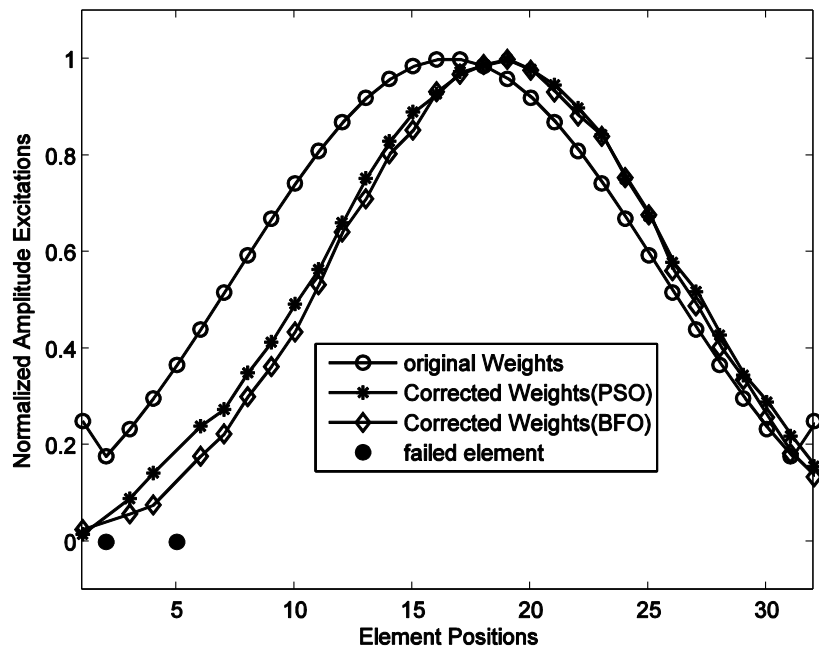


Figure3.19: Amplitude distribution of recovered pattern versus original Chebyshev array  
(Two element failure case)

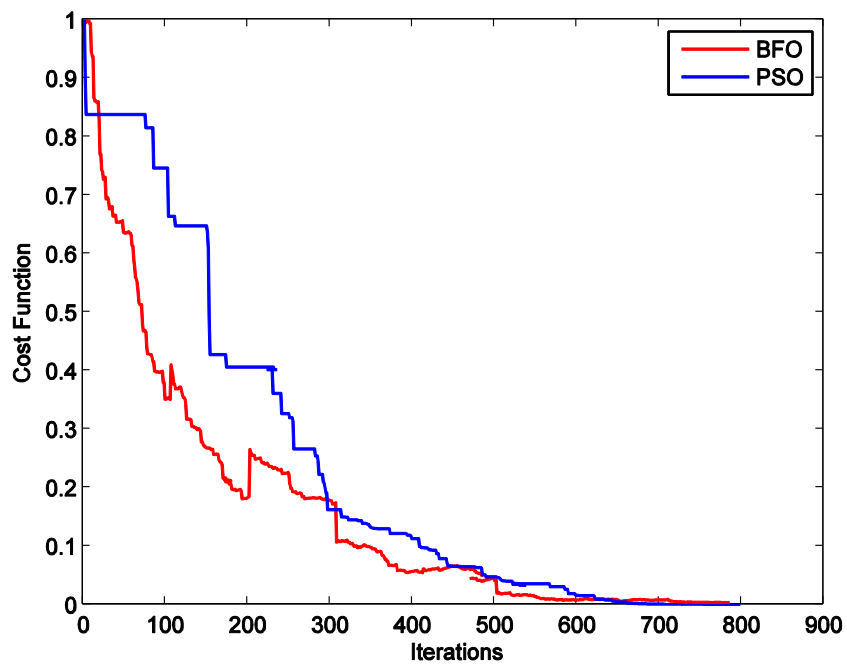


Figure: 3.20 Convergence of fitness function for PSO and BFO

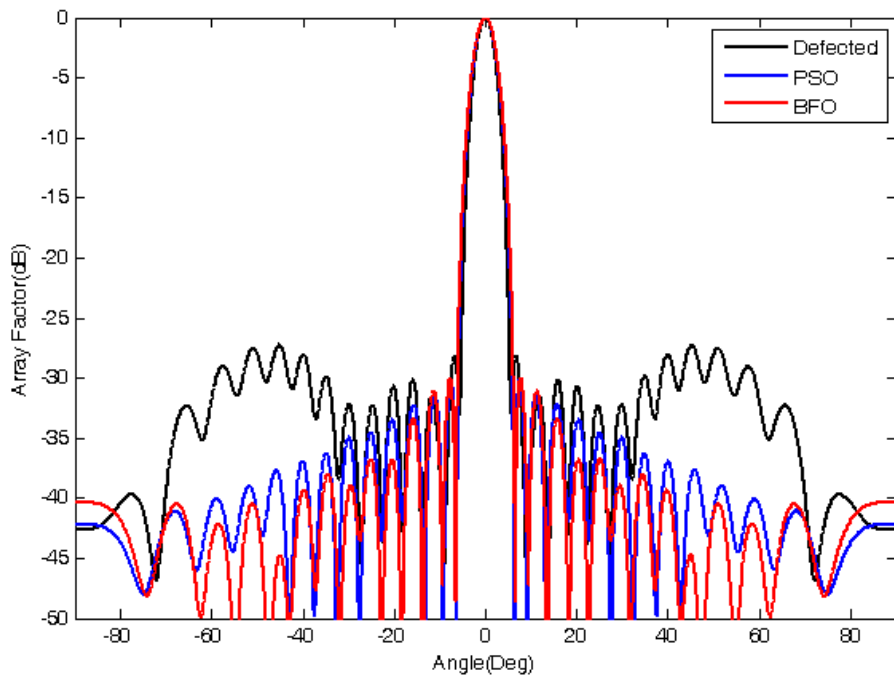


Figure 3.21: Recovered power pattern by PSO and BFO in a two element failed Taylor antenna array

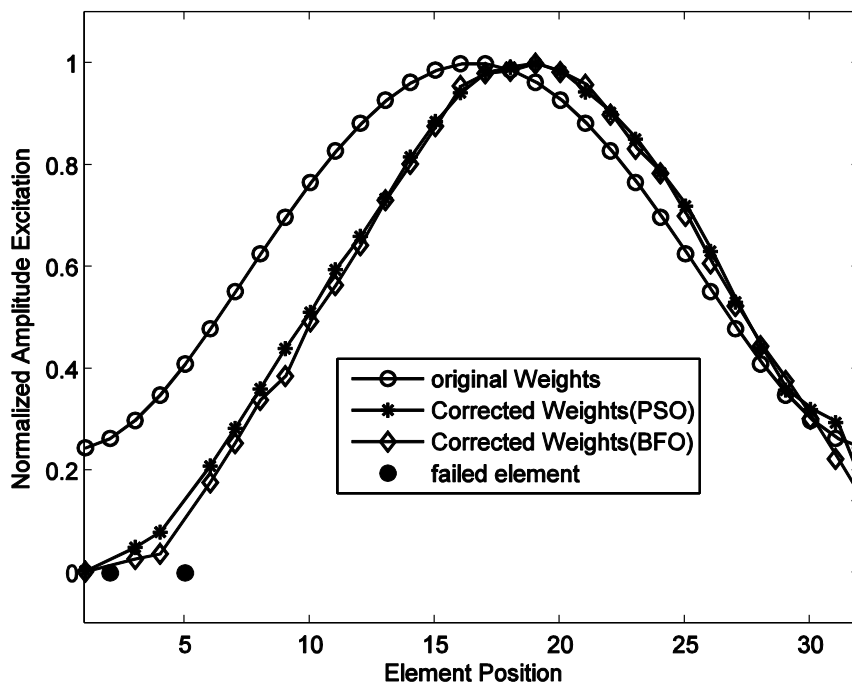


Figure: 3.22 Amplitude distribution of recovered pattern versus Original Taylor array

### **3.6 Performance Comparison of PSO with BFO for SLL Recovery**

In order to compare the performance of these two algorithms, same cost-function was used in both the methods. In addition, both PSO and BFO optimizers were used for the compensation of same failed arrays. The simulations were performed on a 2.33 GHz workstation platform with 4GB RAM. Under this situation, we have observed their rate of convergence and the time of computations. Each optimizer was used for 30 times and the average of the output amplitude weights of the all working elements in the array was determined. It was found that both the optimizers converge to the correct solution, in each case.

However, it was found that PSO required around 826 iterations with an average time of 81 seconds, whereas BFO needed around 770 iterations and time of 1100 seconds to reach the same degree of convergence for obtaining the solution for the two element failure (at 2<sup>nd</sup> and 5<sup>th</sup> positions) in the 32-element linear Chebyshev array. Figure 3.20 shows the performance comparison of both the techniques. The observations reveal that BFO technique converges faster than PSO, but the time taken by PSO for performing each iteration is less compared to BFO, as PSO is much simpler in structure compared to BFO. So, computation time for PSO is less. This trend is also observed in other antenna applications of BFO [110]. The results obtained in the process of compensation for two failed elements in a chebyshev array using these two optimization algorithms and their time of computation are shown in Table 3.11.

It is observed that, for both optimizers, the recovered Chebyshev array pattern, has maximum SLL close to the original one and also maintains a good parity with the pattern before element failure. But the beamwidth of pattern recovered by BFO is slightly broader compared to that in PSO.

While dealing with the case of Taylor array, both PSO and BFO require more number of iterations for convergence compared to the iterations required for the Chebyshev array. PSO and BFO algorithms run for an average of 1050

and 980 iterations, respectively, to produce the corrected Taylor pattern. The computation time required by PSO and BFO was 180 seconds and 1220 seconds, respectively. The recovered pattern by both the optimization techniques have maximum sidelobe level close to the original one, whereas the HPBW value obtained by PSO is 16.9% more and that obtained by BFO is 20% more than the original pattern. So, BFO produced a radiation pattern which has a broader beamwidth compared to the pattern obtained from PSO optimizer. In all the scenarios, the time of computation of BFO is considerably higher than that of PSO. Table 3.12 presents the parameters of the recovered Taylor pattern. With the increase in number of faults, the problem becomes more complex and in such situations, a price has to be paid in terms of reduced directivity while recovering the SLL.

In conclusion it can be said that PSO is preferred optimizer for failed array compensation problem as it is faster and simpler, less costly in terms of computation time, and gives better pattern in similar situations.

Table-3.10: Optimized amplitude-excitation obtained for two element failure at 2nd and 5th positions in 32-element linear Chebyshev and Taylor array

Element Position	Chebyshev Array			Taylor Array		
	Original Excitation	PSO	BFO	Original Excitation	PSO	BFO
1	0.2503	0.0160	0.0026	0.2458	0.0039	0.0027
2	0.1774	<b>0</b>	<b>0</b>	0.2641	0	0
3	0.2341	0.0899	0.0584	0.2994	0.0502	0.0277
4	0.2976	0.1429	0.0767	0.3493	0.0803	0.0377
5	0.3669	<b>0</b>	<b>0</b>	0.4105	0	0
6	0.4406	0.2397	0.1776	0.4795	0.2099	0.1777
7	0.5170	0.2745	0.2237	0.5526	0.2840	0.2551
8	0.5943	0.3503	0.3010	0.6266	0.3615	0.3395
9	0.6703	0.4138	0.3636	0.6988	0.4404	0.3867
10	0.7431	0.4928	0.4353	0.7667	0.5116	0.4943
11	0.8103	0.5645	0.5331	0.8286	0.5956	0.5650
12	0.8700	0.6616	0.6424	0.8830	0.6609	0.6439
13	0.9202	0.7534	0.7111	0.9283	0.7348	0.7320
14	0.9594	0.8301	0.8040	0.9636	0.8168	0.8036
15	0.9863	0.8912	0.8535	0.9877	0.8862	0.8773
16	1.0000	0.9289	0.9331	1.0000	0.9429	0.9561
17	1.0000	0.9749	0.9695	1.0000	0.9825	0.9811
18	0.9863	0.9892	0.9894	0.9877	0.9930	0.9862
19	0.9594	1.0000	1.0000	0.9636	1.0000	1.0000
20	0.9202	0.9794	0.9778	0.9283	0.9847	0.9833
21	0.8700	0.9473	0.9322	0.8830	0.9443	0.9586
22	0.8103	0.8994	0.8824	0.8286	0.9038	0.9001
23	0.7431	0.8440	0.8404	0.7667	0.8518	0.8332
24	0.6703	0.7523	0.7551	0.6988	0.7854	0.7846
25	0.5943	0.6754	0.6780	0.6266	0.7203	0.7011
26	0.5170	0.5793	0.5623	0.5526	0.6314	0.6078
27	0.4406	0.5187	0.4895	0.4795	0.5317	0.5246
28	0.3669	0.4289	0.4035	0.4105	0.4420	0.4449
29	0.2976	0.3458	0.3365	0.3493	0.3590	0.3775
30	0.2341	0.2895	0.2581	0.2994	0.3207	0.3030
31	0.1774	0.2197	0.1834	0.2641	0.2953	0.2241
32	0.2503	0.1566	0.1352	0.2458	0.1712	0.1419

Table: 3.11 Parameters obtained in compensation of two element failure in Chebyshev array

Optimization Techniques	Max <sup>m</sup> Sidelobe Level(SLL)	HPBW	FNBW	No. of Iteration for Convergence	Computation Time (Sec)
PSO	-35.26dB	4.68°	13.2°	826	81
BFO	-35.12dB	4.88°	14.0°	770	720

Table: 3.12 Parameters obtained in compensation of two element failure in Taylor array

Optimization Techniques	Max <sup>m</sup> Sidelobe Level(SLL)	HPBW	FNBW	No. of Iteration for Convergence	Computation Time (Sec)
PSO	-35.1dB	4.7°	12.8°	1170	480
BFO	-35.01dB	4.82°	13.0°	1025	6640

### 3.7 Summary

In this chapter the pattern recovery in a failed antenna array by amplitude only and amplitude-phase approach has been presented. In the first phase of the work, PSO was used to evaluate the fitness function to find the optimized amplitude and amplitude-phase excitations of the working elements in the array. It was observed that the amplitude-only compensation is more suitable compared to amplitude-phase approach for its simplicity and lower computational cost. In the last part of this chapter this compensation problem was solved using BFO. But the obtained results conclude that PSO is more preferred optimizer for failed array compensation problem as it is faster and simpler, less costly in terms of computation time, and gives better pattern in similar situations.

With the growing interest for self-recoverable antenna array for different wireless communication applications, this developed methodology using PSO can be effectively applied to increase the array availability. Although the developed methodology has been used for linear array antennas, the same can be suitably be extended for other array antennas. In the next chapter we have applied the PSO and BFO for the restoration of nulls in a failed antenna array.

# Null Steering in Failed Antenna Array

---

## 4.1 Introduction

The modern wireless communication systems such as mobile communication, radar, sonar, satellite have been the strong candidates to fulfill the growing demands for the wireless services. Presence of the interfering signals in the environment affects the performance of these systems. The effect of these unwanted signals can be suppressed by appropriate antenna pattern synthesis, which requires placing the nulls in the direction of the interference. The goal of the pattern nulling is to minimize the degradation in signal-to-noise ratio performance due to the unwanted interferences. For this reason, null steering is still an active area of research in the field of adaptive beamforming. This goal can be achieved by determining the physical layout of the array and by controlling the amplitude and phase of the excitation current for individual array elements [111-125].

In this chapter, our focus is to develop compensation techniques to restore nulls in phased array antennas in the presence of failed elements. It has been found that the presence of faulty elements can sometimes remove the nulls altogether and replace it by a lobe. In the previous chapter we have discussed the methods for recovering the SLL in a failed antenna array without replacing the faulty elements. In addition to this, the recovery of null(s) in the desired direction(s) is another challenge while dealing with failed arrays.

In this chapter, we show that it is possible to recover the desired SLL and simultaneously, the nulls can be steered back to their original locations. This can be achieved by modifying the excitations of the working elements in

a failed array. Both PSO and BFO have been used for the compensation process.

## 4.2 Problem Formulation

The far-field pattern of an  $N$ -element linear array, equally spaced, non-uniform amplitude and progressive phase excitation is given by (4.1)

$$F(\theta) = EP(\theta) \sum_{n=1}^N a_n e^{j(n-1)kd \cos \theta} \quad (4.1)$$

where

$a_n$ : current excitation of  $n^{\text{th}}$  element

$d$ : inter element spacing

$\theta$ : angle from broad side

$k$ : wave number ( $2\pi/\lambda$ )

$EP(\theta)$ : element pattern ( $EP(\theta) = 1$  for isotropic source)

When some of the elements become non-operational in the antenna array, the value of  $a_n$  becomes 0 for those elements. That is, if two elements failed (2<sup>nd</sup> and 5<sup>th</sup>) in a 32 element array then the current excitation vector becomes  $\mathbf{a} = [a_1, 0, a_3, a_4, 0, a_6, a_7, a_8, \dots, a_{32}]$ . As discussed in the previous chapter, this problem is also approached as an optimization problem and solved by optimizing the weights of the functional elements using evolutionary computational techniques. The system objective is defined in eq. (4.2) as a function of decision variables which is minimized to achieve the desired pattern.

$$I = \sum_{\theta=-90^\circ}^{90^\circ} [W(\theta) |F_{PSO}(\theta) - F_d(\theta)|] + S \quad (4.2)$$

The first term in the objective function is meant for interference suppression, i.e., to place nulls in the direction of undesired sources, in the presence of faulty elements.  $F_{PSO}(\theta)$  is the pattern obtained by using PSO,  $F_d(\theta)$  is the desired pattern, and  $W(\theta)$  is a controlling parameter for creating the null. The term 'S' in the cost function is included to take care of the



sidelobe level of the recovered pattern. It is similar to the cost function that has been used for suppression of side lobe in the eqn. (3.2).

### **4.3 Null Recovery Using PSO**

Like the SLL recovery, the problem of null steering in failed antenna array can be approached as an optimization problem and solved by PSO. The methodology adopted for obtaining the desired pattern can be amplitude-only or amplitude-phase method. The job of PSO optimizer is to return optimum current excitations for the working elements that will lead to the desired radiation pattern with reduced SLL and nulls in the desired direction.

For the implementation of null recovery using PSO, a swarm is initialized with the population of random positions and velocities for the parameters (amplitude of excitation current of all working element in the array for amplitude-only approach or complex weights for amplitude-phase approach) with their minimum and maximum limit. PSO searches for the optimum design parameters of the antenna array within the solution space to obtain a desired radiation pattern. Each point in this solution space represents a possible current excitation for one the remaining working elements of the array. After defining the solution space, the next task is to develop the objective function. An objective function is one which takes the value of all coordinates of a point in the solution space and returns a single number representing the goodness of antenna array design. The form of the fitness function is based on the requirement of the user. In the present case, the objective function was framed as defined in eqn. (4.2). The next task for the PSO optimization process is to select the value of the optimization parameters and execute the PSO program. Like the previous case as discussed in Chapter-3, for this problem also a population size of 30 was chosen,  $c_1$  and  $c_2$  were set to 2 and the inertial weight  $w$  was linearly varied from 0.9 to 0.4 iteratively. The invisible/reflecting boundary conditions were applied for confining the particles with the solution space [97].

### 4.3.1. Analysis for Amplitude-Only Control

The failure of any element in an antenna array makes the pattern distorted. The proposed method using PSO to restore the radiation pattern with suppressed SLL and to place the nulls to their original positions in the presence of faulty elements was implemented by recalculating and adjusting the amplitude weights of remaining working elements. The simulation was performed on the same test antenna array (32-element linear Chebyshev array) as described in section 3.3. The radiation pattern of the original test antenna is shown in Figure 4.1. This section presents the amplitude-only approach to obtain the desired pattern with the recovered nulls for the array with failed elements.

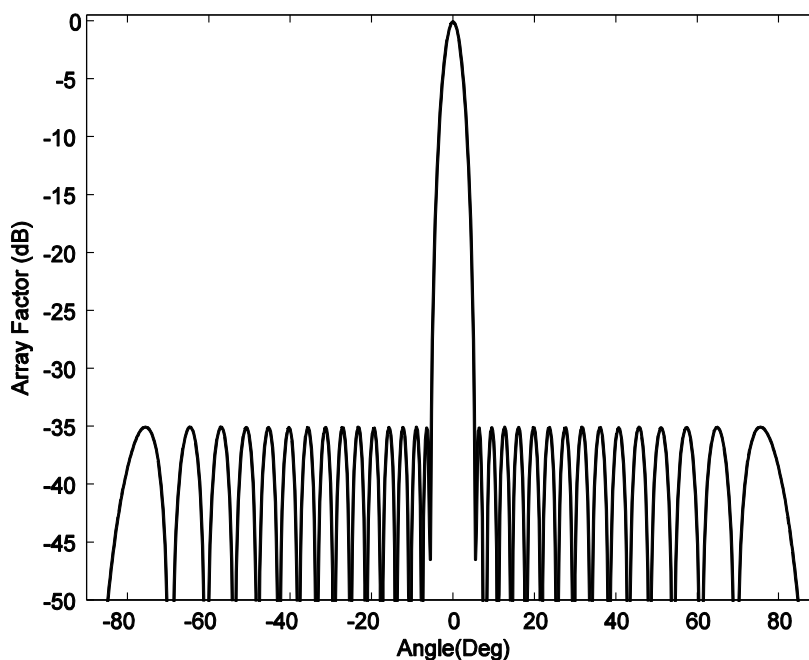


Figure 4.1: A 32-element Chebyshev array pattern with SLL of -35dB.

#### ***Case I: Recovery of single null with element failure***

In order to formulate the null recovery problem, the above mentioned 32-element array was used to make the test antenna array having a radiation pattern with single null at  $20^\circ$  direction, by controlling only the current amplitudes. The corresponding radiation pattern is shown in Figure 4.2. The pattern has the null depth level (NDL) of -121.9 dB and maximum SLL of -34.83dB. The element failure in this test array was considered randomly

at 2<sup>nd</sup> and 5<sup>th</sup> positions. This element failure resulted in increase of SLL and removal of null from its original position. Here the aim was to place the null at its original position in the recovered array pattern along with the suppressed SLL. The PSO optimization was applied to optimize the cost function as defined in eqn. (4.2), w.r.t. to the amplitude excitations of the all working array elements.

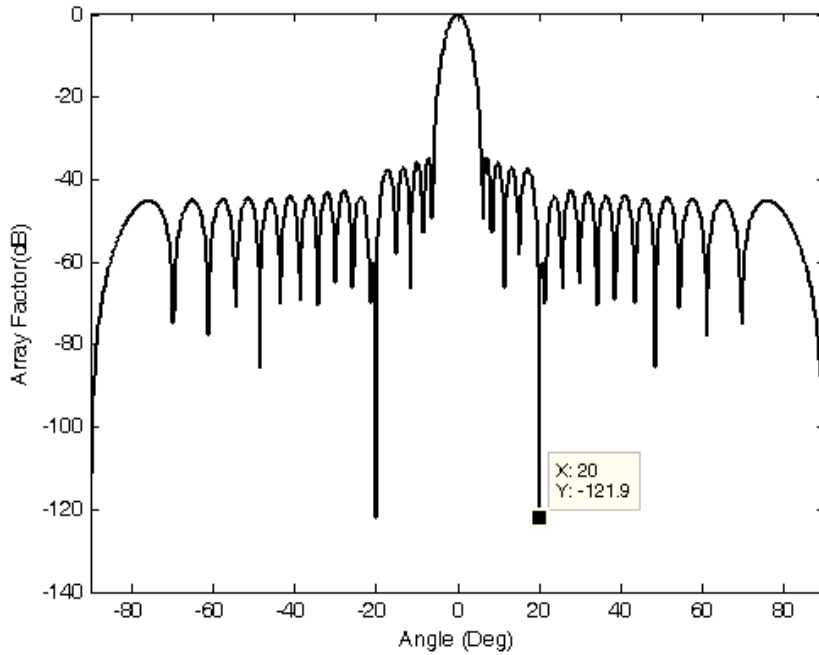


Figure 4.2: Radiation pattern of 32 element linear broadside array with null at 20°.

The values of different parameters in the cost function were selected as:

$F_d(\theta) = 0$ , for  $\theta = \theta_i$ ,  $\theta_i$  is the direction where the null has to be placed.

$W(\theta) = 200$ , for  $\theta = \theta_i$  and  $W(\theta) = 1$ , for other directions.

From figure 4.3 it can be observed that the PSO can recover the pattern with the null at its original position in the presence of faulty elements in the array. It can also be observed that the recovered pattern has a close resemblance with the original pattern having satisfactory null depth level and maximum SLL. The null was placed at 20° with NDL of -110.9 dB and maximum SLL of -34.9 dB.

The effectiveness of the proposed technique for single null recovery was extended to array with more number of faulty elements. In order to study the performance of pattern recovery in 3 element failure condition, the simulation was performed with defective elements located at 2<sup>nd</sup>, 5<sup>th</sup> and 6<sup>th</sup> positions in the same test antenna array. The PSO was executed to correct the damaged pattern by finding the new set of amplitude excitations of the remaining working elements and to relocate the nulls at the desired directions as per the objective function described in eqn. (4.2).

Another element failure scenario was considered in the same array with defected elements located at 2<sup>nd</sup>, 3<sup>rd</sup>, 5<sup>th</sup> and 6<sup>th</sup> positions and the pattern recovery was carried out. Figure 4.4 and Figure 4.5 show the recovered patterns with single null at 20° direction for three and four element failure in the antenna array. The maximum SLL, NDL for the corresponding null and beamwidth of the recovered patterns shown in Figure 4.3-4.5 are given in Table 4.1.

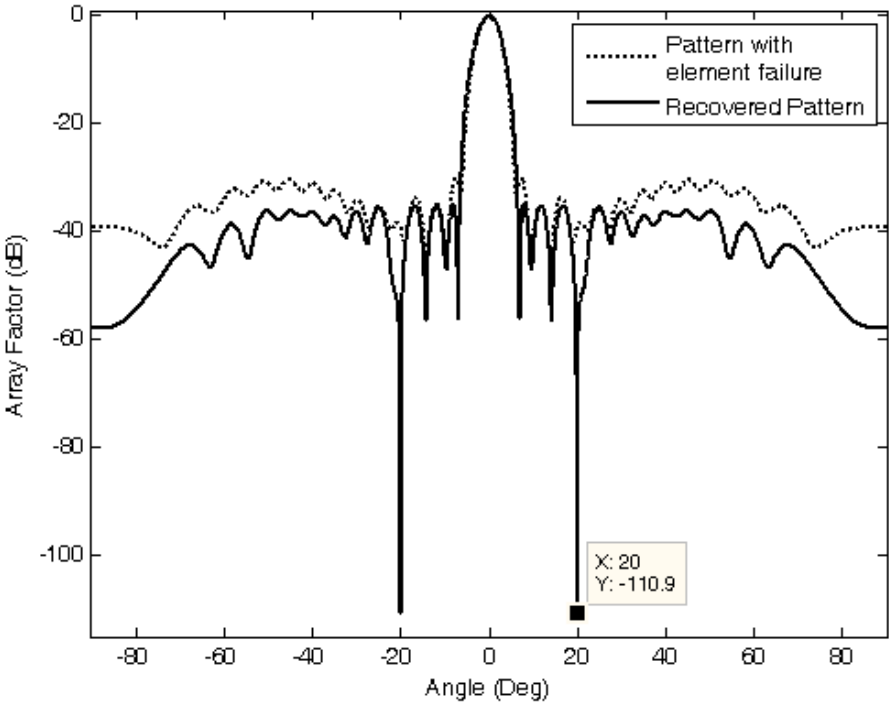


Figure 4.3: Radiation pattern with element failure at 2<sup>nd</sup> and 5<sup>th</sup> positions and null at 20°.

It is apparent from Table 4.1 and Figures 4.3-4.5 that PSO can recover the patterns with satisfactory NDL and SLL. The results obtained in *Case-I* show that the null which was displaced due to element failure can be placed at the original position. But a reduced NDL was achieved compared to the original test array of this case and with the desired SLL. The element excitations for single null recovery with two, three and four element failures are shown in Table 4.2. The convergence curve for this case, with the progress of PSO iterations is shown in Figure 4.6. The PSO simulations were performed on a 2.33GHz workstation platform with 4GB RAM and the computation time required to reach the solution is 128 seconds.

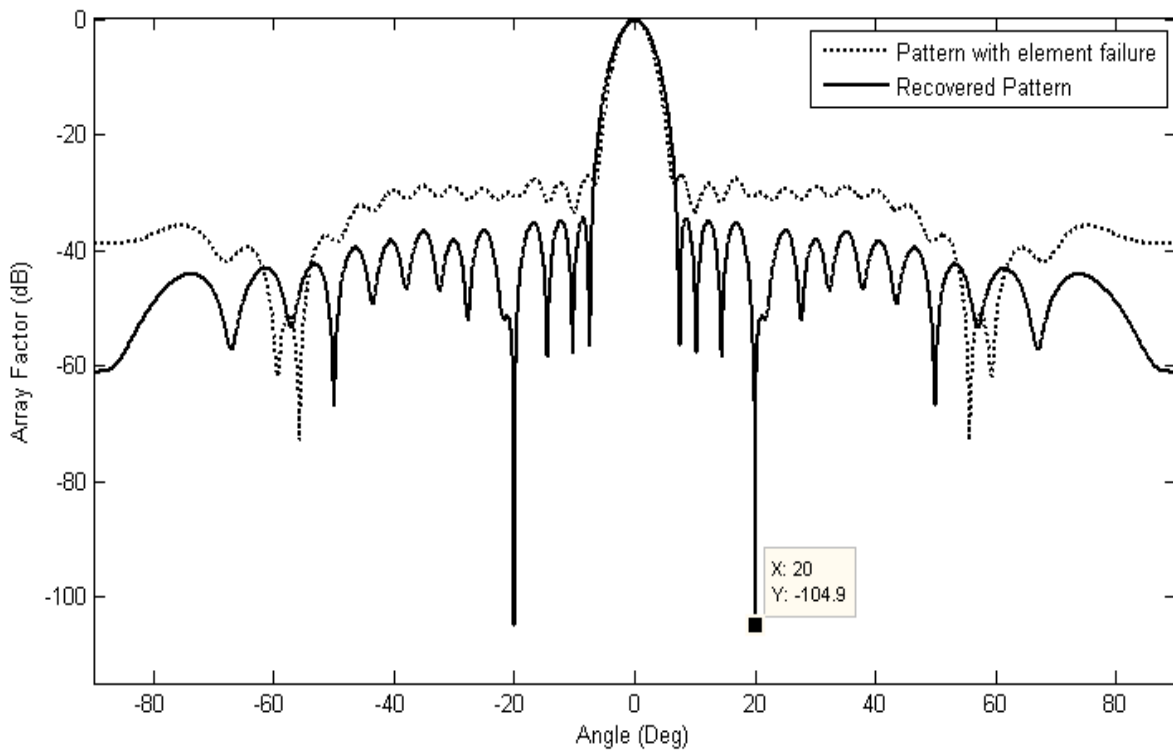


Figure 4.4: Radiation pattern with element failure at 2<sup>nd</sup>, 5<sup>th</sup> and 6<sup>th</sup> positions and null at 20°.

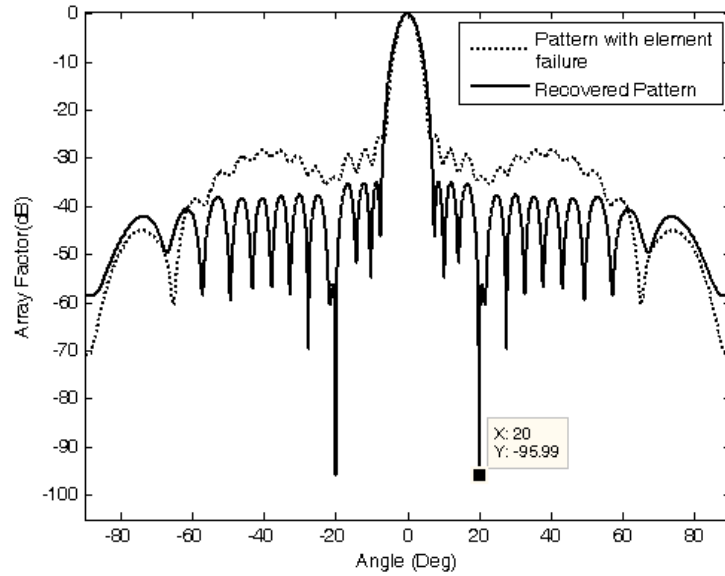


Figure 4.5: Radiation pattern with element failure at 2<sup>nd</sup>, 3<sup>rd</sup>, 5<sup>th</sup> and 6<sup>th</sup> positions and null at 20°

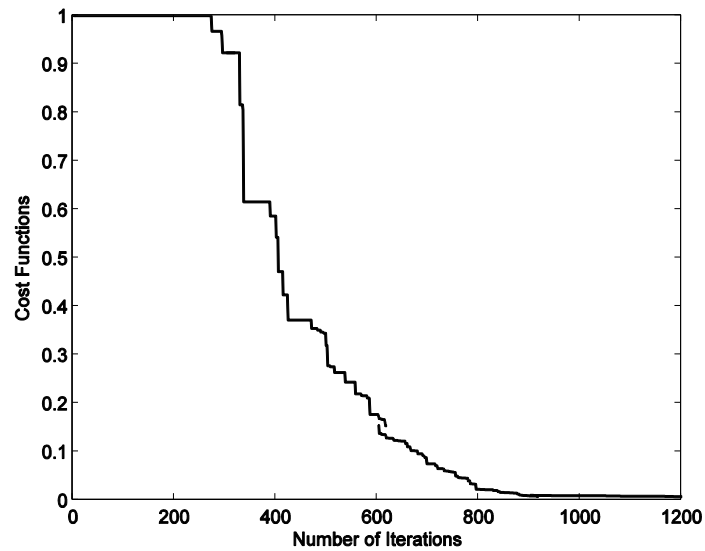


Figure 4.6: Convergence curve for recovery of pattern nulling in the presence of faulty elements in the antenna array.

Table 4.1: Comparison of recovered patterns for the configurations discussed in Case I

	Original test array pattern	Compensated pattern with two element ( 2 <sup>nd</sup> and 5 <sup>th</sup> ) failure	Compensated pattern with three element failure ( 2 <sup>nd</sup> , 5 <sup>th</sup> , 6 <sup>th</sup> )	Compensated pattern with four element failure ( 2 <sup>nd</sup> ,3 <sup>rd</sup> , 5 <sup>th</sup> , 6 <sup>th</sup> )
NDL(dB)	-121.9dB	-110.9dB	-104.9dB	-95.99dB
SLL(dB)	-34.83dB	-34.9dB	-34.8dB	-34.85dB
HPBW	4.36°	4.83°	5.23°	5.25°
BWFN	12.2°	13.5°	14.5°	14.6°

Table 4.2: Element excitations corresponding to recovery of single null

Element Position	Single null in the pattern with no faulty element	Recovery of null with 2 <sup>nd</sup> ,5 <sup>th</sup> element failure	Recovery of null with 2 <sup>nd</sup> ,5 <sup>th</sup> ,6 <sup>th</sup> element failure	Recovery of null with 2 <sup>nd</sup> ,3 <sup>rd</sup> ,5 <sup>th</sup> ,6 <sup>th</sup> element failure
1	0.109123	0.023487	0.004259	0.007916
2	0.137998	0	0	0
3	0.196634	0.088316	0.013976	0
4	0.267514	0.112242	0.044149	0.035117
5	0.335095	0	0	0
6	0.398675	0.201482	0	0
7	0.465396	0.291272	0.150306	0.130495
8	0.545720	0.310633	0.190064	0.155570
9	0.635776	0.429662	0.249726	0.234578
10	0.722141	0.498319	0.353981	0.316015
11	0.793865	0.606783	0.450910	0.407948
12	0.849005	0.676120	0.530129	0.500501
13	0.896751	0.745092	0.622374	0.580281
14	0.940400	0.801728	0.705494	0.670289
15	0.976450	0.902258	0.798791	0.765804
16	1.000000	0.954487	0.888472	0.865514
17	1.000000	1.000000	0.960522	0.940693
18	0.976450	0.984364	1.000000	0.970688
19	0.940400	0.97029	0.996628	0.993166
20	0.896751	0.951613	0.980757	0.995043
21	0.849005	0.920146	0.988853	1.000000
22	0.793865	0.884823	0.951899	0.970576
23	0.722141	0.799609	0.888656	0.914123
24	0.635776	0.705233	0.796514	0.832025
25	0.545720	0.614106	0.698030	0.728130
26	0.465396	0.530277	0.600114	0.626217
27	0.398675	0.468255	0.521222	0.553461
28	0.335095	0.382750	0.430780	0.458737
29	0.267514	0.293752	0.338369	0.366813
30	0.196634	0.235127	0.244051	0.265242
31	0.137998	0.149190	0.166303	0.183424
32	0.109123	0.094176	0.130248	0.163462

### Case II: Recovery of two nulls with element failure

Like Case-I, the test array for this case was also obtained from the original 32-element Chebyshev array with radiation pattern having two nulls at  $\theta_1 = 20^\circ$  and  $\theta_2 = 40^\circ$  by optimizing the amplitude excitations, using PSO. The corresponding pattern is shown in Figure 4.7. The element failure in the antenna array was considered randomly at 2<sup>nd</sup> and 5<sup>th</sup> position. The recovery of two nulls in case of the element failure was approached in a similar manner as discussed in *case-I*. The degraded pattern due to element failure and the recovered optimized pattern with two nulls are shown in Figure 4.8. The SLL and NDL for corresponding nulls are presented in Table 4.3. The new set of optimized amplitude excitations of the working elements that produce the two nulls in the recovered pattern are given in Table 4.4.

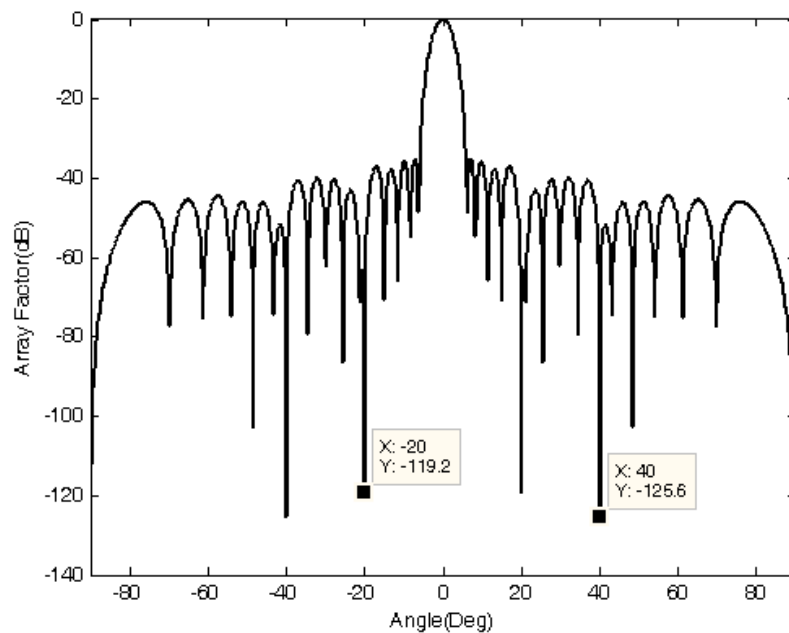


Figure 4.7: Radiation pattern of 32 element linear broadside array with null at  $20^\circ$  and  $40^\circ$

Table 4.3: Pattern characteristics obtained in recovery of two nulls with two element failure in a Chebyshev array

	Test array		Array with failure at two random element positions( 2 <sup>nd</sup> and 5 <sup>th</sup> )	
	$20^\circ$	$40^\circ$	$20^\circ$	$40^\circ$
NDL(dB)	-119.2dB	-125.6dB	-103.7dB	-108.4dB
SLL(dB)	-34.92dB		-34.31dB	
HPBW	$4.36^\circ$		$4.88^\circ$	
BWFN	$12.2^\circ$		$13.5^\circ$	



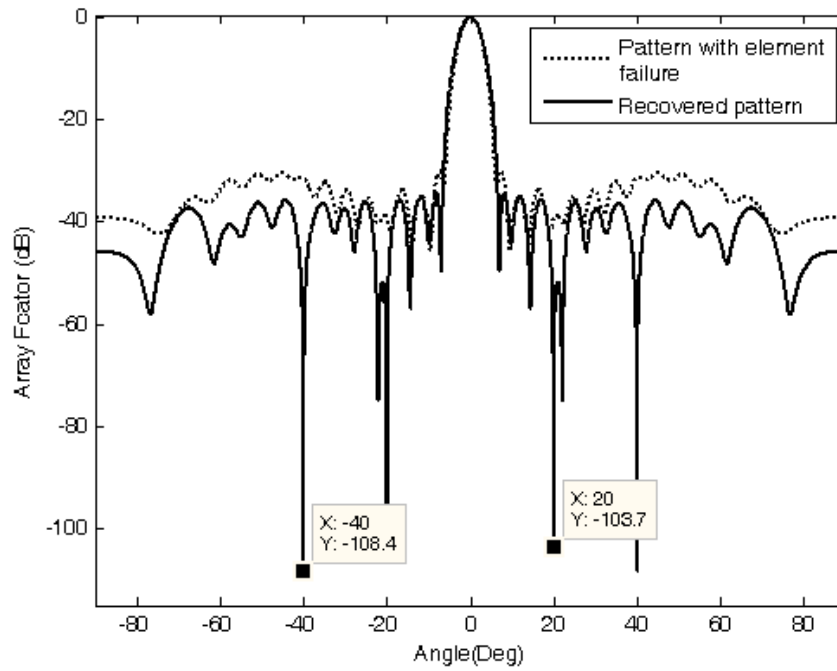


Figure 4.8: Performances of PSO for placing nulls at  $20^\circ$  and  $40^\circ$  with element failure.

Table 4.4: Element excitations corresponding to Case II

Element Position	Two nulls at $-20^\circ$ and $40^\circ$ without any fault	Recovery of nulls with two element failure	Element Position	Two nulls at $-20^\circ$ and $40^\circ$ without any fault	Recovery of nulls with two element failure
1	0.111027	0.009475	17	1.000000	1.000000
2	0.147357	0	18	0.984256	0.981285
3	0.195769	0.070337	19	0.937196	0.967211
4	0.260461	0.094673	20	0.893344	0.955228
5	0.343247	0	21	0.853337	0.959541
6	0.405897	0.176755	22	0.792959	0.876785
7	0.457458	0.219296	23	0.720820	0.829228
8	0.549227	0.298897	24	0.643900	0.747795
9	0.643900	0.376129	25	0.549227	0.635467
10	0.720820	0.453272	26	0.457458	0.571792
11	0.792959	0.581294	27	0.405897	0.500871
12	0.853337	0.634989	28	0.343247	0.395569
13	0.893344	0.683541	29	0.260461	0.312531
14	0.937196	0.789530	30	0.195769	0.262544
15	0.984256	0.866472	31	0.147357	0.161759
16	1.000000	0.912675	32	0.111027	0.104164

### **Case III: Recovery of three nulls with element failure**

In order to verify the proposed procedure further, a test array with three nulls at  $20^\circ$ ,  $33^\circ$ , and  $50^\circ$  were designed out of the original 32-element array by optimizing the amplitude excitations. This radiation pattern of the test array with three nulls is shown in Figure 4.9. In order to restore the nulls of the radiation pattern in the presences of defective element at 2<sup>nd</sup> and 5<sup>th</sup> positions, the PSO was executed to obtain the new amplitude excitations for the remaining working elements. Figure 4.10 shows the recovery of three nulls at angles of  $20^\circ$ ,  $33^\circ$ , and  $50^\circ$  respectively for two element failure in the antenna array. Table 4.5 summarizes the parameters of the recovered radiation pattern. The element amplitude values calculated by the PSO for the recovered pattern given in Figure 4.10 are listed in Table 4.6.

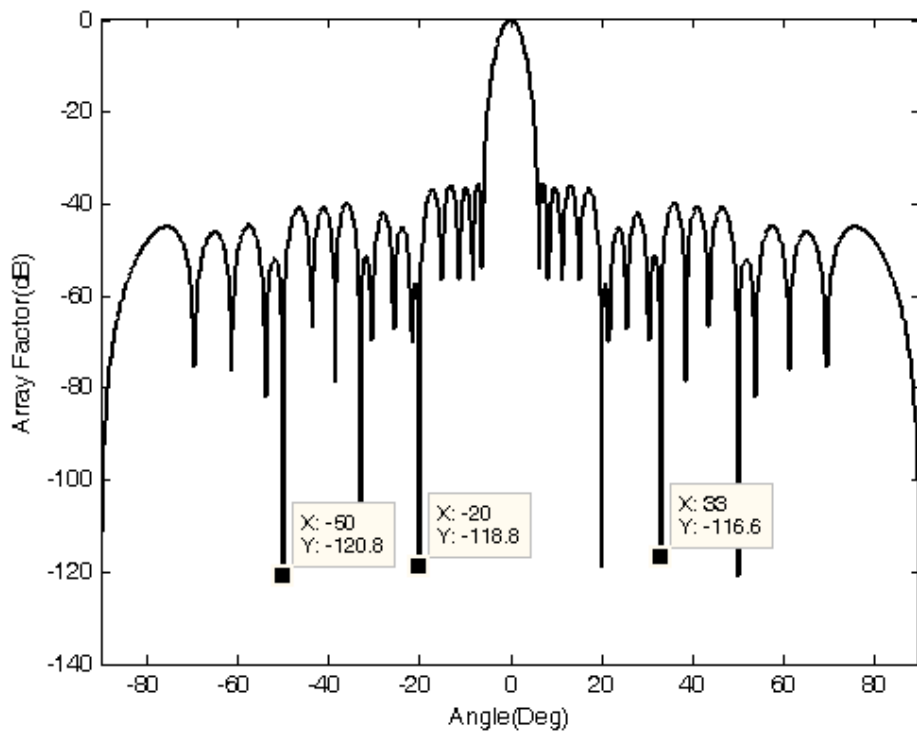


Figure 4.9: Radiation pattern of the linear array with imposed nulls at  $20^\circ$ ,  $33^\circ$  and  $50^\circ$

Table-4.5: Pattern characteristics obtained in recovery of three nulls with two element failure in a Chebyshev array

	Test array			Recovered pattern with failure of two elements		
	20°	33°	50°	20°	33°	50°
NDL(dB)	-118.8dB	-116.6dB	-120.8dB	-110dB	-108.5dB	-99.02dB
SLL(dB)	-34.92dB			-34.62dB		
HPBW (Deg.)	4.37°			4.84°		
FNBW(Deg.)	12.2°			13.6°		

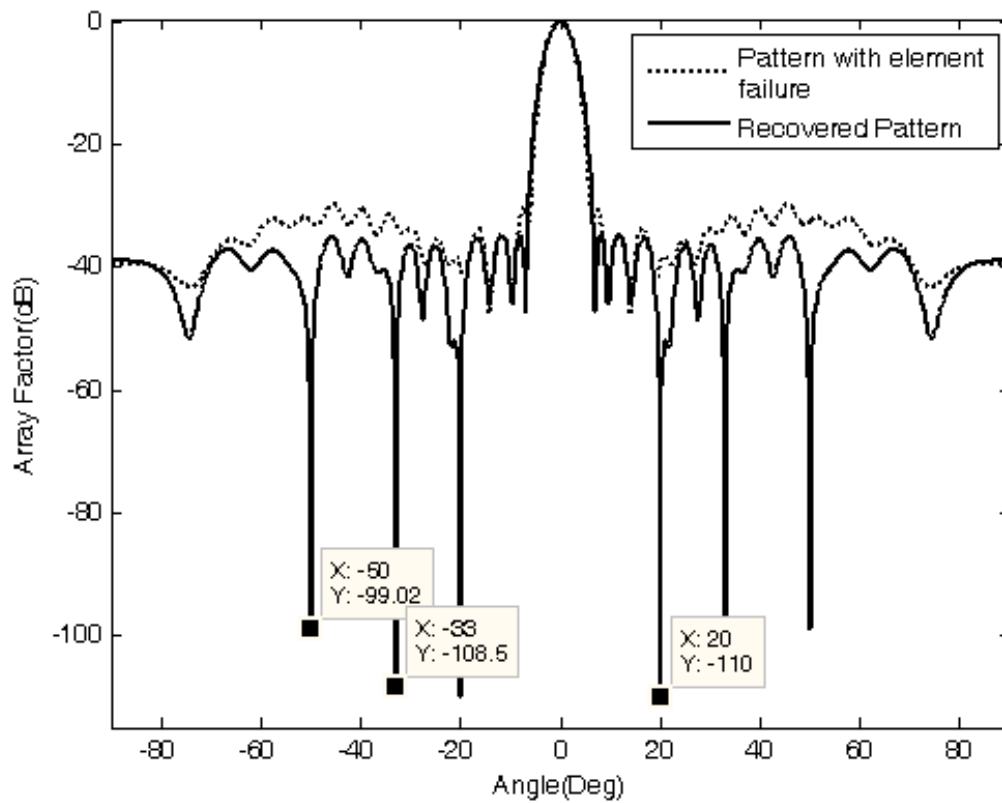


Figure 4.10: Performances of PSO for placing nulls at 20°, 33° and 50° with element failure

Table 4.6 Element excitations corresponding to *Case III*

Element Position	Test array with three nulls at 20°, 33° and 40°	Recovery of nulls with two element failure
1	0.112412	0.015243
2	0.142523	0
3	0.197175	0.048331
4	0.277724	0.115920
5	0.337813	0
6	0.387541	0.174559
7	0.474674	0.229018
8	0.549653	0.301296
9	0.630065	0.373663
10	0.735809	0.486093
11	0.806746	0.555039
12	0.856400	0.641071
13	0.904119	0.737750
14	0.948004	0.747771
15	0.997974	0.885625
16	1.000000	0.958554
17	1.000000	0.982341
18	0.997974	1.000000
19	0.948004	0.984777
20	0.904119	0.996626
21	0.856400	0.963321
22	0.806746	0.912246
23	0.735809	0.875323
24	0.630065	0.760197
25	0.549653	0.653518
26	0.474674	0.606215
27	0.387541	0.498355
28	0.337813	0.434902
29	0.277724	0.334749
30	0.197175	0.266688
31	0.142523	0.201471
32	0.112412	0.125968

#### **Case IV: Recovery of broad nulls with element failure**

In wireless communication, the exact direction of arrival of interference signal may not be available precisely. In this situation a comparatively sharp null would require continuous steering for obtaining a reasonable value of signal-to-noise ratio, which is a difficult task. To tackle this situation, a broad or sector null is needed. For the present case, the test array was designed by perturbing the amplitude excitations of the original 32-element array to have a broad null at  $30^\circ$  with  $\Delta\theta_i = 5^\circ$ . The pattern of this test array is shown in Figure 4.11. The recovery of the broad null was carried out in the presence of defective elements at 2<sup>nd</sup> and 5<sup>th</sup> positions in the antenna array using PSO. The damaged pattern and the corresponding recovered pattern with broad null at its original position are shown in Figure 4.12. The pattern parameters of the recovered pattern are tabulated in Table 4.7 and corresponding excitations are shown in Table 4.8.

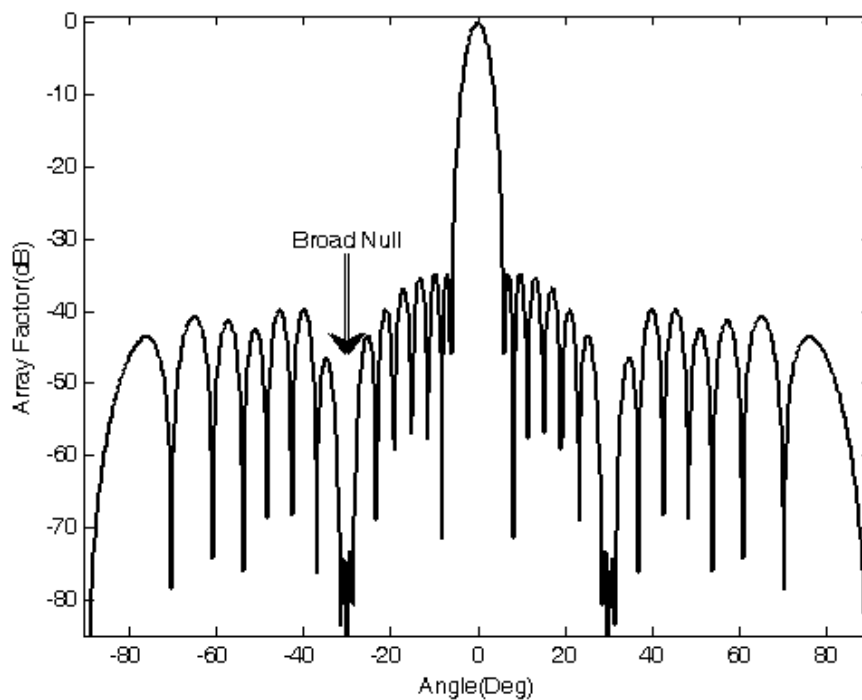


Figure 4.11: Radiation pattern of a linear broadside array with a broad null at  $30^\circ$

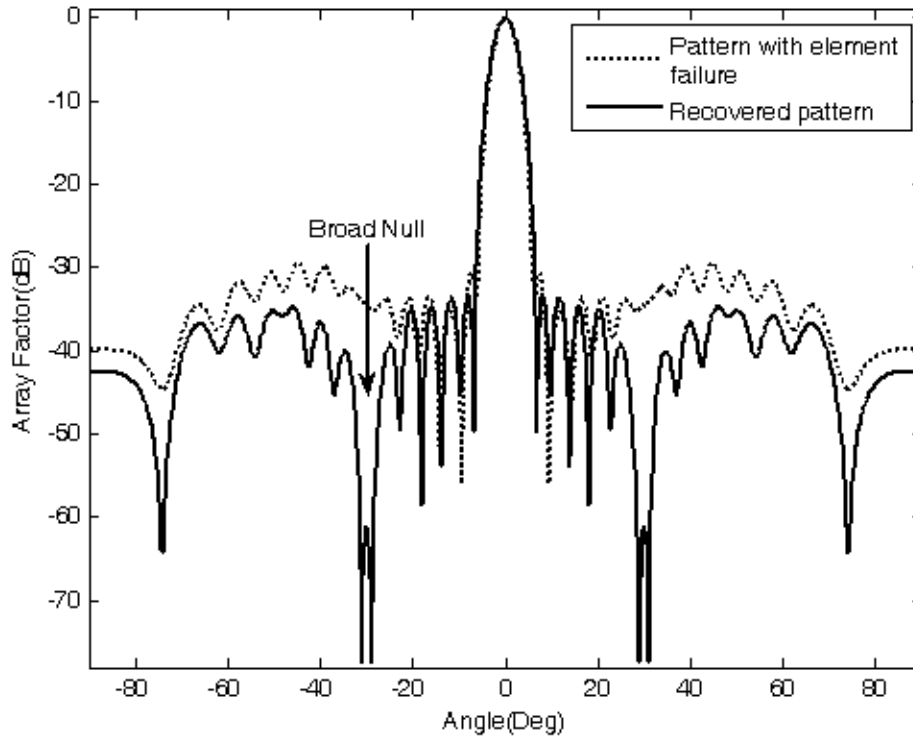


Figure 4.12: Performances of PSO for placing broad null with element failure.

Table 4.7: Pattern characteristics obtained for the configurations discussed in *Case IV*

	Broad null without any fault	With failure of two elements ( 2 <sup>nd</sup> and 5 <sup>th</sup> )
NDL(dB)	-99dB	-77.5dB
SLL(dB)	-34.73dB	-33.51dB
HPBW (Deg)	4.33°	4.8°
FNBW (Deg)	12°	13.5°

Table-4.8: Element excitations corresponding to *Case IV*

Element Position	Test array with broad null	Broad null recovered array with two element failure
1	0.114935	0.072946
2	0.132036	0
3	0.234604	0.052306
4	0.294215	0.097363
5	0.318546	0
6	0.395721	0.224616
7	0.489433	0.246791
8	0.565008	0.332650
9	0.636642	0.422243
10	0.727687	0.487619
11	0.790406	0.564408
12	0.859729	0.659086
13	0.913656	0.751987
14	0.951624	0.823226
15	0.981358	0.893587
16	1.000000	0.930046
17	1.000000	0.999085
18	0.981358	0.989130
19	0.951624	1.000000
20	0.913656	0.997671
21	0.859729	0.952235
22	0.790406	0.897201
23	0.727687	0.820005
24	0.636642	0.752422
25	0.565008	0.696424
26	0.489433	0.597174
27	0.395721	0.482113
28	0.318546	0.417580
29	0.294215	0.344862
30	0.234604	0.287656
31	0.132036	0.193549
32	0.114935	0.127802

#### **4.3.1.1 Observations**

A keen observation to Case-I of single null recovery reveals that the value of NDL of the corresponding null depends on the number of faulty elements present in the array. The increase in the number of faulty elements reduces the NDL of the corresponding recovered null. It was also observed that, in every case, the beamwidth of the recovered patterns are increasing. In the case of multiple null and broad null recovery case also, it was observed that the NDL of the recovered nulls have a values lesser than that of the original test array.

#### **4.3.2 Analysis for Amplitude-Phase Control**

Complex weights (both amplitude and phase) of an array can be changed to make changes in its radiation pattern. In case of element failure in the array, nulls can be recovered by changing both the amplitude and the phase of remaining working elements. In this section, amplitude-phase control is investigated for recovery of nulls in a failed antenna array. The test antennas were the same that was discussed in previous amplitude-only case.

In order to have a valid comparison, the test case of single null in  $20^\circ$  with faults at same 2<sup>nd</sup> and 5<sup>th</sup> position was considered first. The single null in the direction of  $20^\circ$  was recovered in the radiation pattern of the failed antenna array by controlling the complex weights of the remaining functional elements. Figure 4.13 shows the radiation pattern of a fully functional array having single null at  $20^\circ$ . Figure 4.14 shows the performance of PSO in the recovery of the single null. The pattern parameters are detailed in Table 4.9.



Table 4.9: Pattern characteristics of the array with single null

	Pattern characteristics of the original array with single null	Pattern characteristics with failure of two elements (2 <sup>nd</sup> and 5 <sup>th</sup> )
NDL(dB)	-126.5dB	-115dB
SLL(dB)	-34.42dB	-34.3dB
HPBW (Deg)	4.3°	4.86°
FNBW (Deg)	12°	13.5°

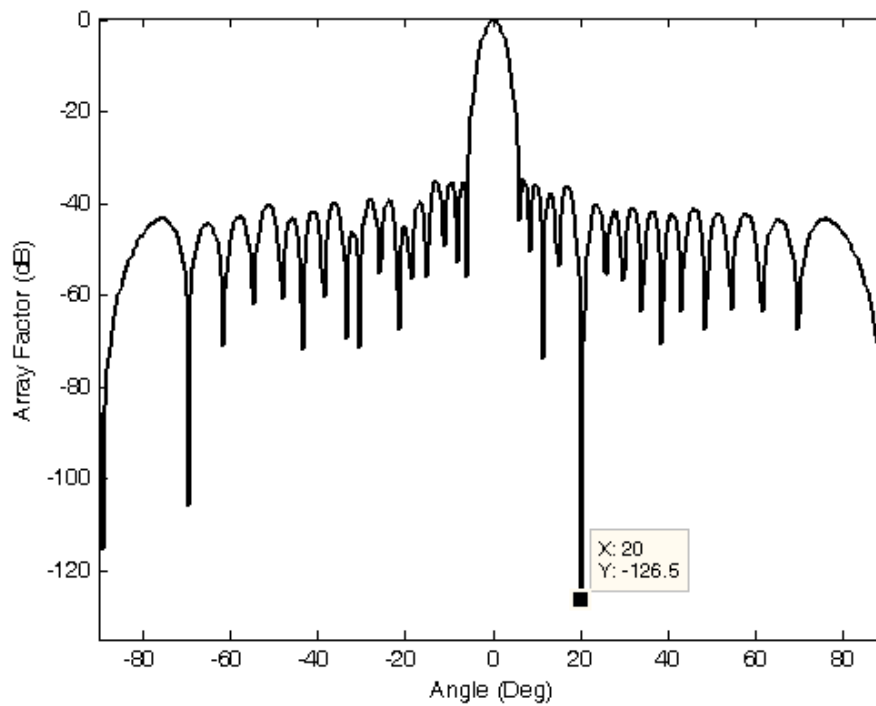


Figure 4.13: Radiation pattern obtained by controlling both the amplitude and the phase with one null at 20°

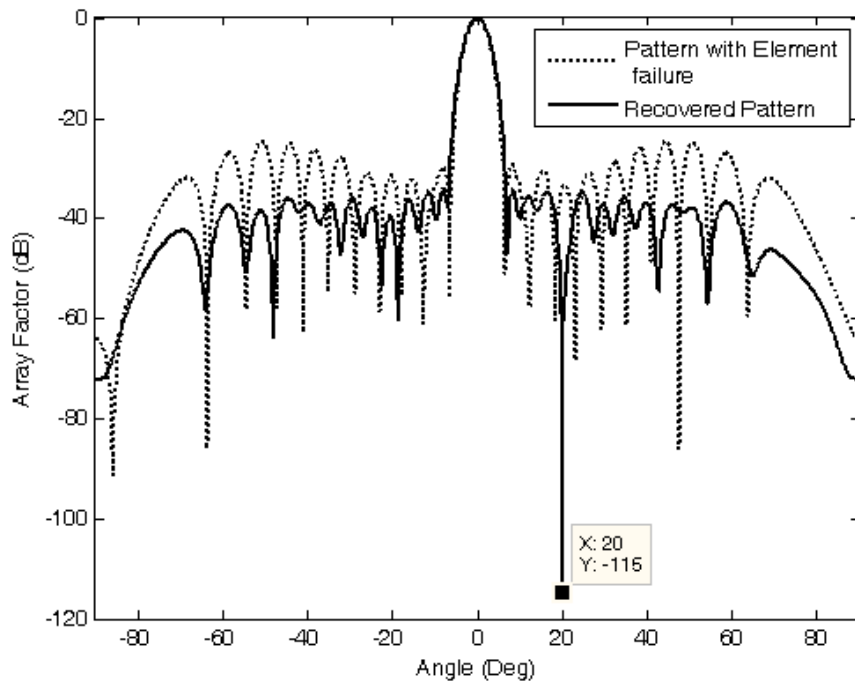


Figure 4.14: Recovered radiation pattern of a failed antenna array obtained by controlling both the amplitude and the phase with one null at 20°

In a similar approach the recovery of two nulls in the directions of 20° and 40° and three nulls in the directions of -20°, 33°, and 50° was successfully achieved. Figure 4.15 and 4.17 shows the radiation patterns of the test arrays with two nulls at angles of 20° and 40° and three nulls at angles of -20°, 33°, and 50° respectively. Figure 4.16 and 4.18 shows the recovery of two and three nulls in their original positions for two element failures. From the null depth and the maximum sidelobe level points of view, the performances of the recovered patterns are very good. The parameters of the recovered radiation pattern having two and three nulls are given in Table 4.10 and Table 4.11 respectively.

The numerical results show that the PSO optimizer is capable of restoring the single and multiple nulls in the radiation pattern which are removed due to element failure.

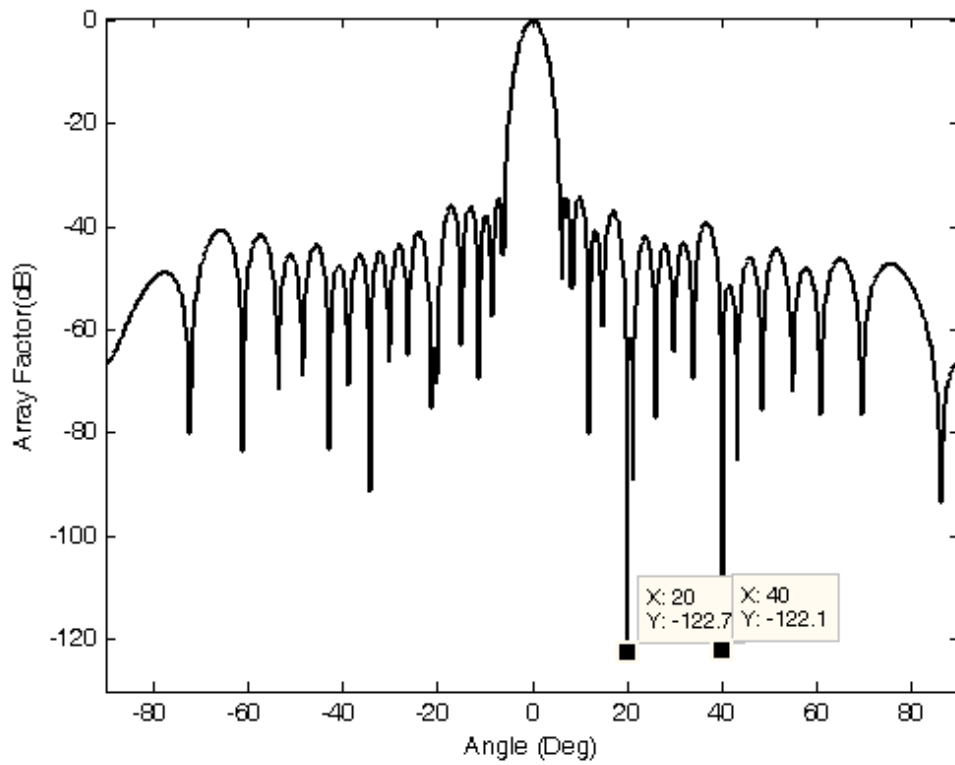


Figure 4.15: Radiation pattern obtained by controlling both the amplitude and the phase excitations to impose nulls at 20° and 40° (Test array pattern)

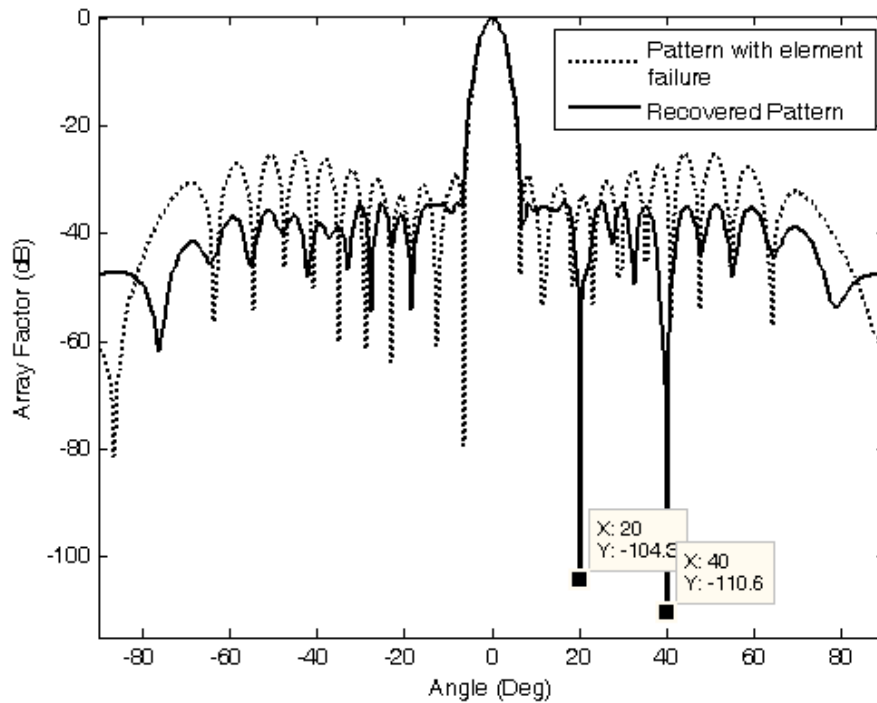


Fig. 4.16: Recovery of pattern with failed elements and have nulls at 20° and 40° directions

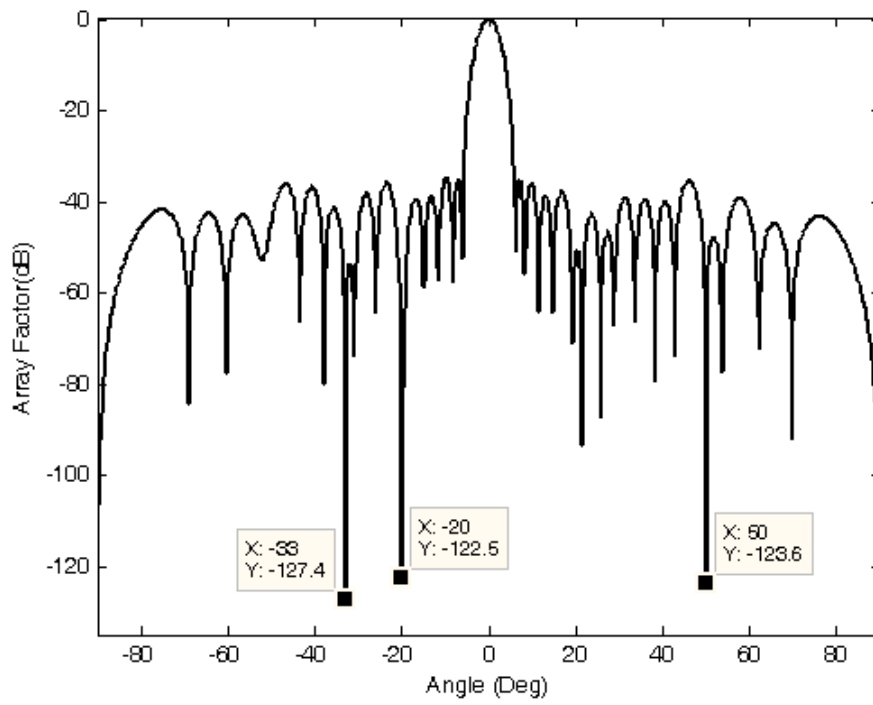


Figure 4.17: Three nulls in the pattern, obtained by re-optimizing complex weights (Test array pattern)

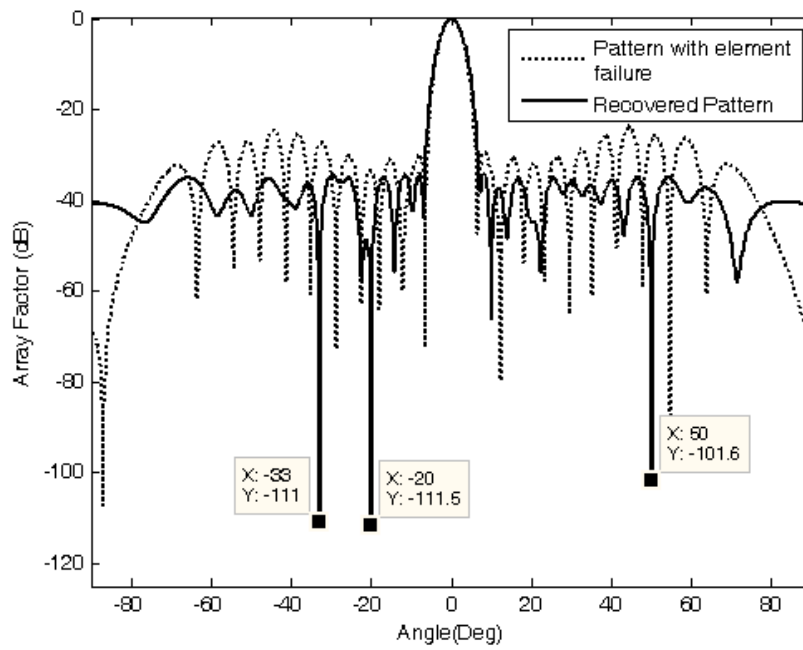


Figure 4.18: Recovery of three nulls in element failure

Table 4.10: Pattern characteristics obtained in recovery of the two null patterns in a failed antenna array

	Pattern characteristics of original test array		Pattern characteristics with failure of two elements( 2 <sup>nd</sup> and 5 <sup>th</sup> )	
	20°	40°	20°	40°
NDL(dB)	122.7dB	122.1dB	-104.3dB	110.6dB
SLL(dB)	-34.44dB		-34.2dB	
HPBW (Deg)	4.36°		4.84°	
FNBW(Deg)	12°		14°	

Table 4.11: Pattern characteristics obtained in recovery of three null patterns in a failed antenna array

	Pattern characteristics of original test array			Recovered pattern characteristics with failure of two elements		
	-20°	-33°	50°	-20°	-33°	50°
NDL(dB)	-127.4	-122.5	-123.6	-111	-111.5	-101.6
SLL(dB)	-34.59			-34.03		
HPBW (Deg)	4.32°			4.9°		
FNBW(Deg)	12°			14°		

### 4.3.2.1 Observations

The recovery of nulls in the radiation pattern of failed antenna array is possible by controlling both amplitude and phase of the remaining working elements. The obtained results in amplitude-phase approach reveals that the value of NDL for the corresponding nulls are slightly higher compared to the NDL obtained in case of amplitude-only approach. The null steering in failed antenna array with amplitude phase control is most effective as it has a larger solution alternative. But at the same time, this approach increases the computational complexity and computation time.

## 4.4 Null Recovery Using BFO

This section discusses the use of BFO [98] for null recovery problem in failed antenna arrays. In order to have a fair comparison between the performance of PSO and BFO in recovering nulls, the same test antennas that were taken for PSO was also considered for BFO. The same problem formulation procedure that was used for PSO was also used here. The parameters of BFO taken for this problem are given in Table 4.12. The simulations were performed on the same platform and with the same objective function as described in the eqn. 4.2. In this section we have limited ourselves to the use of amplitude only approach for BFO to recover the nulls in failed antenna array as the amplitude-phase approach does not provide any significant advantages.

Table 4.12: BFO parameters

Parameters	Value
Number of Bacteria(S)	30
Swimming lenth( $N_s$ )	50
Number of Chemotactic steps $N_c(N_c > N_s)$	50
Number of reproduction ( $N_{re}$ )	10
Number of elimination dispersal events	4
Probability of elimination dispersal ( $P_{ed}$ )	0.25

### ***Case-I: Recovery of Single null with element failure***

In this case the BFO was applied to recover the single null at  $20^\circ$  with two element failure at 2<sup>nd</sup> and 5<sup>th</sup> position in the array. The performance of BFO for placing the null at  $20^\circ$  is demonstrated in Figure 4.19. For ease of comparison, a result from PSO for the same array is overlapped in the same figure. A comparison of the null depth level (NDL) and maximum SLL in the patterns recovered by PSO and BFO is given in Table 4.13.

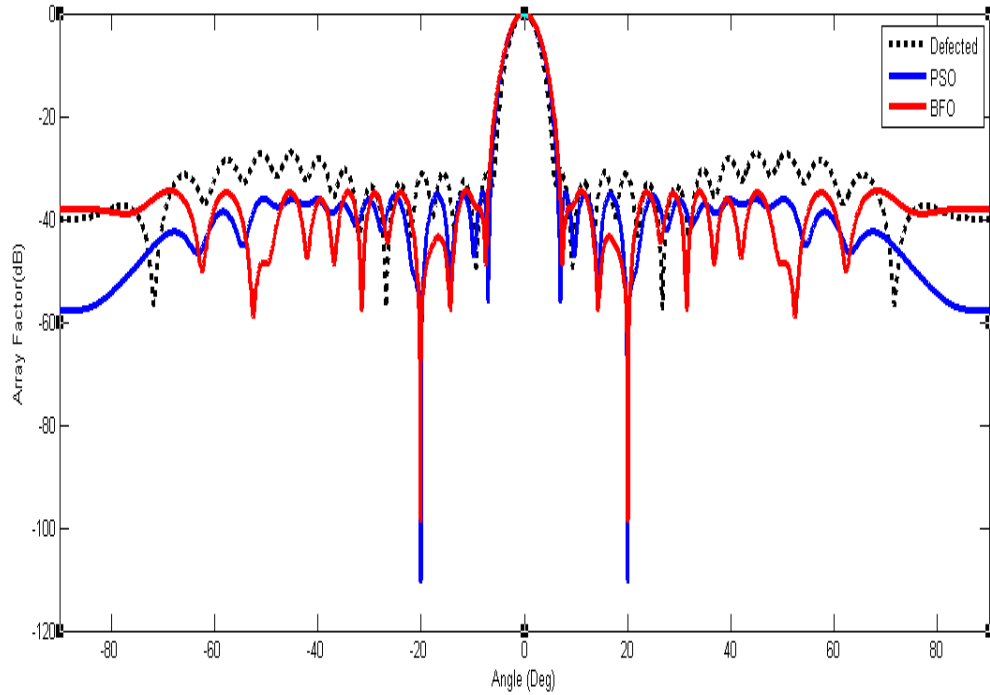


Figure 4.19: Performances of PSO and BFO for placing a null at 20° with element failure.

Table 4.13: Comparison of pattern properties obtained in recovery of single null with two element failure

	PSO	BFO
NDL (dB)	-110.9	-98.56
SLL (dB)	-34.9	-34.47
HPBW	4.83°	5.0°
FNBW	13.5°	14.2°

### ***Case-II: Recovery of two nulls with element failure***

In this case, the same Chebyshev array with the nulls, now at  $\theta_1 = 20^\circ$  and  $\theta_2 = 40^\circ$  with two element failures at 2<sup>nd</sup> and 5<sup>th</sup> position was considered. BFO was executed to place the nulls in its original positions in the failed array. The distorted radiation pattern in the presence of failed elements and the recovered optimized pattern using PSO and BFO with two nulls at 20° and 40° are shown in Figure 4.20. The SLL, NDL and HPBW of the pattern recovered from the implementation of both the optimization process are given in Table 4.14.

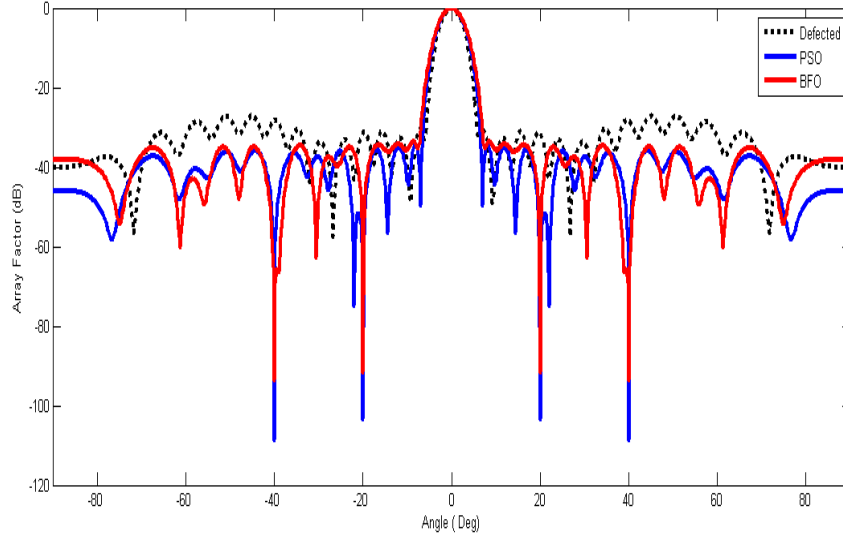


Figure 4.20: Performances of PSO and BFO for placing double null at 20° and 40° with element failure.

Table 4.14: Comparison of pattern properties obtained in recovery of two nulls with two element failure

	PSO	BFO
NDL (dB) at 20°	-103.7	-91.6
NDL(dB) at 40°	-108.4	-93.72
SLL (dB)	-34.31	-33.88
HPBW	4.88°	5.12°
BWFN	13.5°	14.2°

### **Case-III: Recovery of three nulls with element failure**

In this case a pattern with three nulls located at 20°, 33° and 50° was considered. Figure 4.21 shows the performance of application of both the optimization process. The recovery of all the three nulls at the specified positions of the recovered pattern can be clearly marked from this figure. The parameters of the recovered pattern obtained from both the optimization techniques are given in Table 4.15.

Table 4.15: Comparison of pattern properties obtained in recovery of three null with two element failure

	PSO	BFO
NDL (dB) at 20°	-110	-99.07
NDL(dB) at 33°	-108.5	-97.18
NDL (dB) at 50°	-99.02	-92.7
SLL (dB)	-34.62	-34.1
HPBW	4.84°	5.14°
BWFN	13.6°	14.2°



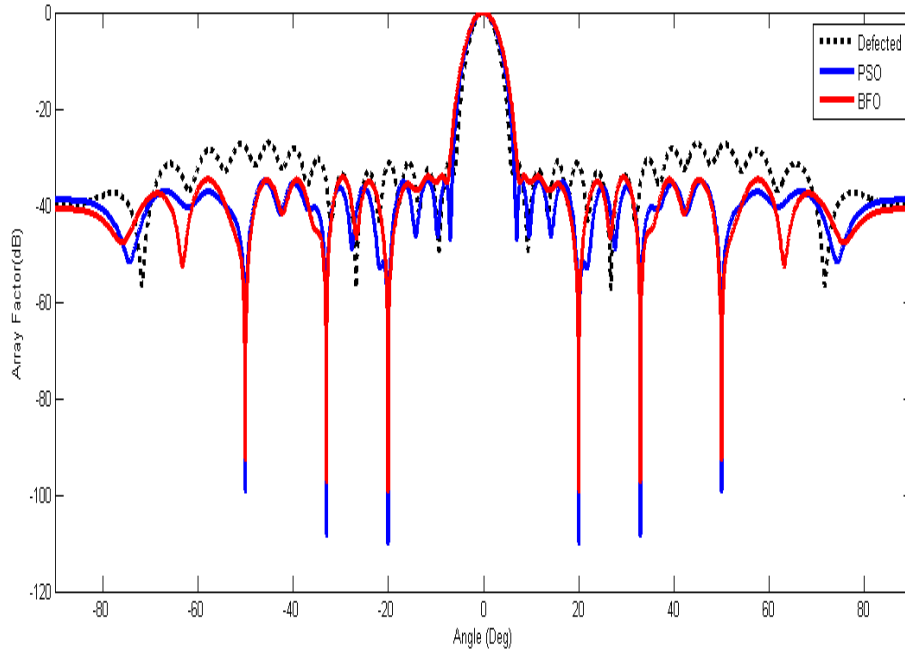


Figure 4.21: Performances of PSO and BFO for placing three nulls at a  $20^\circ$ ,  $33^\circ$  and  $50^\circ$  with element failure.

## 4.5 Performance Comparison of PSO with BFO for Null Recovery

The performances of the two optimization algorithms, PSO and BFO, for null steering in the failed antenna array were observed by performing the simulations on a same platform and with a same objective function. Same stopping criteria was used for the both the optimizers. It was observed that the PSO optimizer converged after 1250 iteration whereas BFO required 1400 iterations to reach the correct solution. The average computation time taken by PSO and BFO for the null steering problem is 128 sec and 560 sec respectively. All the cases of the null steering problem considered in this chapter reveal that the nulls obtained by PSO optimizer are deeper compared to BFO. The optimized amplitudes excitations obtained from BFO for placing the single and multiple nulls are given in Table 4.16.

Table 4.16: Element excitations obtained using BFO

Element Position	Single Null Recovery	Two Null Recovery	Three Null Recovery
1	0.0018	0.0098	0.0011
2	0	0	0
3	0.0493	0.0025	0.0303
4	0.0710	0.0362	0.0878
5	0	0	0
6	0.1885	0.0946	0.1749
7	0.2090	0.0696	0.2924
8	0.2714	0.1157	0.3825
9	0.3159	0.1895	0.4834
10	0.4379	0.2814	0.5779
11	0.4804	0.3235	0.6509
12	0.6051	0.4043	0.7511
13	0.6815	0.4612	0.8237
14	0.7711	0.5913	0.8250
15	0.8465	0.6642	0.9143
16	0.9029	0.7362	1.0000
17	0.9486	0.8529	0.9663
18	1.0000	0.8760	0.9783
19	0.9472	0.8906	0.9243
20	0.9389	0.9209	0.8708
21	0.8926	1.0000	0.8094
22	0.8258	0.9417	0.7107
23	0.8107	0.9011	0.7071
24	0.6635	0.8653	0.5537
25	0.6132	0.7535	0.4558
26	0.5023	0.6923	0.3732
27	0.4747	0.6372	0.3046
28	0.4011	0.5167	0.2503
29	0.2852	0.4362	0.1688
30	0.1653	0.3595	0.1111
31	0.1190	0.2696	0.0621
32	0.1248	0.2182	0.0850

## 4.6 Summary

This chapter analyzed the problem of null recovery in a failed antenna array. This task was formulated as an optimization problem and solved using two optimization techniques i.e., PSO and BFO. The role of the optimization techniques in this problem was to find the optimized set of the current excitations of the remaining working elements in the failed array to reduce the SLL and steer nulls back to their original positions. The effectiveness of the proposed methodology was tested for the recovery of single, multiple and broad nulls in the radiation pattern in the presence of defective elements.

The performance of BFO, which is comparatively a new optimization tool to antenna engineers, was examined with that of PSO. In this problem it was found that PSO performs better in terms convergence, computation time and also the nulls obtained by PSO are deeper compared to BFO. Therefore, PSO can be a better choice for dealing with null steering in failed antenna arrays.



# Limits of Compensation in a Failed Antenna Array

---

## 5.1 Introduction

In the previous chapters, the use of PSO and BFO was discussed for array failure compensation. Although it is not possible to restore the pattern fully by rearranging the excitations of the working elements, these compensation methods focus on restoring one performance parameter of the array and at the same time makes a tradeoff with some other parameters. This chapter focuses on finding the limits on the performance parameters of an array with failed elements.

This limit of compensation is studied from two different aspects. The first investigation is carried out to determine the minimum number of operational elements whose excitations need to be adjusted to restore the radiation pattern of the array, while the second one is to determine the maximum number of element failures in an array that can be compensated. Although results for a specific array have been presented in this thesis, by similar extensive analysis for other arrays, it has been found that the results obtained are quite general in nature and equally applicable for other arrays. In this work, we have employed the amplitude-only weight synthesis process to restore the damaged array pattern, as the variation of the phase of the weights has very little effect on SLL. In practice, methods for changing the complex weights for restoring the sidelobes are slow and ineffective for large antenna arrays because of hardware complexity in its implementation.

## 5.2 Investigation on Minimum Number of Element Excitations Required for Pattern Restoration

In this chapter the investigations are made on a 32-element linear Chebyshev array with inter-element spacing of  $\lambda/2$ . The radiation pattern of the array has the maximum SLL -30dB, BWFN 10.4° and HPBW 3.88°. The method adopted in this phase of the work is the same that was discussed in previous chapters, where the recovery of radiation pattern was approached as an optimization problem and solved using PSO. The performance of the PSO based compensation technique was tested on the Chebyshev array with failure of an element located at different positions. The distorted pattern due to the presence of failed element increases the SLL from -30dB to higher levels and also the half-power beamwidth (HPBW), depending on the failed element position. In this case, the goal is to restore the peak sidelobe power of the failed array near to its original value by re-optimizing the amplitude excitations of minimum number of the remaining working elements.

In the first attempt, the element failure was considered randomly at 5<sup>th</sup> position. The amplitude excitations of 6 working elements were considered as the optimization parameters and new amplitude excitations were calculated for those six working elements to restore the pattern. The performance of PSO for this case is shown in Figure 5.1 for a broadside array. The obtained corrected pattern has SLL of -29.99dB and HPBW of 4.14°. So for this array with element failure at 5<sup>th</sup> position, pattern recovery is possible even by perturbing a minimum of 6 elements, i.e., 19% of the total elements.

In each subsequent attempt, investigations were carried out to determine the minimum number of elements whose excitations need to be changed for pattern recovery, when the location and number of the failed elements are varied in the array. First the compensation process was observed by changing the position of the failed element and then by varying the number of failed elements in the array. After recovering the pattern successfully for a

failed element at 5<sup>th</sup> position, the compensation procedure was applied on an array having faults located at 6<sup>th</sup>, 7<sup>th</sup>, 8<sup>th</sup> and 9<sup>th</sup> positions, consecutively. The aim in each case of pattern recovery is to obtain the minimum number of functional elements whose excitations have to be adjusted. It was found that the excitations of minimum 8, 12, 14 and 16 numbers of the elements have to be adjusted when the element failure occurred at 6<sup>th</sup>, 7<sup>th</sup>, 8<sup>th</sup> and 9<sup>th</sup> positions, respectively, to produce a pattern with minimal loss of quality in the system performance.

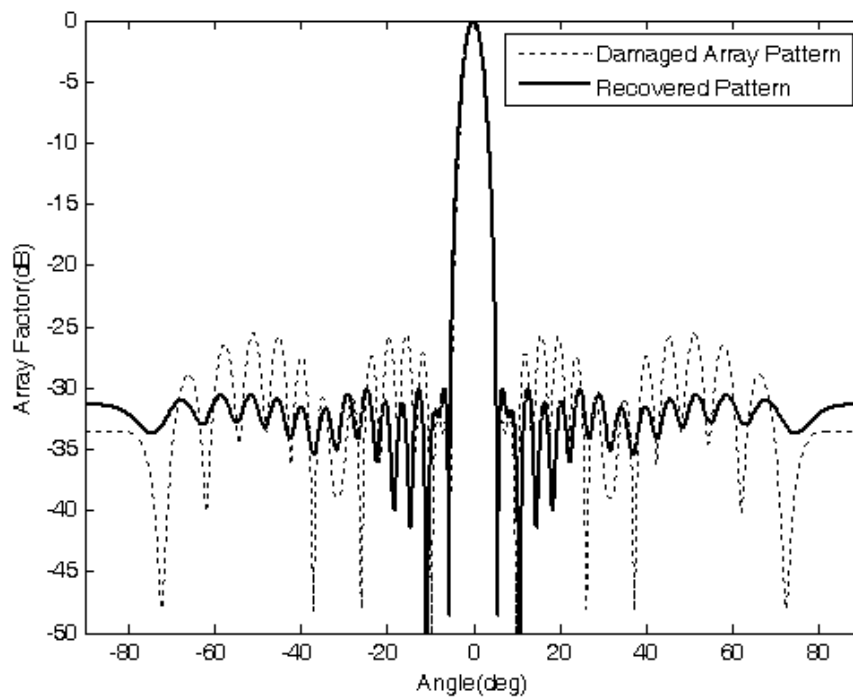


Figure 5.1: Compensation for element failure at 5<sup>th</sup> position by adjusting 6 of the remaining elements (solid line shows the corrected pattern, dotted line shows the defected pattern)

The results of this compensation process for failure of elements at different positions are shown in Table 5.1. The corresponding distorted and recovered patterns are shown in Figures 5.1-5.5.

This shows that the array failure compensation can be possible by perturbing the excitation values of some of the working elements near to the defective one and this limiting value is different for faults at different positions. If the designer has apriori information about these limitations, the compensation process will be easier.

Table 5.1: Compensation for single element failure at different positions in the array carried out by optimizing minimum number of working elements

Failed Position	Maximum SLL of Damaged Pattern	HPBW of damaged Pattern	No. of Elements excitation adjusted	Position of the Compensating Element	Recovered SLL (dB)	HPBW of Recovered Pattern
5	-25.52dB	3.95°	6	1 <sup>st</sup> , 6 <sup>th</sup> , 7 <sup>th</sup> , 8 <sup>th</sup> , 9 <sup>th</sup> , 32 <sup>nd</sup>	-29.99	4.14°
6	-25.1dB	3.94°	8	1 <sup>st</sup> , 2 <sup>nd</sup> , 7 <sup>th</sup> , 8 <sup>th</sup> , 9 <sup>th</sup> , 10 <sup>th</sup> , 11 <sup>th</sup> , 32 <sup>nd</sup>	-29.8	4.2°
7	-24.38dB	3.93°	12	1 <sup>st</sup> , 2 <sup>nd</sup> , 3 <sup>rd</sup> , 4 <sup>th</sup> , 5 <sup>th</sup> , 6 <sup>th</sup> , 8 <sup>th</sup> , 9 <sup>th</sup> , 10 <sup>th</sup> , 11 <sup>th</sup> , 12 <sup>th</sup> , 32 <sup>nd</sup>	-29.85	4.35°
8	-23.9dB	3.91°	14	1 <sup>st</sup> , 2 <sup>nd</sup> , 3 <sup>rd</sup> , 4 <sup>th</sup> , 5 <sup>th</sup> , 6 <sup>th</sup> , 7 <sup>th</sup> , 9 <sup>th</sup> , 10 <sup>th</sup> , 11 <sup>th</sup> , 12 <sup>th</sup> , 13 <sup>th</sup> , 14 <sup>th</sup> , 32 <sup>nd</sup>	-29.27	4.5°
9	-23.43dB	3.89°	16	1 <sup>st</sup> , 2 <sup>nd</sup> , 3 <sup>rd</sup> , 4 <sup>th</sup> , 5 <sup>th</sup> , 6 <sup>th</sup> , 7 <sup>th</sup> , 8 <sup>th</sup> , 10 <sup>th</sup> , 11 <sup>th</sup> , 12 <sup>th</sup> , 13 <sup>th</sup> , 14 <sup>th</sup> , 15 <sup>th</sup> , 16 <sup>th</sup> , 32 <sup>nd</sup>	-29.6	4.8°

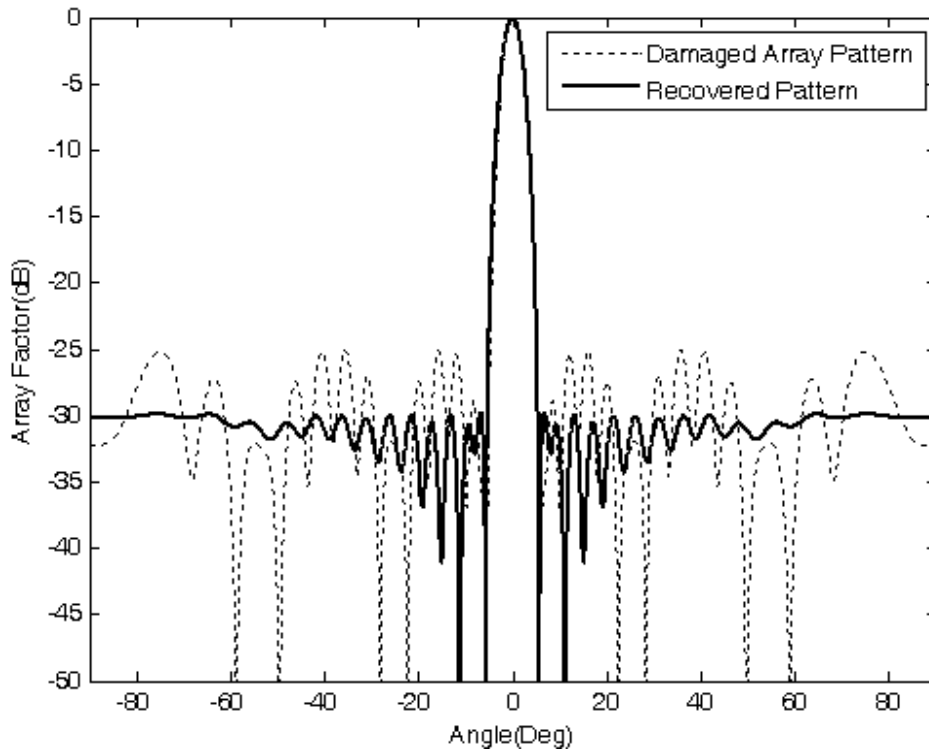


Figure 5.2: Compensation for element failure at 6<sup>th</sup> position by adjusting 8 of the remaining elements



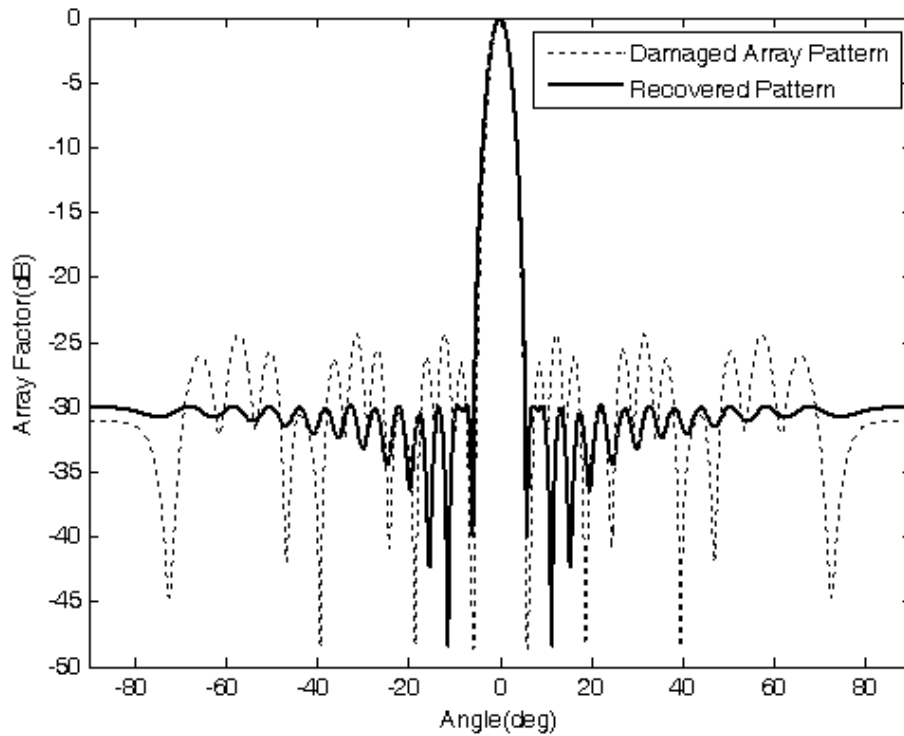


Figure 5.3: Compensation for element failure at 7<sup>th</sup> position by adjusting 12 of the remaining elements

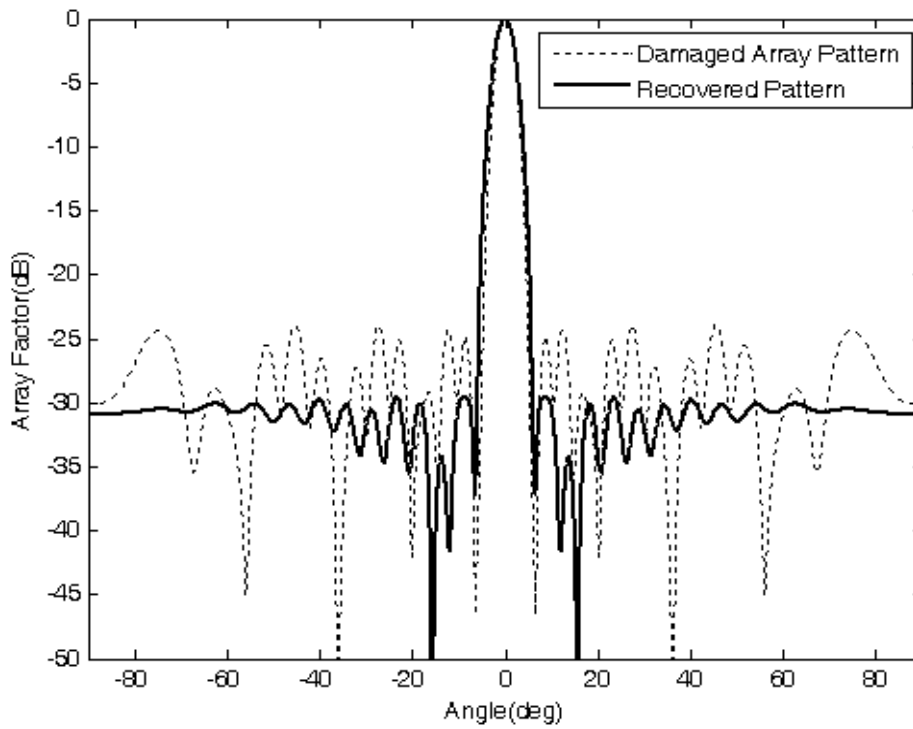


Figure 5.4: Compensation for element failure at 8<sup>th</sup> position by adjusting 14 of the remaining elements

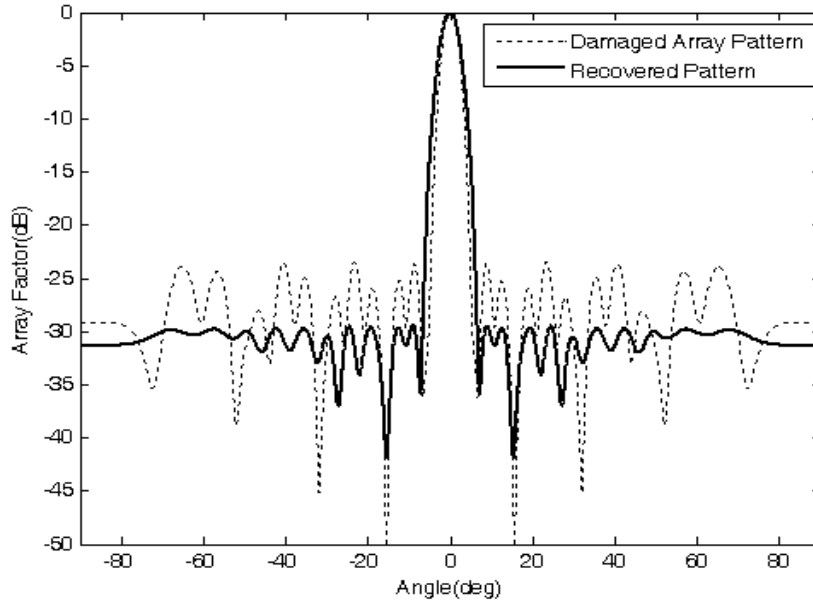


Figure 5.5: Compensation for element failure at 9<sup>th</sup> position by adjusting 16 of the remaining elements

In the next phase, the same compensation approach was applied to the array having multiple failed elements with an aim to produce a pattern with minimal loss of quality in the system performance. Initially, a two element failure was considered randomly at 2<sup>nd</sup> and 7<sup>th</sup> positions in the array and for the recovery of radiation pattern the amplitude excitations of a minimum of 12 elements were adjusted. Another two element failure at 2<sup>nd</sup> and 8<sup>th</sup> positions was also considered and it was found that in this case, the excitations of the 14 elements need to be adjusted. Similarly, two different cases of three element failure and four element failure were taken into consideration and the minimum number of functional elements required for the compensation was obtained. The results for the compensation process are shown in Table 5.2.

It was observed that when there is a single element failure at 7<sup>th</sup> position, a minimum of 12 elements took part in the compensation. At the same time the pattern recovery for the cases of two element failure (2<sup>nd</sup> and 7<sup>th</sup>), three element failure (2<sup>nd</sup>, 3<sup>rd</sup> and 7<sup>th</sup>), and four element failure (2<sup>nd</sup>, 3<sup>rd</sup>, 5<sup>th</sup> and 7<sup>th</sup>) in the same antenna array was possible by adjusting the excitations of same numbers of elements. So it is possible to recover the radiation pattern by changing the excitations of 12 elements when four elements at different positions before the 7<sup>th</sup> positions became nonoperational. Similar results

were obtained for all the cases that were investigated. The optimized excitations of the functional elements which were involved in the process of compensation are reported in Table 5.3 and Table 5.4.

Table 5.2: Compensation for multiple element failure in the array carried out by optimizing minimum number of working elements

<b>Two Element Failure</b>						
Failed Position	Damaged Pattern		No of Elements excitation adjusted	Position of the Compensating Element	Recovered Pattern	
	Max <sup>m</sup> SLL (dB)	HPBW			Max <sup>m</sup> SLL (dB)	HPBW
2,7	-22.93	4.0°	12	1 <sup>st</sup> , 3 <sup>rd</sup> , 4 <sup>th</sup> , 5 <sup>th</sup> , 6 <sup>th</sup> , 8 <sup>th</sup> , 9 <sup>th</sup> , 10 <sup>th</sup> , 11 <sup>th</sup> , 12 <sup>th</sup> , 13 <sup>th</sup> , 32 <sup>nd</sup>	-29.83	4.4°
2,8	-22.76	3.98°	14	1 <sup>st</sup> , 3 <sup>rd</sup> , 4 <sup>th</sup> , 5 <sup>th</sup> , 6 <sup>th</sup> , 7 <sup>th</sup> , 9 <sup>th</sup> , 10 <sup>th</sup> , 11 <sup>th</sup> , 12 <sup>th</sup> , 13 <sup>th</sup> , 14 <sup>th</sup> , 15 <sup>th</sup> , 32 <sup>nd</sup>	-29.79	4.64°
<b>Three Element Failure</b>						
Failed Position	Damaged Pattern		No of Elements excitation adjusted	Position of the Compensating Element	Recovered Pattern	
	Max <sup>m</sup> SLL (dB)	HPBW			Max <sup>m</sup> SLL (dB)	HPBW
2,3,7	-22.44	4.08°	12	1 <sup>st</sup> , 4 <sup>th</sup> , 5 <sup>th</sup> , 6 <sup>th</sup> , 8 <sup>th</sup> , 9 <sup>th</sup> , 10 <sup>th</sup> , 11 <sup>th</sup> , 12 <sup>th</sup> , 13 <sup>th</sup> , 14 <sup>th</sup> , 32 <sup>nd</sup>	-29.95	4.66°
2,5,8	-20.4	4.06°	14	1 <sup>st</sup> , 3 <sup>rd</sup> , 4 <sup>th</sup> , 6 <sup>th</sup> , 7 <sup>th</sup> , 9 <sup>th</sup> , 10 <sup>th</sup> , 11 <sup>th</sup> , 12 <sup>th</sup> , 13 <sup>th</sup> , 14 <sup>th</sup> , 15 <sup>th</sup> , 16 <sup>th</sup> , 32 <sup>nd</sup>	-29.82	4.82°
<b>Four Element Failure</b>						
Failed Position	Damaged Pattern		No of Elements excitation adjusted	Position of the Compensating Element	Recovered Pattern	
	Max <sup>m</sup> SLL (dB)	HPBW			Max <sup>m</sup> SLL (dB)	HPBW
2,3,5,7	-21.6	4.17°	12	1 <sup>st</sup> , 4 <sup>th</sup> , 6 <sup>th</sup> , 8 <sup>th</sup> , 9 <sup>th</sup> , 10 <sup>th</sup> , 11 <sup>th</sup> , 12 <sup>th</sup> , 13 <sup>th</sup> , 14 <sup>th</sup> , 15 <sup>th</sup> , 32 <sup>nd</sup>	-29.87	4.78°
3,4,6,8	-20.55	4.16°	14	1 <sup>st</sup> , 2 <sup>nd</sup> , 5 <sup>th</sup> , 7 <sup>th</sup> , 9 <sup>th</sup> , 10 <sup>th</sup> , 11 <sup>th</sup> , 12 <sup>th</sup> , 13 <sup>th</sup> , 14 <sup>th</sup> , 15 <sup>th</sup> , 16 <sup>th</sup> , 17 <sup>th</sup> , 32 <sup>nd</sup>	-29.8	4.96°

Table 5.3: Amplitude weights computed for single element failure at different positions (as given in Table 5.1) in a 32- element array

Element Position	Initial Chebyshev Pattern	Optimized weights computed for single element failure at different positions as given in Table-I in the antenna array				
		5	6	7	8	9
1	0.44388	<b>0.168256</b>	<b>0.116</b>	<b>0.01346</b>	<b>0.00005</b>	<b>0.0001</b>
2	0.24331	0.24331	<b>0.1174</b>	<b>0.12482</b>	<b>0.061533</b>	<b>0.089</b>
3	0.30354	0.30354	0.30354	<b>0.16248</b>	<b>0.1112</b>	<b>0.038</b>
4	0.36838	0.36838	0.36838	<b>0.24568</b>	<b>0.144267</b>	<b>0.0403</b>
5	0.43670	<b>0</b>	0.43670	<b>0.33968</b>	<b>0.2323</b>	<b>0.0559</b>
6	0.50723	<b>0.560467</b>	<b>0</b>	<b>0.44534</b>	<b>0.329383</b>	<b>0.125</b>
7	0.57851	<b>0.515578</b>	<b>0.624775</b>	<b>0</b>	<b>0.449783</b>	<b>0.198</b>
8	0.64897	<b>0.55978</b>	<b>0.587075</b>	<b>0.61244</b>	<b>0</b>	<b>0.2971</b>
9	0.71699	<b>0.6324</b>	<b>0.60885</b>	<b>0.61578</b>	<b>0.615267</b>	<b>0</b>
10	0.78094	0.78094	<b>0.739525</b>	<b>0.67658</b>	<b>0.646867</b>	<b>0.529</b>
11	0.83923	0.83923	<b>0.7662</b>	<b>0.74736</b>	<b>0.70785</b>	<b>0.5009</b>
12	0.89036	0.89036	0.89036	<b>0.79814</b>	<b>0.765767</b>	<b>0.5374</b>
13	0.93301	0.93301	0.93301	0.93301	<b>0.832683</b>	<b>0.6252</b>
14	0.96604	0.96604	0.96604	0.96604	<b>0.893117</b>	<b>0.67</b>
15	0.98858	0.98858	0.98858	0.98858	0.98858	<b>0.7507</b>
16	1.00000	1.00000	1.00000	1.00000	1.00000	<b>0.803</b>
17	1.00000	1.00000	1.00000	1.00000	1.00000	1.00000
18	0.98858	0.98858	0.98858	0.98858	0.98858	0.98858
19	0.96604	0.96604	0.96604	0.96604	0.96604	0.96604
20	0.93301	0.93301	0.93301	0.93301	0.93301	0.93301
21	0.89036	0.89036	0.89036	0.89036	0.89036	0.89036
22	0.83923	0.83923	0.83923	0.83923	0.83923	0.83923
23	0.78094	0.78094	0.78094	0.78094	0.78094	0.78094
24	0.71699	0.71699	0.71699	0.71699	0.71699	0.71699
25	0.64897	0.64897	0.64897	0.64897	0.64897	0.64897
26	0.57851	0.57851	0.57851	0.57851	0.57851	0.57851
27	0.50723	0.50723	0.50723	0.50723	0.50723	0.50723
28	0.43670	0.43670	0.43670	0.43670	0.43670	0.43670
29	0.36838	0.36838	0.36838	0.36838	0.36838	0.36838
30	0.30354	0.30354	0.30354	0.30354	0.30354	0.30354
31	0.24331	0.24331	0.24331	0.24331	0.24331	0.24331
32	0.44388	<b>0.174067</b>	<b>0.119</b>	<b>0.13028</b>	<b>0.121433</b>	<b>0.1095</b>

Table 5.4: Optimized amplitude weights computed for multiple element failure at different positions (as given in Table 5.2) in a 32- element array

		Optimized weights computed for multiple element failure at different positions as given in Table-II in the antenna array					
Element Positions	Initial Chebyshev Pattern	Two element failure		Three element failure		Four element failure	
		2,7	2,8	2,3,7	2,5,8	2,3,5,7	3,4,6,8
1	0.44388	0.06121	0.01865	0.0059	0.00055	0.016025	0.000133
2	0.24331	0	0	0	0	0	0.000933
3	0.30354	0.1059	0.0524	0	0.023	0	0
4	0.36838	0.20956	0.102433	0.1502	0.068875	0.13335	0
5	0.43670	0.3044	0.167817	0.1556	0	0	0.154633
6	0.50723	0.39943	0.269483	0.2929	0.220288	0.325075	0
7	0.57851	0	0.376433	0	0.344688	0	0.2855
8	0.64897	0.58233	0	0.4955	0	0.2899	0
9	0.71699	0.546	0.5545	0.5053	0.466813	0.5131	0.3316
10	0.78094	0.58775	0.55045	0.5193	0.462563	0.477275	0.553433
11	0.83923	0.68051	0.62165	0.6179	0.64225	0.50665	0.4735
12	0.89036	0.80571	0.681067	0.6896	0.6086	0.6356	0.507333
13	0.93301	0.81741	0.759	0.7207	0.697375	0.7006	0.639167
14	0.96604	0.96604	0.852733	0.7898	0.73485	0.748625	0.7296
15	0.98858	0.98858	0.889717	0.98858	0.8467	0.877925	0.808633
16	1.00000	1.00000	1.00000	1.00000	0.927863	1.00000	0.887667
17	1.00000	1.00000	1.00000	1.00000	1.00000	1.00000	0.954
18	0.98858	0.98858	0.98858	0.98858	0.98858	0.98858	0.98858
19	0.96604	0.96604	0.96604	0.96604	0.96604	0.96604	0.96604
20	0.93301	0.93301	0.93301	0.93301	0.93301	0.93301	0.93301
21	0.89036	0.89036	0.89036	0.89036	0.89036	0.89036	0.89036
22	0.83923	0.83923	0.83923	0.83923	0.83923	0.83923	0.83923
23	0.78094	0.78094	0.78094	0.78094	0.78094	0.78094	0.78094
24	0.71699	0.71699	0.71699	0.71699	0.71699	0.71699	0.71699
25	0.64897	0.64897	0.64897	0.64897	0.64897	0.64897	0.64897
26	0.57851	0.57851	0.57851	0.57851	0.57851	0.57851	0.57851
27	0.50723	0.50723	0.50723	0.50723	0.50723	0.50723	0.50723
28	0.43670	0.43670	0.43670	0.43670	0.43670	0.43670	0.43670
29	0.36838	0.36838	0.36838	0.36838	0.36838	0.36838	0.36838
30	0.30354	0.30354	0.30354	0.30354	0.30354	0.30354	0.30354
31	0.24331	0.24331	0.24331	0.24331	0.24331	0.24331	0.24331
32	0.44388	0.1247	0.11405	0.1233	0.116363	0.1367	0.120033

### **5.2.1 Observations**

From the above analysis of pattern recovery with minimum number of working element excitations, the following important observations were made:

- The minimum number of working elements required for compensation mostly depends on the position of the faulty elements. When the position of the failed element is nearer to the centre of the array, the excitations of more number of functional elements need to be adjusted for performance restoration.
- It can also be observed that the set of working elements that take part in the compensation process must include the corner elements i.e. the first and last element of the array. Another important observation is that, all the elements whose excitations need to be adjusted lie in that half of the array in which the faulty element is located.
- Furthermore, it was observed that the failure of the elements have a more profound effect on SLL while HPBW is less affected. But the restoration of the SLL to the desired value is possible at the cost of a broader main beam.

## **5.3 Investigation on maximum number of element failure that can be compensated**

In this section the investigation was performed to determine another limiting parameter, i.e. the maximum number of element failures in the antenna array for which the compensation is possible, without a substantial degradation in its performance. As the number of failed elements increases, the gain of the antenna array in the desired direction decreases. The compensation techniques applied to a failed array can recover the pattern only for a certain maximum number of element failures, beyond which the performance of compensated array falls below a specified level of acceptability. Different numbers of element failures were considered in the array with a goal for determining the maximum number of element failures for which the pattern can be recovered. Specifically, the criteria were to

achieve a SLL close to -30dB and the HPBW within a specified limit, which was considered to be 50% greater than the value of the original array. Table 5.5 shows the SLL, HPBW and BWFN of the recovered pattern for different number of element failures in the test array. It is evident from the results that the compensation technique applied on the failed antenna array effectively performs the job of sidelobe suppression. The SLL can be successfully recovered even for larger number of failures. Although the recovery of SLL is accompanied by a reduction in BWFN, the recovered pattern has a broader beamwidth compared to that of the original pattern. Thus the SLL recovery is at the cost of some loss in directivity and gain. The results presented in Table 5.5 show that in a 32-element array, a maximum of 10-element failures can be compensated. The recovered pattern for the 10-element failure has SLL of -30 dB and HPBW  $5.76^\circ$  which is 48% larger and BWFN is  $14.8^\circ$  which is 43% larger than their respective original values. It was found that if the number of failed elements is increased beyond 10, the recovered pattern will have SLL of -29.97dB with HPBW of  $6.0^\circ$ . In that case the beamwidth crosses the limiting value and hence the gain falls below the level of acceptability. Therefore, for the present array, the compensation technique enables the recovery of reasonable antenna performance when a maximum of 10 elements, i.e., nearly 30% of elements are not operational.

To further investigate this, the same procedure was also implemented on a 20-element linear Chebyshev broadside array having SLL -30dB, BWFN of  $17^\circ$ , HPBW of  $6.3^\circ$ . The compensation method applied on the array for different number of failures and the obtained results are presented in Table 5.6. It can be seen that in a 20-element array, when a maximum of 6 elements become non-operational, it is possible to recover the pattern having SLL close to -30dB and the HPBW below the limit, i.e. 50% larger than the original pattern. When one more element fails in the array, the beamwidth goes beyond this limit. So, in this case also, pattern restoration is possible for 30% of element failure in array. The results in Table 5.5 and Table 5.6 show that the maximum SLL of the recovered antenna is achieved by sacrificing some other parameters within the limit of acceptability. The

optimized amplitude excitations obtained for the above cases are given in Table 5.7 and Table 5.8, respectively.

Table 5.5: Pattern Recovery for maximum number of element failure in a 32-element linear array

NO. OF FAILED ELEMENTS	POSITION OF FAILED ELEMENTS	%AGE OF FAILURE	FAILED ANTENNA ARRAY PATTERN CHARACTERISTICS			RECOVERED ARRAY PATTERN CHARACTERISTICS		
			MAX <sup>M</sup> SLL (DB)	HPBW (DEG.)	BWFN (DEG.)	MAX <sup>M</sup> SLL (DB)	HPBW (DEG.)	BWFN (DEG.)
2	2,3	6	-26.48	4.0	16.0	-30.0	4.1	10.6
3	2,3,4	9	-25.19	4.08	18.0	-30.0	4.3	11.2
4	2,3,4,5	12	-23.81	4.16	18.0	-30.02	4.58	11.8
5	2,3,4,5,6	16	-22.26	4.24	18.0	-30.01	4.75	12.4
6	2,3,4,5,6,7	19	-20.85	4.34	18.0	-30.04	5.0	13.2
7	2,3,4,5,6,7,8	22	-19.91	4.45	20.0	-30.01	5.2	13.8
8	2,3,4,5,6,7,8,9	25	-19.63	4.58	20.0	-30.01	5.44	14.0
9	2,3,4,5,6,7,8,9,10	28	-21.6	4.72	32.0	-30.0	5.74	14.8
10	1,2,3,4,5,6,7,8,9,10	31	-20.53	5.1	22.0	-30.0	5.76	14.8

Table 5.6: Pattern recovery for maximum number of element failure in a 20-element linear array

NO. OF FAILED ELEMENTS	POSITION OF FAILED ELEMENTS	%AGE OF FAILURE	FAILED ANTENNA ARRAY PATTERN CHARACTERISTICS			RECOVERED ARRAY PATTERN CHARACTERISTICS		
			MAX <sup>M</sup> SLL (DB)	HPBW (DEG.)	BWFN (DEG.)	MAX <sup>M</sup> SLL (DB)	HPBW (DEG.)	BWFN (DEG.)
2	2,3	10%	-23.62	6.6	18	-30.09	7.8	22
3	2,3,4	15%	-21.32	6.8	20	-30.04	8.0	22
4	2,3,4,5	20%	-18.27	7.1	20	-30.01	8.6	24
5	2,3,4,5,6	25%	-15.99	7.6	20	-30.01	9.2	26
6	1,2,3,4,5,6	30%	-14.44	8.0	22	-30.03	9.4	26



Table 5.7: Optimized amplitude weights computed for multiple element failure at different positions (as given in Table 5.5) in a 32- element array

Element Positions	Initial Chebyshev Pattern	Two element failure	Three element failure	Four element failure	Five element failure	Six element failure	Seven element failure	Eight element failure	Nine element failure	Ten element failure
		2,3	2,3,4	2,3,4,5	2,3,4,5,6	2,3,4,5,6,7	2,3,4,5,6,7,8	2,3,4,5,6,7,8,9	2,3,4,5,6,7,8,9,10	1,2,3,4,5,6,7,8,9,10
1	0.44388	0.178	0.0489	0.0289	0.0074	0.0002	0.0048	0.0011	0.0283	0
2	0.24331	0	0	0	0	0	0	0	0	0
3	0.30354	0	0	0	0	0	0	0	0	0
4	0.36838	0.2923	0	0	0	0	0	0	0	0
5	0.43670	0.386	0.3436	0	0	0	0	0	0	0
6	0.50723	0.3556	0.2266	0.2981	0	0	0	0	0	0
7	0.57851	0.4232	0.333	0.3076	0.3161	0	0	0	0	0
8	0.64897	0.423	0.3944	0.3641	0.261	0.3571	0	0	0	0
9	0.71699	0.5294	0.4943	0.2847	0.3437	0.2347	0.2373	0	0	0
10	0.78094	0.6101	0.4905	0.5894	0.4427	0.2845	0.2863	0.27	0	0
11	0.83923	0.7248	0.6275	0.5678	0.4457	0.4299	0.294	0.3583	0.2272	0.2186
12	0.89036	0.7499	0.6421	0.5868	0.6168	0.5157	0.4153	0.3406	0.2616	0.2328
13	0.93301	0.7608	0.8319	0.8354	0.6322	0.6022	0.4652	0.3953	0.3181	0.2817
14	0.96604	0.9084	0.8279	0.7832	0.7293	0.6786	0.582	0.5298	0.4288	0.3801
15	0.98858	0.8719	0.8495	0.8022	0.8246	0.7316	0.6712	0.6768	0.4819	0.5494
16	1.00000	0.9567	1.0000	0.8939	0.9498	0.8186	0.7529	0.6995	0.6241	0.5605
17	1.00000	0.8656	0.9712	0.9595	0.8995	0.8996	0.7473	0.7741	0.7056	0.6688
18	0.98858	1.0000	0.9763	1.0000	0.9586	0.9313	0.8643	0.9212	0.771	0.7919
19	0.96604	0.9191	0.9902	0.9835	0.9456	0.9652	0.9131	0.8926	0.9353	0.856
20	0.93301	0.935	0.9946	0.8808	0.9864	1	1	0.9009	0.8667	0.9347
21	0.89036	0.8965	0.9223	0.92	1	0.9044	0.7982	1	0.9866	0.8935
22	0.83923	0.7593	0.9191	0.9526	0.9346	0.9308	0.9251	0.8924	0.9412	1
23	0.78094	0.8743	0.8761	0.8375	0.8085	0.9126	0.8959	0.9562	1	0.9801
24	0.71699	0.6992	0.7671	0.7926	0.8292	0.8057	0.7649	0.8042	0.8654	0.8523
25	0.64897	0.6463	0.7379	0.6383	0.743	0.7632	0.8034	0.7808	0.8515	0.8713
26	0.57851	0.6093	0.6711	0.6036	0.6692	0.657	0.6105	0.6867	0.755	0.8293
27	0.50723	0.4347	0.6249	0.5384	0.5491	0.5332	0.5593	0.6165	0.6696	0.6877
28	0.43670	0.5084	0.4248	0.4393	0.5525	0.506	0.4954	0.4753	0.6108	0.571
29	0.36838	0.3926	0.4339	0.4075	0.3397	0.3576	0.3443	0.4374	0.4672	0.4687
30	0.30354	0.3513	0.3322	0.2831	0.2802	0.3958	0.3471	0.3439	0.315	0.4271
31	0.24331	0.2563	0.3245	0.2834	0.3569	0.2706	0.275	0.2216	0.3436	0.3173
32	0.44388	0.2606	0.365	0.2215	0.2486	0.2028	0.211	0.2744	0.2966	0.3502

Table 5.8: Optimized amplitude weights computed for multiple element failure at different positions (as given in Table-5.6) in a 20- element array

Element Positions	Initial Chebyshev Pattern	Two element failure	Three element failure	Four element failure	Five element failure	Six element failure
		2,3	2,3,4	2,3,4,5	2,3,4,5,6	1,2,3,4,5,6
1	0.3256	0.0226	0.0296	0.0002	0.0373	0
2	0.2856	0	0	0	0	0
3	0.3910	0	0	0	0	0
4	0.5046	0.1851	0	0	0	0
5	0.6203	0.3224	0.2878	0	0	0
6	0.7315	0.3325	0.3361	0.2020	0	0
7	0.8310	0.5497	0.4504	0.2755	0.2697	0.6371
8	0.9124	0.6595	0.6084	0.3768	0.3449	0.3029
9	0.9701	0.8143	0.7613	0.6285	0.5459	0.3352
10	1.0000	0.8779	0.8310	0.6782	0.6777	0.5653
11	1.0000	1.0000	0.9047	0.8547	0.7861	0.6987
12	0.9701	0.9472	1.0000	0.9944	0.9672	0.8472
13	0.9124	0.9542	0.9368	0.9870	1.0000	0.9709
14	0.8310	0.8892	0.9203	1.0000	0.9088	1.0000
15	0.7315	0.7345	0.8204	0.9554	0.8721	0.9009
16	0.6203	0.6931	0.6529	0.8682	0.7533	0.8339
17	0.5046	0.4667	0.5490	0.6260	0.5727	0.6534
18	0.3910	0.4483	0.3971	0.5722	0.4054	0.4805
19	0.2856	0.2743	0.2500	0.3917	0.2985	0.3548
20	0.3256	0.0928	0.2087	0.2969	0.1649	0.1842

## 5.4 Summary

In this chapter, an attempt was made to quantify the tolerance level of the compensation in a failed antenna array. An investigation was carried out to determine the minimum number of elements whose excitations need to be

changed to recover the desired SLL. It is found that this number depends on the position(s) of the failed element(s). Another investigation was carried to determine the maximum number of element failures that can be compensated for the pattern recovery within a specified acceptable limit. It is found that for a 50% relaxation in the HPBW, pattern restoration is possible for faults in around 30% of the elements. However, this value varies with the location of the faults. At the same time it was found that if the central element fails the correction of damaged pattern becomes a difficult task. PSO was unable to provide any improvement even by changing its different tuning parameters. Although the results are presented for 32-element and 20-element Chebyshev arrays, the conclusions drawn from the study are equally applicable for other arrays as well. As there is a growing demand to add flexibility in large arrays, these results should be useful while developing self-healing arrays.



# Effect on DoA Estimation in Failed Array

---

## 6.1 Introduction

Antenna arrays play a leading role in meeting the challenges of the modern communication systems such as mobile communication, radar, sonar, wireless LANs etc. It spatially directs the electromagnetic power towards the targets of interest by steering the main beam in that directions and placing the nulls in the direction of interferences. This process is usually known as beamforming. However to maintain the main beam of the radiation pattern of the antenna array in the desired direction, the spatial signature of the source has to be known. This spatial signature of the sources can be estimated by estimating their direction of arrivals (DoAs). This information can be employed to track the sources of interest and null out the other sources as interference.

The DoA estimation is one of the most challenging problems in the field of array signal processing for a quite long time. The purpose of DoA estimation is to estimate the direction of source by using the data received by the array. It exploits either the parametric structure of the array manifold or the properties of the signals. The parameters which affects the estimation of DoA are the inter element spacing of the array, angular separation between the incident signals, signal-to-noise ratio (SNR) etc. A large number of parametric and non parametric methods have been proposed in the literature for estimating unknown signal parameters [126]. These widely used methods include Multiple Signal Classification (MUSIC) [81], Estimation of Signal Parameters via Rotational Invariance Techniques (ESPRIT) [83], and their variants (e.g. Root MUSIC) [82], and Matrix Pencil [127].

The increased interest in DoA estimation leads to new requirements such as estimation with reduced number of snapshots, i.e. the number of temporal samplings of the array. In order to reduce the computational burden of DoA estimation process, use of evolutionary computational techniques have been reported in the literature [84-91].

In this chapter, the focus is to see the effect of element failure on the DoA estimation of a phased array antenna. An attempt has been made to investigate the use of evolutionary algorithm, specifically, PSO for DoA estimation in failed antenna array, which can be used as an input for the beamformer.

## 6.2 Problem Formulation

Let us consider a linear antenna array of N-elements with inter-element spacing  $d$  (Figure 6.1). It is assumed that M numbers of uncorrelated far-field sources transmit signals to the antenna array. The sources are positioned at  $\theta = [\theta_1 \ \theta_2 \ \dots \ \theta_M]^T$ , where  $[\cdot]^T$  represents the transpose operator. The received signals at the terminals of antenna elements can be expressed as a superposition of signals from all the sources and linearly added noise, represented by

$$\mathbf{x}(t) = \sum_{m=1}^M \mathbf{a}(\theta_m) S_m(t) + \mathbf{n}(t) \quad (6.1)$$

where  $\mathbf{x}(t)$  is the received signal vector at the antenna array at time  $t$ , that can be written as:

$$\mathbf{x}(t) = [x_1(t) \ x_2(t) \ \dots \ x_N(t)]^T \quad (6.2)$$

$S_m(t)$  is the incoming plane wave from  $m^{\text{th}}$  source and the signal is arriving from  $\theta_m$  direction

$\mathbf{n}(t)$  represents a  $N \times 1$  vector of additive white Gaussian noise. The noise is either sensed along with the signal or generated inside the system.

Eqn (6.1) can be represented in matrix form as:

$$\mathbf{x}(t) = \mathbf{A}(\boldsymbol{\theta})\mathbf{s}(t) + \mathbf{n}(t) \quad (6.3)$$

where  $\mathbf{A}(\boldsymbol{\theta})$  represent the array response matrix of size  $N \times M$ . It must time-invariant over the observation interval.

Each column of this matrix represents the array response vector for each incident plane wave, represented as:

$$\mathbf{A}(\boldsymbol{\theta}) = [\mathbf{a}(\theta_1) \ \mathbf{a}(\theta_2) \ \cdots \ \mathbf{a}(\theta_M)] \quad (6.4)$$

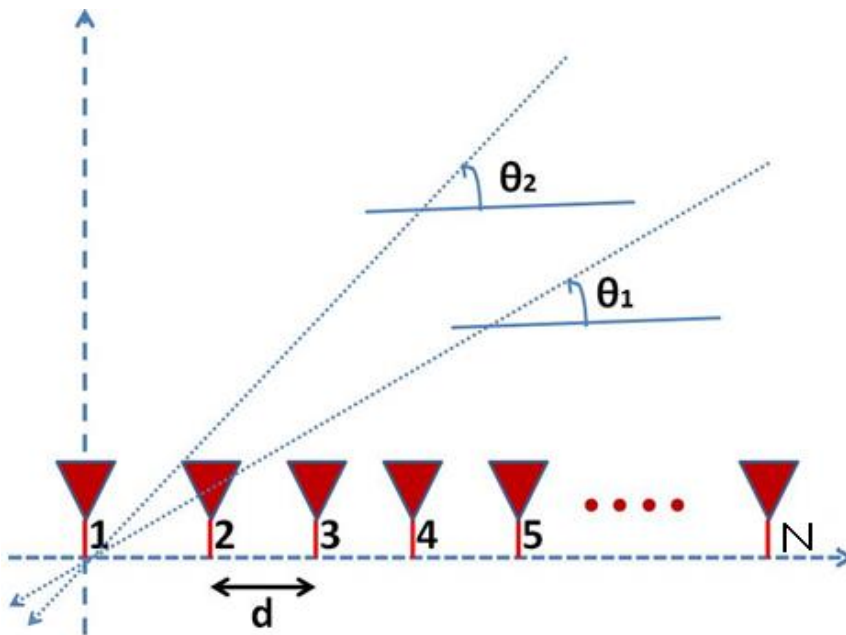


Figure: 6.1 Linear uniform array for DoA estimation

The array response vector for one signal source of a uniform linear array (ULA) consisting of  $N$  isotropic antennas (Figure 6.1) with element spacing  $d$  can be expressed as:

$$\mathbf{a}(\theta_m) = \left[ 1, \exp\left(-j\frac{2\pi}{\lambda}d \cos\theta_m\right), \dots, \exp\left(-j\frac{2\pi}{\lambda}(N-1)d \cos\theta_m\right) \right]^T \quad (6.5)$$

$\mathbf{s}(t)$  is the vector of incoming signals from each source, and can be represented as:

$$\mathbf{s}(t) = [s_1(t) \ s_2(t) \ \cdots \ s_M(t)]^T \quad (6.6)$$

In eqn. (6.3), a single observation of  $\mathbf{x}(t)$  from the array is known as a snapshot. In the present work, the DoA estimation problem was approached with single snapshot. In that case,  $t$  can be assumed as 0 ( $t=0$ ).

The vector  $\mathbf{x}$  of voltages received at the output of the array can be expressed as

$$\mathbf{x} = \sum_{m=1}^M \mathbf{a}(\theta_m) S_m + \mathbf{n} = \mathbf{A}(\boldsymbol{\theta})\mathbf{s} + \mathbf{n} \quad (6.7)$$

which in turn for the N element antenna array can be represented as

$$\mathbf{x} = \left[ \sum_{m=1}^M (s_m + n_1) \quad \sum_{m=1}^M (s_m e^{-j\frac{2\pi}{\lambda} d \cos \theta_m} + n_2) \cdots \sum_{m=1}^M (s_m e^{-j\frac{2\pi}{\lambda} (-1) d \cos \theta_m} + n_N) \right]^T \quad (6.8)$$

In the present case, the aim is to investigate the effects on DoA estimation in the presence of failed antenna elements in the array. When an antenna element encounters a failure it does not receive any signal from the sources. Hence, only noise is present at the output of those faulty elements. Under this circumstance, when the fault is at  $i^{\text{th}}$  element, the array output vector can be represented as:

$$\mathbf{x}(t) = [x_1(t) \quad x_2(t) \cdots x_{i-1}(t) \quad n_i \quad x_N(t)]^T \quad (6.9)$$

From this received signal, the angular directions ( $\theta_i$ ) of the sources have to be determined. This problem can be approached as an optimization problem and solved by using PSO. Because in the present scenario, M numbers of sources are present, therefore according to PSO terminology the search for the solution has to be performed in an M-dimensional space with each dimension representing a possible direction of arrival. These known values of DoA can vary between  $0^\circ$  and  $180^\circ$ .

In order to solve the problem using PSO, the fitness function was framed as the correlation between the estimated and actual signal received at the antenna array. The estimated signal is generated by the PSO optimizer corresponding to each candidate point in the solution space. This estimated signal is called as synthetic snapshot, represented by  $\mathbf{x}_g$ . Hence, the fitness function can be expressed as:



$$f = 1 - \frac{\sum_{i=1}^M x_i x_{gi}^*}{\|x\| \|x_g\|} \quad (6.10)$$

where  $\|x\| = \sqrt{\sum_{i=1}^M x_i x_i}$

The role of the PSO is to update the candidate solution point in each iteration and hence to minimize the difference between the actual and synthetic snapshot.

### 6.3 PSO for DoA Estimation

Before starting the PSO iteration process, the unknown parameters (DoAs) were initialized with suitable lower and upper bounds. For the present problem these bounds are  $0^\circ$  and  $180^\circ$ . As it was assumed that M numbers of sources are there, the number of dimensions was set to M in the solution space for PSO. Each point in the solution space represents a possible candidate solution. Having defined the solution space and fitness function, the remaining task is to set the values of the PSO parameters and to execute the PSO program. The PSO parameters given previously in Table 3.1 were used in this case also. The invisible/reflecting boundary condition was applied that confines the particles within the solution space. In this case the PSO iterations were terminated by fixing the maximum number of iterations.

The DoA estimation was performed for three different scenarios. In the first case, the DoA was estimated for a single source and the effect of element failure was investigated. The second and third cases were performed for two sources with two different angle of separation between those sources. The simulations were performed on the 32-element uniform linear array separated by a half wavelength distance. The performance of PSO based DoA estimation was studied in terms of root mean square error (RMSE) and the ability to resolve closely spaced sources, that is in terms of the probability of resolution (PR). The RMSE is given by:

$$RMSE = \sqrt{\frac{1}{MN_{run}} \sum_{i=1}^{N_{run}} \sum_{l=1}^M [\hat{\theta}_l(i) - \theta_l]^2} \quad (6.11)$$

where  $M$  is the number of sources,

$\hat{\theta}_l$  is the estimated DoA of  $l^{\text{th}}$  source,

$\theta_l$  is the actual DoA of  $l^{\text{th}}$  source.

PR is a measure of the ability to separate two closely spaced signals. The two sources are said to be separated in a given run if both  $|\hat{\theta}_1 - \theta_1|$  and  $|\hat{\theta}_2 - \theta_2|$  are smaller than  $|\theta_1 - \theta_2|/2$ .

Taking into account the heuristic nature of PSO algorithm, the simulations were carried out for multiple times to have final averaged result.

### 6.3.1 DoA Estimation in a Failed Antenna Array for Single Source

In this case, the array was assumed to receive the signal from a single source. The angle of arrival of the signal was randomly selected at  $\theta_i = 140^\circ$ . The simulation was performed in the presence of noisy environments. The SNR was made to vary from 0 dB to 30 dB with a step size of 5 dB. The PSO was executed for 1000 iterations and the simulation was run for 100 times. The performance of single source direction finding is shown in Figure 6.2.

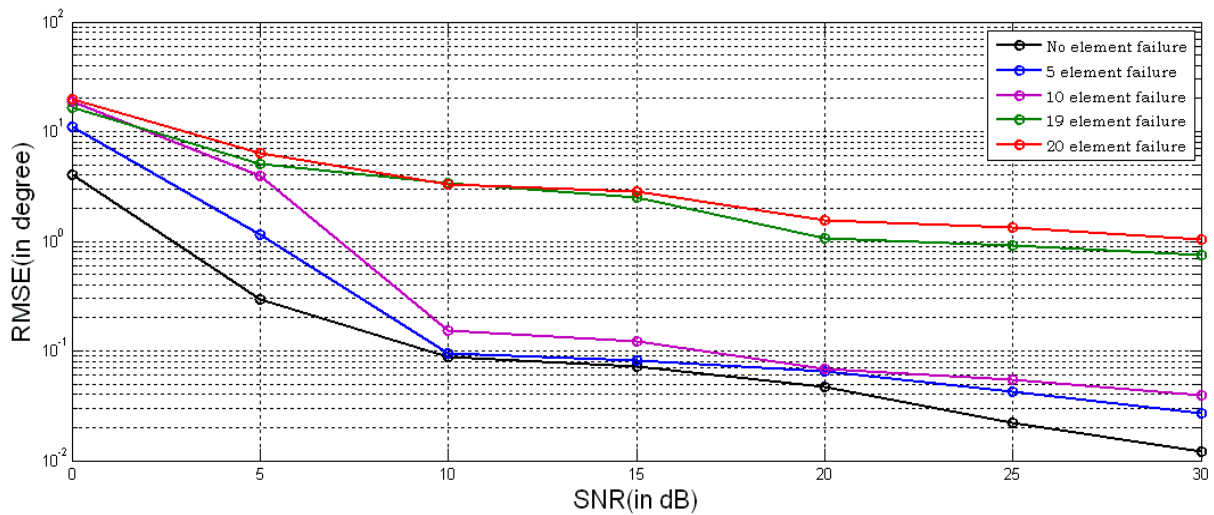


Figure 6.2: RMS error of the estimated DoA vs SNR (Single source incident on the antenna array having different number of faulty elements)

After applying the PSO for single snapshot DoA estimation for the test array, the same procedure was extended to failed antenna array with faults at different random locations. The antenna element that encounters a failure will not receive any signal. Hence the output of the faulty element will be noise only. Figure 6.2 shows the RMSE in DoA estimation, obtained using PSO, as a function of SNR for some typical cases of element failure. It can be observed that the error is small at higher SNR values. On the other hand the error is more profound when the number of element failure in the array is more.

From figure 6.2, it can be seen that, in this 32-element array if an error of  $1^\circ$  in the DoA estimation is tolerable, then a maximum permissible failure of 19 elements is allowed, at an SNR of 25-30dB. In this analysis, the observations are made for SNR values of 25-30dB, because in most of the wireless communication systems, more than 25dB SNR is considered as very good signal. For 20 element failure case, it was found that the error in DoA exceeds more than  $1^\circ$ . The root mean square error in DoA estimation remain within  $1^\circ$  for faults in around 60% of the elements in a 32-element linear array.

### **6.3.2 DoA Estimation in a Failed Antenna Array for Two Sources**

The feasibility of using PSO for DoA estimation in failed antenna array was tested in a multiple source environment. The simulation was performed on same antenna array with two incoming signals with true DoA's of  $130^\circ$  and  $140^\circ$ . Similar observations were made for two incoming signal sources in noisy environments for failed antenna array. The performances obtained through the simulation are plotted Figure 6.3. It was found that the RMS error in the DoA estimation remain within  $1^\circ$  till the number of faulty element in the array reach to 7, for SNR value of 25-30dB. The error became more than  $1^\circ$  when the number of defective element was 8 in the array. So two sources separated by  $10^\circ$  can be detected till seven number of faults in the array. Figure 6.4 show the probability of resolution (PR) obtained in case of multiple sources and multiple element failures. From the figure it is

clear that it is difficult to separate out the two sources when the numbers of failure in the array is 8. So the DoA estimation in this case is possible in the failed antenna array with around 22% of element failure.

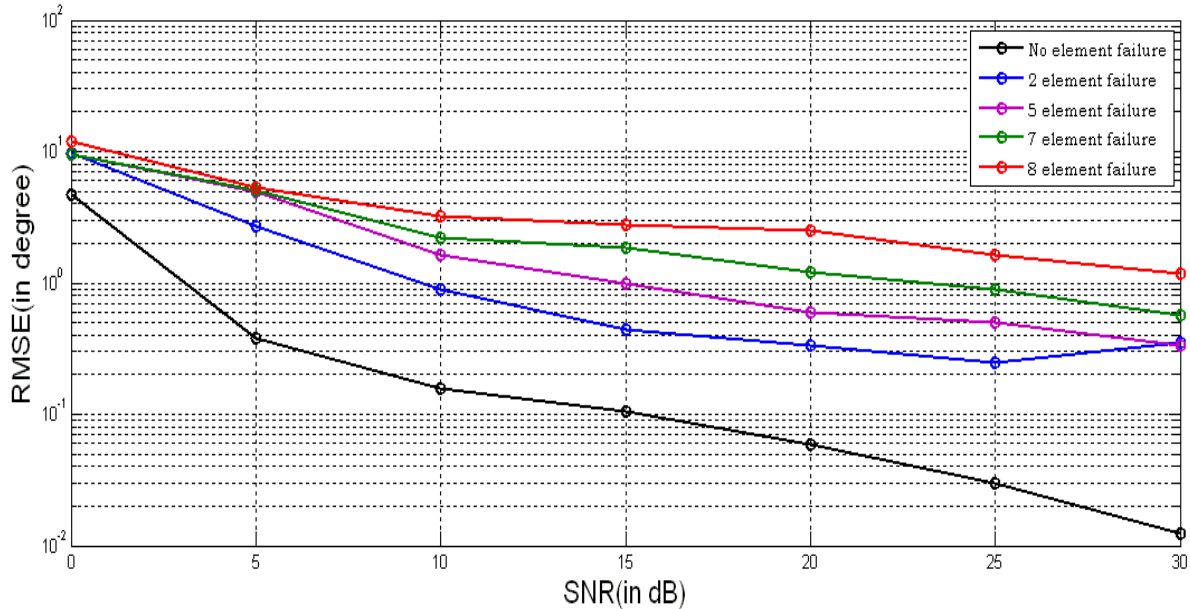


Figure 6.3: RMS Error of the estimated DoA vs SNR (Two sources incident on the antenna array having different number of faulty elements)

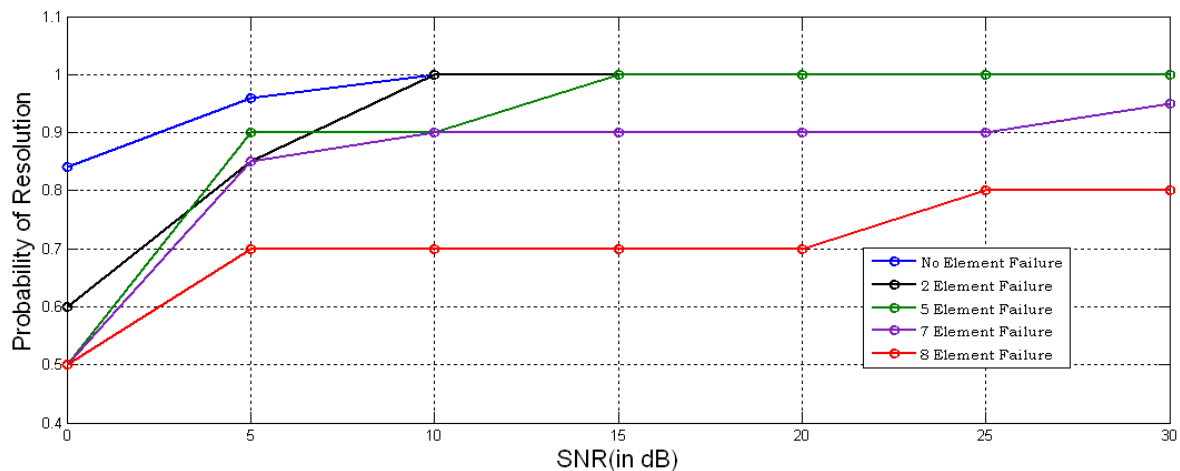


Figure 6.4 Probability of resolution (PR) vs SNR for DOA estimation by PSO in a failed antenna array (Two sources separated by  $10^\circ$ )

The same DoA estimation problem was implemented for the two sources directed at  $130^\circ$  and  $135^\circ$ , that is the sources separated by  $5^\circ$ . The DoA estimation was performed under array failure scenarios. It was found that the number of faults in the array without affecting much the DoA estimation

is 4. Hence in this case, the DoA estimation is possible with 12.5% of element failure in the array. Furthermore, when the sources are present more closely, then the estimation of the DoA is a difficult task in failed arrays. Figure 6.5 shows the PSO performance under this circumstance in terms of RMSE. Extending this simulation process with more closely sources, it was found that when the separation is less than  $3^\circ$ , DoA estimation is not possible for any kind of failure in the array.

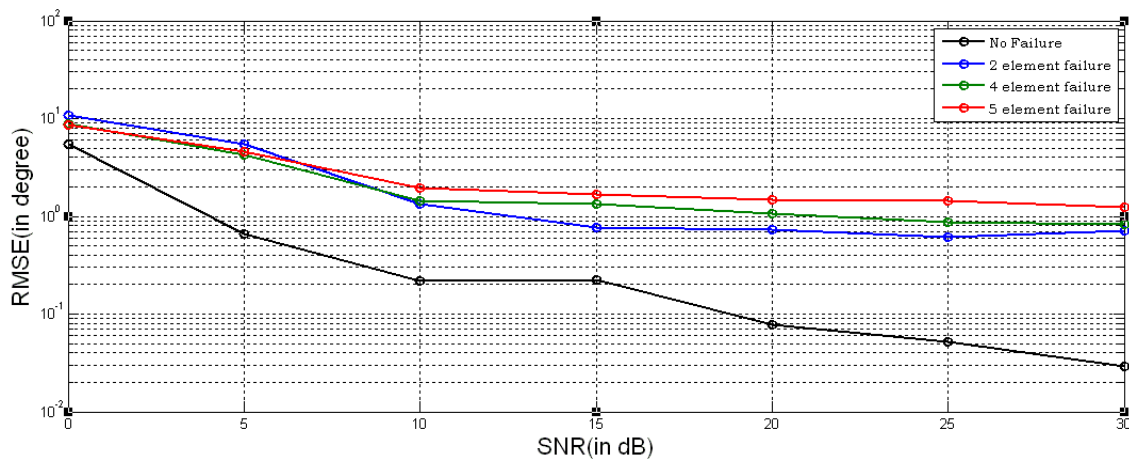


Figure 6.5: RMS Error of the estimated DoA vs SNR (Two sources separated by  $5^\circ$  incident on the antenna array having different number of faulty elements)

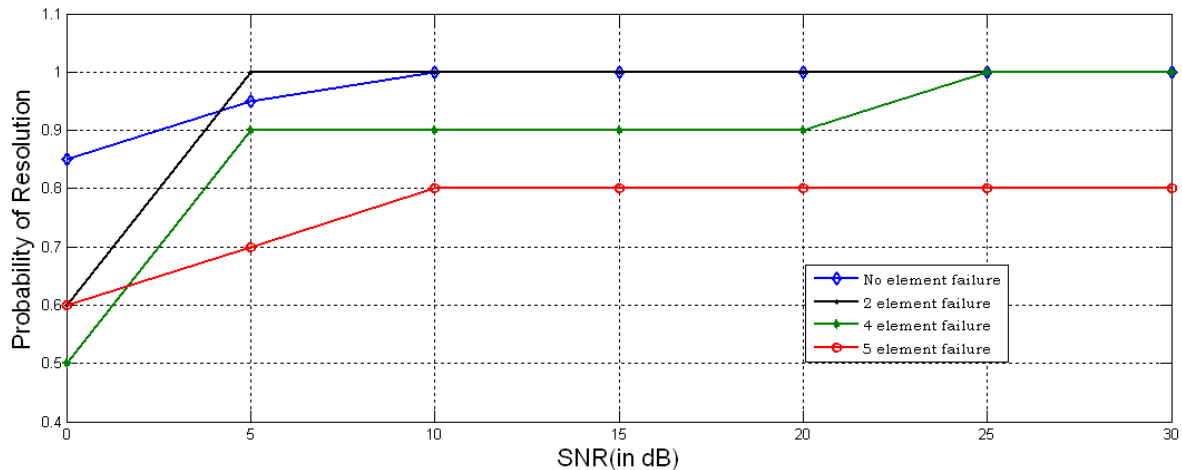


Figure 6.6: Probability of resolution (PR) vs SNR for DOA estimation by PSO in a failed antenna array (Two sources separated by  $5^\circ$ )

### 6.3.3 Observations

It was observed in the above investigation that the element failure in the array has a little effect on DoA estimation when the array is illuminated by a single source. The RMS error of the estimated DoA of the single source is

remain within  $1^\circ$  for 60% element failure in a 32-element linear array. But when the array is illuminated by two sources, the error increases rapidly with element failure. For a 32-element array illuminated by two sources separated by  $10^\circ$ , the error in estimated DoA crosses  $1^\circ$  when 8 elements became nonoperational. When the sources are placed more closely to each other, then detection becomes more difficult with element failure. In the above simulation when the sources are considered at  $5^\circ$ , only 12% of the element failure can be tolerable to estimate the DoA of the signals with a RMS error less than  $1^\circ$ . If the signals come closer than  $3^\circ$  then a single element failure in the array affects the estimation of DoA.

## 6.4 Beamforming in Failed Array

Beamforming in antenna array is used for directional signal transmission and reception. It provides an effective way to interfere the signals constructively at desired directions, whereas the signals at other directions interfere destructively [83]. Beamforming is to enhance the spectral efficiency and ease the effects of multipath problem in far-field, by looking at the strongest one of the multipath signals. The rest of the multipath signal is treated as the interfering signals. The beamformer forms the beam by controlling the phase and amplitude of the each radiating element of the array, to provide constructive and destructive interference in the wavefront [37].

After performing the DoA estimation, the next job for the failed phased array is beamforming, that is to direct the main beam in that direction. In a normal array this can be achieved only by phase perturbations. But in a failed antenna array, the designed beam pattern has to be obtained by amplitude-phase perturbations, because the amplitude perturbation has the better performance on the restoration of SLL of the damaged pattern, also. Here a search procedure based on PSO is used to obtain the required perturbations for the designed optimal beam patterns.

Considering a linear array of  $N$ -equispaced isotropic antenna elements, as shown in Fig. 6.7, the far-field pattern can be expressed as:

$$AF(\theta) = w^T S(\theta) \quad (6.11)$$

where  $w$ :  $N$ - dimensional complex weight vector

$$w = [w_1 \ w_2 \ w_3 \ \cdots \ w_n \ \cdots \ w_N]^T \quad (6.12)$$

$$w_n = a_n e^{j\beta_n} \quad (6.13)$$

$a_n$ : Amplitude weight of the  $n^{\text{th}}$  element

$\beta_n$ : Phase shifter weight at  $n^{\text{th}}$  element

$S$ :  $N$ -dimensional steering vector

$$S(\theta) = [\exp(j2\pi f\tau_1) \exp(j2\pi f\tau_2) \cdots \exp(j2\pi f\tau_n) \cdots \exp(j2\pi f\tau_N)] \quad (6.14)$$

where  $\{\tau_n, \ n=1,2,\dots,N\}$  are the propagation delay between the plane wavefront and antenna elements, which can be expressed as:

$$\tau_n = \frac{d_n \cos \theta}{v}$$

$d_n$ : distance of the  $n^{\text{th}}$  element from the reference antenna element.

$v$ : propagation speed of the radio waves.

To point the main beam in desired direction, the steering vector has to be modified as:

$$S = \exp \left\{ j \frac{2\pi}{\lambda} d_n \cdot (\cos \theta - \cos \theta_m) \right\}. \quad (6.15)$$

In the array, the weight of an element is assumed to be zero, which is considered as failed.

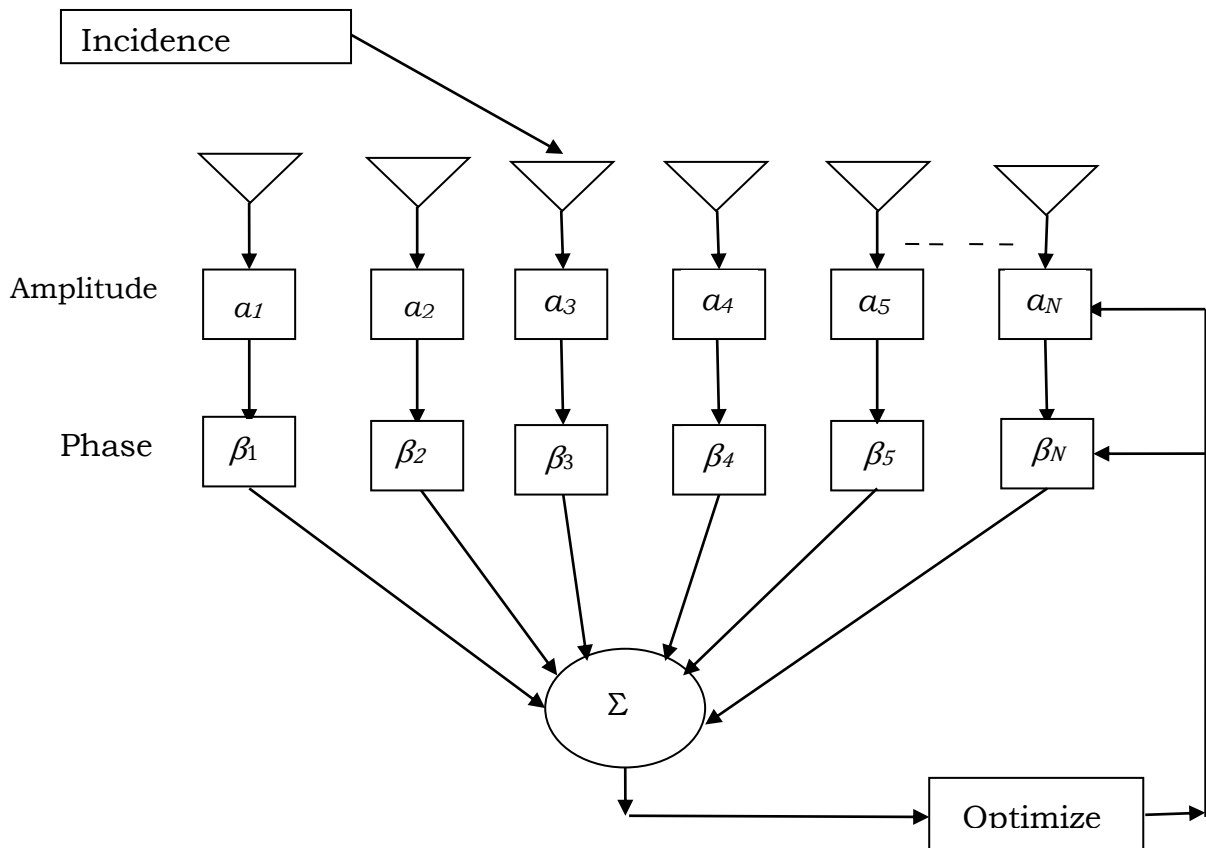


Figure 6.7 : Beamformer

## 6.5 Beamforming Implementation

In the present case, the task is to show that a failed array can make a beam in  $130^\circ$  direction, and for that matter in any direction and not only in broadside direction as verified in the previous chapters. In order to testify that, the same 32-element linear array having  $\lambda/2$  interelement spacing was considered as the candidate antenna. The current excitations of the each element was adjusted, such that the main beam of the radiation pattern directed in the  $130^\circ$  direction and the SLL was maintained at -30dB level. The HPBW and the FNBW of the pattern have the value  $3.8^\circ$  and  $10.4^\circ$  respectively. But when the element failure occurs in the array, the pattern gets distorted. In such scenario, pattern recovery can be possible by reconfiguring both amplitude and phase excitation, which will restore the pattern.



Here we considered a case of element failure, in the above considered array and tried to restore the SLL and main beam direction of the pattern. Two elements located at 2<sup>nd</sup> and 5<sup>th</sup> position were considered as non-radiating in the array. The distorted pattern have the value of SLL, HPBW and FNBW as -24.2 dB, 4° and 11° respectively. The PSO optimizer adjusts the amplitude and phase weights of all the remaining functional elements of the array, with a goal to minimize the SLL and to direct the main beam in the desired direction. The values assigned to different PSO parameters are same as mentioned in Table 3.2. The recovered pattern, after applying the PSO formulation is shown in Figure 6.5. From the figure, the recovered values of SLL, HPBW and FNBW are -29.99 dB, 4.2°, and 11.2° respectively.

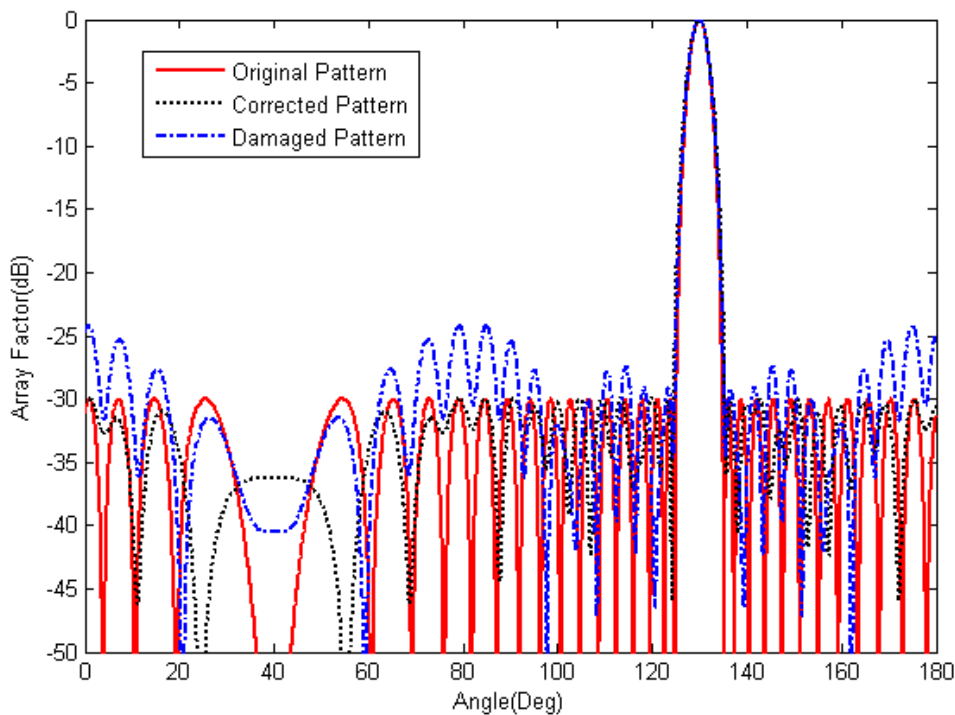


Figure 6.8: Beamforming in a 32- element linear array having two failed elements

## 6.6 Summary

In this chapter, the problem of DoA estimation was formulated as an optimization problem and solved using PSO for an antenna array having faulty elements. The RMSE in the DoA estimation for different number of

element failure was determined at different SNR values. This investigation was performed to determine the maximum number of element failure in the array, for which the variation in the DoA estimation is in an acceptable limit, at a given SNR. With the knowledge of number of failure in a particular array which has no significant effect of DoA estimation, the pattern restoration procedure can be initiated. After obtaining the DoA of the sources the beam can be directed in that direction by phase perturbation.

## **Conclusion and Future Scope of Work**

---

Strategy for recovery of different radiation parameters of a failed phased array antenna has been developed in this thesis, with the goal to use the failed array as a normal array. The parameters in focus are side-lobe level, null position, estimation of direction-of-arrival and the corresponding beamforming. Because compensation of one parameter affect the other parameters, therefore research focus have also been made, in this thesis, to quantify the limits of these compensations. The process of compensation of each parameter was approached as an optimization problem and solved using two evolutionary computational techniques, viz. PSO and BFO. The reason of applying evolutionary computational techniques in the present scenario is twofold: (i) when faults develop in an antenna array, it becomes unsymmetric and hence difficult to handle analytically; (ii) evolution based optimizers are capable of reaching to the global minima/maxima and their application process is easy.

The work started with a review on phased array antennas and evolutionary computational techniques. The requirement for compensation in a failed array and approaches applied so far has been highlighted in this review chapter. Because the application process of PSO is easy and it is one of the widely used evolutionary optimization techniques in microwave engineering, so this was a common choice for the present problem. At the same time, because BFO was relatively new to microwave community, it was chosen as the next choice method for solving the array compensation problem. The main motive was to find a suitable method of compensation that can be realized in real time.

The major effect of faults in antenna arrays is the rise in SLL, removal/shifting of the null positions and change in HPBW. Methods of compensating all these parameters were outlined and successfully handled in Chapters 3 and 4. It was found that compensation of one parameter has effects on the compensated value of the other parameters of failed antenna array. For this reason, in order to give a quantitative measure to the extent compensation is possible; a comprehensive analysis was carried out. It was found that compensation in SLL and null position is possible for failure upto 30% of elements, if one is ready to compromise 50% in HPBW. Furthermore, it was also found that, there is no need to perturb the excitation of all the working elements to have the compensation. Perturbation of few working element excitations is enough to get an acceptable compensation. From the conducted research, it has been revealed that, this number is mostly a function of position of the faulty element in the array and depends less on the number of faulty elements.

It was found that the presence of faulty elements also affects the DoA estimation capability of a phased array. Because of this, the probability of resolution, that is, the ability of the phased array to resolve two closely spaced sources deteriorates. Solutions have been found, in this thesis, for the array to make correct beamforming.

Both PSO and BFO were used in the compensation process of the failed array parameters. It has been found that, although the convergence of BFO is faster than that of PSO but the time of computation of PSO is much less than that is required for BFO. Therefore for a real-time implementation of a self-recoverable antenna array PSO is the preferred technique than BFO.

The developed methodology can be helpful in increasing the life span of the arrays, particularly for the arrays without direct human access. At the same time it can save the hardware replacement cost.

## **7.1 Future Scope of Work**

The work done in the thesis gives hopes of using a failed array as a normal array, that can, not only increase the life-time of the arrays, but also can be used as a resort in emergency situation. Particularly to deal with situations in emergency and also for the phased arrays placed in inaccessible regions; research focus needs to be expended to develop self-recoverable antennas. In order to develop those kinds of antennas, the work done in this thesis can be used as a starting point.



# References

- [1] <http://sat-nd.com/failures>
- [2] IEEE Trans.on AES, Oct.1999.
- [3] A. K. Agrawal, E. L. Holzman, "Active phased array design for high reliability", *IEEE Trans. Aerospace and Electronic Systems*, vol. 35, no. 4, pp. 1204 -1211, 1999.
- [4] D. J. Ramsdale, R. A. Howerton, "Effect of element failure and random errors in amplitude and phase on sidelobe level attainable with a linear array", *J. Acoust. Soc. Am.*, vol. 68, no. 3, pp. 901-906, Sept. 1980.
- [5] L. A. Rondinelli, "Effects of random errors on the performance of antenna arrays of many elements", *IRE Natl. Conv. Rec. 7*, pp. 174-189, 1959.
- [6] R. J. Malloux, "Phased array antennas handbook", *Artech House*, 1994.
- [7] J. Redvik, B. I. Svensson, "Compensation of faulty elements in array antennas" US patent no.: US 6339398B1, Jan. 2002.
- [8] J. S. R. Jang, C. T. Sun and E. Mizutani, "*Neuro-Fuzzy and Soft Computing*" Prentice Hall, NJ, 1997.
- [9] R. K. Shukla and A. Biswas, "Application of genetic algorithm for computer-aided design and optimization of microwave circuits," *IETE Journal of Research* vol. 47, no. 3&4, pp. 1-4, 2001.
- [10] Y. Rahmat-Samii, C. G. Christoudoulou (Editors), Special issue on synthesis and optimization techniques in electromagnetics and antenna system design, *IEEE Trans. On Antenna and Prop.*, vol. 55, no. 3, part 1, 2007.
- [11] R. L. Haupt, "An introduction to genetic algorithm for electromagnetic" *IEEE Antenna and Propagation magazine*, vol. 37, no. 2, pp. 7-15, Apr. 1995.
- [12] Michael Johnson, Y. Rahmat-Samii, "Genetic algorithms in engineering," *IEEE Antennas Propag. Mag.*, vol. 39, no. 4, pp. 7-21, Aug.1997.
- [13] G.K. Mohanti, A. Chakrabarty and S. Das, "Phase-only and amplitude-phase synthesis of dual-pattern linear antenna arrays using floating-point genetic algorithms," *Progress in Electromagnetic Research PIER*, 68, pp. 247-259, 2007.
- [14] G. K. Mohanti, S. Das and A. Chakraborty, "Design of phase differential reconfigurable array antennas with minimum dynamic range ratio," *IEEE Antennas and Wireless Propagation Letters*, vol. 5, pp. 262-264, 2006.
- [15] G.K. Mohanti, A. Chakraborty and S. Das, "Discrete phase-only synthesis of a dual-beam collinear dipole antenna array using genetic algorithms," *International Journal of Theoretical and Applied Computer Sciences*, vol. 1, no.1, pp. 63-70, 2006.
- [16] J. Robinson, Y. Rahmat-Samii, "Particle swarm optimization in electromagnetic," *IEEE Transactions on Antennas and Propagation*, vol. 52, no.2, pp. 397-407, February 2004.

- [17] S. Baskar, A. Alphones, P. N. Suganthan and J. J. Liang, "Design of yagi-uda antennas using comprehensive learning particle swarm optimization," *Microwave, Antennas and Propagation, IEE Proceedings*, vol. 152, no. 5, pp. 340-346, 2005.
- [18] D. W. Boeringer and D. H. Werner, "Particle swarm optimization versus genetic algorithm for phased array synthesis" *IEEE Trans Antennas and Propagation*, vol. 52, no. 3, pp. 771-779, Mar. 2004.
- [19] R. K. Mishra, A. Patnaik, "Neural network based CAD model for design of square patch antennas," *IEEE Trans Antennas and Propagation*, vol. 46, no. 12, pp. 1890-1891, Dec. 1998.
- [20] A. Patnaik, D. E. Anagnostou, R. K. Mishra, C. G. Christodoulou and J. C. Lyke, "Applications of neural networks in wireless communications", *IEEE Antennas and Propagation Magazine*, vol. 46, no.3, pp. 130-137, June 2004.
- [21] A.P Engelbrecht, "Computational intelligence-An introduction", JohnWiley and Sons, Ltd., 2002.
- [22] K. Deb, "Optimization for engineering design algorithms and examples", Prentice-hall India, New Delhi, 2003.
- [23] S. Kharche, G. S. Reddy, B. Mukherjee, R. Gupta, and J. Mukherjee, "MIMO Antenna for bluetooth, Wi-Fi, Wi-Max and UWB applications", *Progress In Electromagnetics Research C*, Vol. 52, pp 53-62, 2014.
- [24] A. Sanyal, A. Basu, S. K. Koul, M. Abegaonkar, S. Varughese and P. B. Venkatesh Rao, "A planar end-fire array in S-band for airborne applications," *IETE Journal of Research*, vol. 58, no. 1, pp. 34-43, 2012.
- [25] L. A. Berge, M. Reich and B. D. Braaten, "A Compact Dual-Band Bow-tie Slot Antenna for 900 MHz and 2400 MHz ISM Bands," *IEEE Antennas and Wireless Propagation Letters*, vol. 10, 2011, pp. 1385-1388.
- [26] M. S. Khan, M. F. Shafique, A. Naqvi, A. - D. Capobianco, B. Ijaz and B. D. Braaten, "A Miniaturized Dual-Band Diversity Antenna for WLAN Applications," *IEEE Antennas and Wireless Propagation Letters*, vol. 14, 2015, pp. 958-961.
- [27] M.S. Khan, A. - D. Capobianco, A. Naqvi, M. S. Shafique, B. Ijaz and B. D. Braaten, "Compact Planar UWB MIMO Antenna with On-Demand WLAN Rejection," *IET Electronics Letters*, vol. 51, no. 13, pp. 963-964, Jun. 2015.
- [28] D. E. Anagnostou, M. T. Chryssomallis, B. D. Braaten, J. Ebel, and N. Sepulveda, "Reconfigurable UWB antenna with RF-MEMS for On-demand WLAN rejection", *IEEE Transactions on Antennas and Propagation*, vol. 62, no. 2, pp. 1-7, Feb. 2014.
- [29] P. Prakash, M.P. Abegaonkar, A. Basu, and S. K. Koul, "Gain enhancement of a CPW-fed monopole antenna using polarization-insensitive AMC Structure," *IEEE Antennas and Wireless Propagation Letters*, vol. 12, pp. 1315-1318, 2013.



- [30] P. Mukherjee, B. Gupta, and R. Bhattacharjee, "Dual band coplanar microstrip antenna with polarization diversity" *Journal of Electromagnetic Waves and Applications*, vol. 17, no. 9, pp. 1323-1330, 2003.
- [31] A. Gupta, M. P. Abegaonkar, A. Basu, and S. K. Koul, "A tunable high impedance surface and its application to dual-band microstrip antenna," *Progress In Electromagnetics Research C*, vol. 43, pp. 231-246, 2013.
- [32] R. Jana and R. Bhattacharjee, "A Novel matched feed structure for achieving wide cross-polar bandwidth for an offset parabolic reflector antenna system", *IEEE Antenna and Wireless Propagation Letters*, vol. 14, pp. 1590-1593, 2015.
- [33] R. K. Chaudhary, K. V. Srivastava and A. Biswas, "A broadband dumbbell shaped dielectric resonator antenna", *Microwave and Optical Technology Letters*, vol. 56, no. 12, pp. 2944-2947, Dec. 2014.
- [34] S. Mukherjee, A. Biswas, K. V. Srivastava, "Broadband Substrate Integrated Waveguide Cavity Backed Bow-Tie Slot Antenna," *IEEE Antennas and Wireless Propag. Letters*, vol. 13, pp- 1152-1155, 2014.
- [35] R. C. Reddy and R. Bhattacharjee, "Investigation on L-slot loaded dual-band compact patch antenna" *Proc. IEEE Asia-Pacific Conference on Antennas and Propagation*, Singapore, Aug 2012.
- [36] S. Shelley, J. Costantine, C. G. Christodoulou, D. E. Anagnostou and J. C. Lyke, "FPGA Controlled Switch-Reconfigured Antenna", *IEEE Antennas and Wireless Propagation Letters*, Vol. 9, pp. 355-358, April 2010.
- [37] C.A Balanis, *Antenna Theory and Design*, John Wiley and Sons, Inc., 2005.
- [38] M. T. Chryssomallis and C. G. Christodoulou, "Antenna Radiation Patterns Encyclopedia of RF and Microwave Engineering", 2005.
- [39] T. T. Taylor, "Design of line-source antennas for narrow beamwidth and low sidelobes", *IRE Trans., Antenna Propag.* vol. 3, pp. 16-28, Jan. 1955.
- [40] C. L. Dolph, "A current distribution for broadside arrays which optimises the relationship between beamwidth and sidelobe level", *Proc. IRE*, vol. 34, pp 335-348, Jun.1946.
- [41] C. J. Drane, "Dolph-Chebyshev excitation coefficient approximation," *IEEE Trans.*, vol. AP-12, pp. 781-782, Nov. 1964.
- [42] S.A, Schelkunov, "A mathematical theory of linear arrays," *Bell System Tech. J.*, pp. 80-107, 1943.
- [43] P.M. Woodward, "A method of calculating the field over a plane aperture required to produce a given polar diagram," *Proc IEE, Part IIIA*, vol. 93, pp. 1554-1555, 1947.
- [44] T. S. Fong and R. A. Birgenheier, "Method of conjugate gradients for antenna pattern synthesis," *Radio Sci.*, vol. 6, pp. 1123-1130, 1971.

- [45] Leo I. Vaskelainen, "Constrained least-squares optimization in conformal array antenna synthesis," *IEEE Trans. Antennas Propagation*, vol. 55, no. 3, Mar. 2007.
- [46] H. Elmikati and A. A. Elsohly, "Extension of projection method to nonuniformly linear antenna arrays," *IEEE Trans. Antennas Propagat.*, vol. AP-32, pp. 507-512, 1984.
- [47] G. Mazzarella and G. Panariello, "A projection-based synthesis of non-uniform array", *Proc. of Antennas Propag. Symp.* London, Ont., Canada, 1991.
- [48] G. Miaris, M. Chryssomallis, E. Vafiadis, and J. N. Sahalos, "A unified formulation for Chebyshev and Legendre superdirective endfire array design" *Electrical Engineering*, vol. 78, pp. 271-280, 1995.
- [49] Keen-keong Yan, Yilong Lu, "Sidelobe Reduction in Array-Pattern Synthesis Using GA," *IEEE Trans. on Antenna and Propagation*, vol.45, no.7, July 1997.
- [50] R. L. Haupt, "Thinned arrays using genetic algorithms", *IEEE Trans. Antennas and Propagation*, vol. 42, no. 7, pp. 993-999, 1994.
- [51] Ling Cen, Zhu Liang Yu, Wee Ser, and Wei Cen, "Linear aperiodic array synthesis using an improved genetic algorithm," *IEEE Trans. Antennas and Propagation*, vol. 60, no. 2, Feb. 2012.
- [52] S. Baskar, A. Alphones and P. N. Suganthan, " Genetic algorithm based design of reconfigurable antenna array with discrete phase shifter" *Microw. Opt. Technol. Lett.*, vol. 45, no. 6, pp. 461-465, June 2005.
- [53] M.M. Khodier and C.G. Christodoulou "Linear array geometry synthesis with minimum sidelobe level and null control using particle swarm optimization" *IEEE Trans. Antenna and Propagation*, vol.53, no.8, pp.2674-2679, 2005.
- [54] M. Khodier and M. Al-Aqeel "Linear and circular array optimization: A study using particle swarm intelligence," *Progress In Electromagnetics Research B*, vol. 15, pp. 347-373, 2009.
- [55] M. H. Bataineh, and J. I. Ababneh, "Synthesis of a periodic linear phased antenna array using particle swarm optimization," *Electromagnetics*, vol. 26, no. 7, pp. 531-541, Oct. 2006.
- [56] Boeringer, D. W. and D. H. Werner, "Particle swarm optimization versus genetic algorithms for phased array synthesis," *IEEE Trans. on Antennas and Propagation*, vol. 52, no. 3, pp. 771-779, Mar. 2004.
- [57] Dennis, G. and Y. Rahmat-Samii, "Particle swarm optimization for reconfigurable phase differentiated array design," *Microwave and Optical Technology Letters*, vol. 38, no. 3, pp. 168-175, Aug. 2003.
- [58] Chen, T. B., Y. L. Dong, Y. C. Jiao, and F. S. Zhang, "Synthesis of circular antenna array using crossed particle swarm optimization algorithm," *Journal of Electromagnetic Waves and Applications*, vol. 20, no. 13, pp. 1785-1795, 2006.
- [59] O. P. Acharya, A. Patnaik, S.N. Sinha , "Antenna Array Synthesis for Desired Radiation Pattern using Particle Swarm Optimization," *12th International Symposium*

- on *Microwave and Optical Technology (ISMOT-2009)*, New Delhi, India, pp. 771-774, Dec. 16-19, 2009.
- [60] T. Datta, I. S. Mishra, B. B. Mangaraj, S. Imtiaj, "Improved adaptive bacteria foraging algorithm in optimization of antenna array for faster convergence," *Progress in Electromagnetic Research C*, 1, pp. 143 – 157, 2008.
- [61] K. Guney, and S. Basbug, "Interference suppression of linear antenna array by amplitude-only control using bacteria foraging algorithm," *Progress in Electromagnetic Research PIER* 79, pp. 475 – 497, 2008.
- [62] K. Guney, and S. Basbug, "Bacteria foraging algorithm for null synthesizing of linear antenna arrays by controlling only the element positions," *J. Optim. Theory Appl.* 150, pp. 635–656, 2011.
- [63] J. A. Ferreira and F. Ares, "Pattern synthesis of conformal arrays by the simulated annealing technique," *Electron. Lett.*, vol. 33, no. 14, pp. 1187-1189, July 1997.
- [64] Murino, V., A. Trucco, and C. S. Regazzoni, "Synthesis of unequally spaced arrays by simulated annealing," *IEEE Trans. on Signal Processing*, vol. 44, no.1, pp. 119-123, Jan. 1996.
- [65] C. Rocha-Alicano, D. Covarrubias-Rosales, C. Brizuela Rodriguez, and M. Panduro-Mendoza, "Differential evolution algorithm applied to sidelobe level reduction on a planar array," *AEU International Journal of Electronic and Communications*, vol. 61, no. 5, pp. 286-290, 2007.
- [66] T. J. Peters, "A conjugate gradient-based algorithm to minimize the sidelobe level of planar array with element failures," *IEEE Trans. on Antenna and Propagation*, vol. 39, No. 10, pp. 1497-1504, 1991.
- [67] S.Z.Bu and A.S. Daryoush, "Comparison of reconfigurable methods of active phased array antenna," *IEEE AP-S Int. Symp. Digest*, pp. 214-217, Ann Arbor, Michigan, USA 1993.
- [68] Robert J. Mailloux, "Array failure correction with digitally beamformed array," *IEEE Trans. Antennas Propagation*, vol. 44, no. 12, pp. 1543-1550, Dec. 1996.
- [69] Menachem Levitas, David A. Horton, and Theodore C. Cheston, "Practical failure compensation in active phased arrays," *IEEE Trans. Antennas Propagation*, vol.47, no.3, pp. 524-535, 1999.
- [70] S.H. Zainud-Deen et. al., "Array failure correction with orthogonal methods," *Proc. of the 21st National Radio Science Conference, (NRSC 2004)* pp. B7:1-9, March 2004.
- [71] B. K. Yeo and Y. Lu, "Array failure correction with a genetic algorithm", *IEEE Trans. Antennas Propag*, vol. 47, no. 5, pp. 823-828, May 1999.
- [72] Jung-Hoon Han, Sang-Ho Lim, and Noh-Hoon Myung, "Array antenna TRM failure compensation using adaptively weighted beam pattern mask based on genetic algorithm" *IEEE Antennas and Wireless Propagation Letters*, vol. 11, pp.18-21, 2012.

- [73] S. A. Mitilineos, S. C. A. Thomopoulos and C. N. Capsalis "Genetic design of dual-band, switched-beam dipole arrays, with elements failure correction, retaining constant excitation coefficients," *Journal of Electromagnetic Waves and Applications*, vol. 20, no. 14, pp. 1925–1942, 2006.
- [74] J. A. Rodriguez and F. Ares, "Optimization of the performance of arrays with failed elements using simulated annealing technique," *Journal of Electromagnetics Wave and Applications*, vol.12, pp.1625-1638, 1998.
- [75] M. V. Lozana, J. A. Rodriguez, F. Ares, "Recalculating linear array antennas to compensate for failed elements while maintaining fixed nulls," *Journal of Electromagnetics and Applications*, vol. 13, pp. 397-412, 1999.
- [76] L. L. Wang and D.G. Fang, "Combination of genetic algorithm and fast fourier transform for array failure correction," *Proc. 6th International Symposium on Antennas, Propagation and EM Theory*, 28 Oct.-1 Nov. 2003.
- [77] S. Biswas, P.P.Sarkar and B. Gupta, "Array factor correction using artificial neural network model", *International Journal of Electronics*, vol.91, pp. 301-308, May 2004.
- [78] L.C. Godara, *Smart Antennas*. Boca Raton: CRC Press, 2004.
- [79] Frank Gross, *Smart Antennas for Wireless Communications with Matlab*: McGraw-Hill, 2005.
- [80] Michael Chryssomallis, "Smart Antennas" *IEEE Antennas and Propagation Magazine*, vol. 42, no. 3, June 2000.
- [81] R. O. Schmidt, "Multiple emitter location and signal parameter estimation," *IEEE Trans. Antennas Propag.*, vol. 34, no. 3, pp.276–280, Mar. 1986.
- [82] B. D. Rao and K. V. S. Hari, "Performance analysis of root-MUSIC," *IEEE Trans. Acoust., Speech, Signal Process.*, vol. 37, pp. 1939–1949, Dec. 1989.
- [83] R. Ray and T. Kailath, "ESPRIT-estimation of signal parameter via rotational invariance techniques," *IEEE Trans. Acoust., Speech, Signal Process.*, vol. 37, pp. 984-995, 1989.
- [84] Minghui Li and Yilong Lu, "A refined genetic algorithm for accurate and reliable DoA estimation with a sensor array" *Wireless Personal Communications*(Springer) vol. 43, pp. 533-547, 2007.
- [85] Yiping Yang, Yunshan Hou, Xianxing Liu "Two dimensional DoA estimation by ant colony optimization" *proc.International Conference on Intelligent System Design and Engineering Application*, 2010.
- [86] D. Poyatos et.al. "Evaluation of particle swarm optimization applied to single snapshot direction of arrival estimation" *J. of Electromagn. Waves and Appl.*, vol. 22, pp. 2251–2258, 2008.

- [87] Jui-Chung Hung "Modified particle swarm optimization structure approach to direction of arrival estimation" *Applied Soft Computing (Elsevier)*, vol. 13, pp. 315–320, 2013.
- [88] B. Errasti, D. Escot , D. Poyatos, I. Montiel, "Performance Analysis of the Particle Swarm Optimization Algorithm when applied to Direction Of Arrival Estimation" *Proc. Int. Confreance on Electromagnetics in Advanced Application, (ICEAA 09)*, Torino, pp. 447-450, 14-18 Sept. 2009.
- [89] Borja Errasti-Alcala, Raul Fernandez-Recio," On the Use of Particle Swarm Optimization for Single Snapshot DOA and Frequency Estimation", *Proc. 6th European Conference on Antennas and Propagation (EUCAP)*, pp.3635-3639, 2011.
- [90] B. Errasti-Alcala, D. Escot-Bocanegra, D. Poyatos-Martínez, A. Jurado-Lucena and R. Fernández-Recio, "Joint Direction of Arrival and Amplitude Estimation using Particle Swarm Optimization and a Single Snapshot," *Proc.14th Biennial IEEE Conf. on Electromagnetic Field Computation (CEFC)*, p.1, May 2010.
- [91] Borja Errasti-Alcala and Raul Fernandez-Recio, "Performance Analysis of Metaheuristic Approaches for Single-Snapshot DOA Estimation," *IEEE Antennas and Wireless Propagation Letters*, vol. 12, pp. 166-169, 2013.
- [92] L. Godara, "Application of antenna arrays to mobile communications, Part II: Beamforming and direction-of-arrival considerations," *IEEE proceedings*, vol.85, no.8, pp. 1195-1245, 1997.
- [93] N. K. Jablon, "Adaptive beamforming with generalized sidelobe canceller in the presence of array imperfections," *IEEE Trans. Antennas Propag.*, vol. AP-34, pp. 996–1201, Aug. 1986.
- [94] C. Y. Tseng and L. J. Griffiths, "A unified approach to the design of linear constraints in minimum variance adaptive beamformers," *IEEE Trans. Antennas Propag.*, vol. 40, pp. 1533–1542, Dec. 1992.
- [95] W. A. Press, B. P. Flannery, S. A. Teukolsky and W. T. Vetterling, "Conjugate gradient methods in multidimensions," in *Numerical Recipes. Cambridge: Cambridge Univ. Press*, 1988, pp. 301-307.
- [96] X. S. Yang, "Nature-inspired metaheuristic algorithms" *Lunver Press, UK*, 2010.
- [97] J. Kennedy and R. C. Eberhart, "Particle swarm optimization", *IEEE Conf Neural Networks IV*, NJ, 1995.
- [98] Kevin M. Passino, "Biomimicry of bacteria foraging", *IEEE Control System Magazine* vol.22, no.3, pp.52-67, 2002.
- [99] J. Kennedy, "The particle swarm: Social adaptation of knowledge," *Proc. 1997 Int. Conf. Evolutionary Computation Indianapolis, IN*, pp. 303–308, Apr.1997.
- [100] Y. Shi, and R. C. Eberhart, "A modified particle swarm optimizer," *Proceedings of the IEEE International Conference on Evolutionary Computation*, Piscataway, NJ IEEE Press, pp. 69–73, 1998.

- [101] S. L. Ho, S. Yang, G. Ni, et al., "A particle swarm optimization method with enhanced global search ability for design optimizations of electromagnetic devices," *IEEE Transactions on Antennas and Propagation*, vol. 42, pp.1107-1110, 2006.
- [102] Jai N Tripathi, J Mukherjee and P R Apte, "Design automation, modeling, optimization and testing of analog/RF circuits and systems by particle swarm optimization", *Swarm Intelligence for Electric and Electronic Engineering*, IGI Global Publishers, Dec. 2012.
- [103] S. Kamisetty, J. Garg, J. N. Tripathi and J. Mukherjee, "Optimization of analog RF circuit parameters using randomness in particle swarm optimization", *Proc. Information and Communication Technologies conf. (WICT)* Mumbai, India, pp. 274-278, 2011.
- [104] Nanbo Jin and Y. Rahmat-Samii, "Particle swarm optimization of miniaturized quadrature reflection phase structure for low-profile antenna," *Proc. of IEEE Antennas Propag. Symp.*, Washington DC, July 2005.
- [105] Nanbo Jin and Yahya Rahmat-Samii, "Advances in particle swarm optimization for antenna design: real-number, binary, single-objective, and multi-objective Implementation" *IEEE Transactions on Antennas and Propagation*, vol. 55, no.3, pp. 556-567, Mar 2007.
- [106] Nanbo Jin and Y. Rahmat-Samii, "Particle swarm optimization for antenna designs in engineering electromagnetics," *Journal of Artificial Evolution and Application*, (Hindawi) Article ID 728929, 2008.
- [107] A. Rezaee Jordehi and J Jasni, "Parameter selection in particle swarm optimization: A survey," *Journal of Experimental and Theoretical Artificial Intelligence*, vol. 25, no. 4, pp. 527-542, 2013.
- [108] David W. Stephens and John R. Krebs, "Foraging theory" Princeton academic press, USA, 1986.
- [109] Y. Liu and K. M. Passino, "Biomimicry of Social Foraging Bacteria for Distributed Optimization: Models, Principles, and Emergent Behaviors," *Journal of optimization theory and applications*, vol. 115, No. 3, pp. 603-628, Dec. 2002.
- [110] T. Datta and I. S. Mishra, "A comparative study of optimization techniques in adaptive antenna array processing: The bacteria foraging algorithm and particle swarm optimization," *IEEE Antenna and Propagation Magazine*, vol. 51, no. 6, pp.69-79, Dec. 2009.
- [111] H. Steyskal, R. A. Shore, and R. L. Haupt, "Methods for null control and their effects on the radiation pattern," *IEEE Trans. on Antennas and Propagation*, vol. AP-34, pp. 404-409, March 1986.

- [112] T. H. Ismail and M. M. Dawoud, "Null steering in phase arrays by controlling the element positions," *IEEE Trans. on Antennas and Propagation*, vol. 39, pp. 1561-1566, Nov. 1991.
- [113] B.E. Stuckman and J.C. Hill, "Method of null steering in phased array antenna systems", *Electron Lett* 26, pp. 1216-1218, 1990.
- [114] T.B. Vu, "Simultaneous Nulling in sum and difference patterns by amplitude control," *IEEE Trans. Antennas and Propagation*, vol. AP-34, pp. 214-218, 1986.
- [115] Er, M. H., "Linear antenna array pattern synthesis with prescribed broad nulls," *IEEE Trans. on Antennas Propagation*, vol. 38, pp.1496-1498, 1990.
- [116] W. P. Liao and F. L. Chu, "Array pattern synthesis with null steering using genetic algorithms by controlling only the current amplitudes," *Int. Journal of Electronics*, vol. 86, pp.445-457, 1999.
- [117] B. Babayigit, A. Akdagli, and K. Guney, "A clonal selection algorithm for null synthesizing of linear antenna arrays by amplitude control," *Journal of Electromagnetic Waves and Applications*, vol. 20, pp.1007-1020, 2006.
- [118] Guney, K. and M. Onay, "Amplitude-only pattern nulling of linear antenna arrays with the use of bees algorithm," *Progress In Electromagnetics Research*, PIER 70, pp.21-36, 2007.
- [119] R. L.Haupt, "Phase-only adaptive nulling with a genetic algorithm," *IEEE Trans. Antennas Propagat.*, vol. 45, pp.1009-1015, 1997.
- [120] M. Mouhamadou, P. Armand, P. Vaudon, and M. Rammal, "Interference suppression of the linear antenna arrays controlled by phase with use of SQP algorithm," *Progress In Electromagnetics Research*, PIER 59, pp.251-265, 2006.
- [121] W. P. Liao and F. L. Chu, "Array pattern nulling by phase and position perturbations with the use of the genetic algorithm," *Microwave and Optical Technology Letters*, Vol. 15, pp. 251-256, 1997.
- [122] A. Akdagli., K. Guney, and D. Karaboga, "Pattern nulling of linear antenna arrays by controlling only the element positions with the use of improved touring ant colony optimization algorithm," *Journal of Electromagnetic Waves and Applications*, Vol. 16, pp.1423-1441, 2002.
- [123] A. Alphones and V. Passoupathi, " Null steering in phased array by position perturbations: A genetic algorithm approach" *Proc. IEEE Int. symposium on phased array systems and technology*, Boston, MA, pp. 203-207, Oct 1996.
- [124] M.M. Dawoud, "Null steering in scanned linear arrays by element position perturbations," *Int J Electron* 78, pp. 743-757, 1995.
- [125] A. Tennant, M.M. Dawoud and A.P. Anderson, "Array pattern nulling by element position perturbations using a genetic algorithm," *Electronics Lett.*, Vol. 30, pp. 174-176, 1994.

- [126] H. Krim and M. Viberg, "Two decades of array signal processing research: The parametric approach," *IEEE Signal Process. Mag.*, vol. 13, no. 4, pp. 67–94, Jul 1996.
- [127] N. Yilmazer, R. Fernandez-Recio and T. K. Sarkar, "Matrix pencil method for simultaneously estimating azimuth and elevation angles of arrival along with the frequency of the incoming signals". Elsevier, *Digital Signal Processing*. Vol 16, Issue 6. Nov. 2006. Pages: 796 - 816.



# Author's Publications

## Journal

- [1] **O.P. Acharya**, A. Patnaik, S.N. Sinha "Limits of compensation in a failed antenna array," International Journal of RF and Microwave Computer-Aided Engineering (John Wiley & Sons). Vol 24, No. 6, pp. 635-645, Nov 2014.
- [2] **O.P. Acharya**, A. Patnaik, S.N. Sinha "Null Steering in Failed Antenna Array", International journal of Applied Computational Intelligence and Soft Computing, vol. 2011, article ID 692197, 9 pages, 2011.
- [3] **O.P. Acharya**, A. Patnaik and S.N. Sinha, "Antenna array failure correction: A metaheuristic approach" IET Microwaves, Antennas and Propagation (Under Review)

## Conference

- [4] **O.P.Acharya**, A.Patnaik, S.N.Sinha "Comparative study of bio-inspired optimization techniques in antenna array failure compensation," IEEE International Symposium on Antennas and Propagation, AP-S,2013, Florida, USA, July 7-13, 2013.
- [5] **O. P. Acharya**, A. Patnaik, S.N. Sinha "Pattern recovery in failed antenna array," IEEE Applied Electromagnetics Conference, AEMC -2011, Kolkata, India, Dec 18-22, 2011.
- [6] **O. P. Acharya**, A. Patnaik, S.N. Sinha "Null steering in failed antenna array", National conference on Communication, NCC-2011, Indian Institute of Science, Bangalore, India, Jan 28-30, 2011.
- [7] **O. P. Acharya**, A. Patnaik, S.N. Sinha, "Tolerance on element failure for DoA estimation: A soft-computation approach" IEEE Applied Electromagnetics Conference, AEMC -2015, IIT Guwahati, India Dec 18-21, 2015.